INSTITUTO SUPERIOR DE ENGENHARIA DE LISBOA
Departamento de Engenharia Eletrónica e Telecomunicações e de Computadores

5G-NR Radio Planning for Connected and Autonomous Vehicles Services

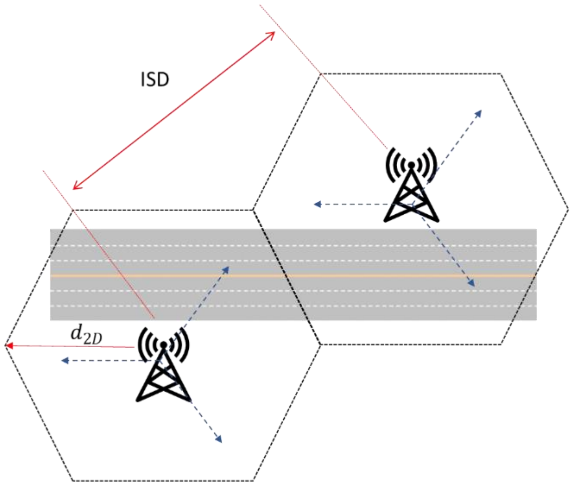

GRAZIELLE BONALDO TEIXEIRA
(Graduated in Electronic Engineering)

Thesis to obtain the Master of Science degree in Electronic and Telecommunications Engineering with minor in Telecommunications

Supervisor:	Prof. Doctor António João Nunes Serrador
Chairmain:	Prof. Doctor Nuno Miguel Machado Cruz
Jury:	Prof. Nuno Antonio Fraga Juliano Cota

February 2021

Grazielle Bonaldo Teixeira

5G-NR Radio Planning for Connected and Autonomous Vehicles Services

2021

Acknowledgement

Life is better when you are surrounded by nice people. I would like to thank to my family specially my parents Rosicler and Clovis, for had provided me all the privileges my entire life, which took me where I am now, for had supported me while this long path, and especially during this rough scenario where Brazil (my country) is, and the rest of the world with the pandemic. I would like to thank my friend Jessica and João for so many advices and friendship during years and specially my last months in Portugal and Alexandra for all patience, support, and care with me. A special acknowledgement for Professor António Serrador, for all dedicated time in supervise me while this work, for always being extremely compromised in provide us weekly meetings for discussions and change ideas regarding this thesis, and for being very ethic and professional all the time. My sincere admirations!

Abstract

The 5G network development is enabling many emerge technologies as connected and autonomous vehicles (CAV), promising a significant impact in the telecommunications industry in the future. In this thesis, was performed 5G radio planning by coverage and capacity, entirely when CAV applications are provided, requiring minimum and maximum user data rates according to different services categories from 5GMOBIX project. 5G air interface was explored joint to MIMO and modulation orders configurations, intending to analyse the different results in two diverse highways around Lisbon, for urban and rural propagation environments. Vehicles traffic model was simulated using real statistic numbers, aiming to compute more effective KPIs while the radio planning. The final number of sites calculated were compared regarding to each scenario simulated as well as the number of vehicles supported for each service category. The results showed that the cell ranges reached in DL were tens of kilometres, despite of some meters in UL for some network configurations. Also, the radio resources showed being enough when minimum user data rate is required, nevertheless when maximum user data rate is required, new cell and vehicle ranges recalculation were needed, reaching much higher number of sites due to the cell capacity limitation. The number of sites required in urban environment showed being the double when comparing to rural, due to the higher vehicles traffic.

Keywords: 5G-NR, connected and autonomous vehicles, V2X, radio planning.

Resumo

O desenvolvimento das redes móveis 5G está permitindo o surgimento de muitas outras tecnologias como veículos autónomos e conectados (CAV), prometendo impacto significativo na indústria das telecomunicações no futuro. Nesta tese, foi realizado planeamento rádio 5G por cobertura e capacidade, para aplicações CAV (e.g. *Vehicle platooning, Advanced driving, Extend sensors, Remote driving and Vehicle QoS support*), quando estes exigem mínima e máxima taxa de dados do utilizador de acordo com o projeto 5GMOBIX. Considerando que CAVs podem ter seis níveis de automação, de 0 à 5, de acordo com as tarefas que estes desempenhem, foram considerados veículos de nível 3. As comunicações V2X foram criadas para desenvolver mais segurança e eficiência no tráfego e economia no consumo de energia nas ruas e rodovias. Estas foram padronizadas em comunicações baseadas em WLAN e redes celulares. O primeiro apoia-se no mesmo protocolo do Wi-Fi IEEE 802.11p e o segundo (C-V2X) nos protocolos do 3GPP desenvolvidos para redes móveis como LTE, onde foi primeiramente definido e 5G, que é a base desta tese. A arquitetura 5G apresenta é padronizada pelo 3GPP e apresenta-se em duas formas, Standalone (SA) e Non-Standalone (NSA), onde o segundo apoia-se na estrutura core e radio do 4G mas tirando vantagem da interface rádio do 5G. Esta confuguração, permite que o 5G alcance o alto padrão de qualidade de serviço requisitado pelos estudos de caso que são: *(i) enhanced mobile broadband (eMBB), (ii) ultra-reliable and low-latency communications (URLLC) and (iii) massive machine-type communications (mMTC).* CAV se enquandra no segundo grupo. A interface rádio do 5G, herdou características do 4G e introduziu outras significativas. No 5G, há dois ranges de frequências. FR1 até 7125 MHz e FR2 de 24 à 52 MHz, ambos grupos com diferentes larguras de banda disponíveis. Para esta tese foi utilizado 3.5 GHz de frequência central, e largura de banda de 10 à 100 MHz. Esta banda, é definida pelo 3GPP como sendo TDD, ou seja, é necessário apenas um canal para que transmissor e receptor se comuniquem, e os símbolos OFDM são dispostos no domínio do tempo e configurados como DL, UL ou flexíveis dentro de cada time slot. O método de multiplexação é o mesmo utilizado no 4G, OFDM,

que devido à orthogonalidade das subportadoras, permite que estas não interfiram entre si, e assim possam compartilhar o espectro rádio. Uma das principais características do 5G que difere do 4G, é a introdução das numerologias que referem-se ao espaçamento entre subportadoras. Estas, são diferentes, de acordo com o range de frequência a ser utilizado. Nesta tese, numerologias 0, 1 e 2 são aplicadas, ou seja, 15, 30 e 60 KHz de espaçamento. Considerando o formato de onda OFDM, e que um radioframe tem 10 ms e 14 símbolos, desta forma, é possível calcular o tempo de símbolo e número de *resource blocks* para as diferentes configurações de numerologia, largura de banda, e frequência utilizada, tornando o acesso radio mais flexível e possibilitando a aplicação de diferentes configurações para diferentes serviços. As modulações QPSK, 16QAM, 64QAM e 256QAM foram utilizadas neste trabalho, todas em UL e DL, uma vez que no 5G, são utilizadas diferentes modulações para diferente tipos de mensagens (e.g. dados, controle). MIMO também foi utilizado em matrizes de 2x2, 4x4 e 8x8, alterando o ganho de transmissão de acordo com o aumento do número de layers de antennas.

O modelo desenvolvido para simular o planeamento rádio do 5G pra CAVs, foi baseado nas definições do 3GPP. O planeamento foi realizado em cobertura e capacidade, considerando os ambientes rural e urbano, em duas autoestradas do distrito de Lisboa em Portugal. Foram calculados KPIs relevantes e seus limites foram comparados, explorando todas as configurações aplicadas.

No planeamento pela cobertura, foi utilizado o modelo do 3GPP para cálculo do *PL* de acordo com a distancia ao gNB*,* utilizando a componente aleatória fornecida de acordo com o ambiente de propagação de maneira a atingir valores mais realistas. Estes, resultaram em valores médios de 30 dB de diferença entre LOS e NLOS devido aos valores de desvio padrão definidos, sendo maiores em NLOS devidos às obstruções do sinal. Os valores médios do PL, foram utilizados para calcular a potência do signal recebido RSS, também com sua componente aleatória. Os valores mais baixos encontrados para RSS foram na borda da célula de -95, -113, -94 e -126 dBm em UL, e -71, -89, -70 e -102 dBm em DL, para RMa LOS, RMa NLOS, UMa LOS e UMa NLOS, respectivamente. Posteriormente, os valores de SNR para cada modulação foram definidos, utilizando a simulação de um canal AWGN hipotético que resultou em um gráfico de BER por EB/N0, onde BER foi definido como 1%, e os valores de SNR foram considerados como sendo os de Eb/N0 (i.e. 4, 8, 12 e 16). Estes foram valores de entrada para calcular a sensibilidade dos veículos e do gNB, que apresentaram aumento significativo com a largura de banda e diferença de 1 dB entre as numerologias em ambos ambientes. O PL maximo permitido MAPL, foi calculado considerando 99% de cobertura, onde os maiores valores foram em DL principalmente quando a modulação QPSK e MIMO 8x8 são utilizados. A distância máxima gNB-veículos foi também simulada, apresentando ser menor de acordo com o aumento da largura de banda, atingindo máximo de 23 km em ambiente rural LOS em DL, e mínimo de 72 m em ambiente urbano para NLOS em UL. A distância entre sites foi calculada em todos os cenários, utilizando a máxima distância gNB-veículos resultando em máximo de 40 km e mínima de 12 km para ambiente rural e LOS para DL e UL respectivamente, sendo que 1/3 dessa distância é atingida para largura de banda de 100 MHz. O número final de sites necessários para cobrir a área simulada de 5 km para largura de banda de 100 MHz resultou em 13 à 25 sites em ambiente rural e 20 á 70 sites em ambiente urbano. De acordo com as configurações utilizadas para o planeamento pela cobertura, foi também simulado o número máximo de veículos suportado por célula de acordo com o serviço.

O planeamento pela capacidade, baseou-se na modelagem realista do tráfego na hora de ponta em duas autoestradas de Lisboa, a comparação do tráfego de dados exigido dos veículos com a capacidade da rede e destacados os pontos em que a rede é limitada pela cobertura e pela capacidade, calculando também KPIs relevantes para a análise. O resultado da modelagem de tráfego encontrou 23 veículos por km em ambiente urbano e 9 veículos por km em ambiente rural. Sabendo a taxa de dados por serviço do projecto 5GMOBIX, e aplicando percentagem à esses serviços de acordo com uma presumida penetração, atingiu-se taxa de dados total mínima e máxima requerida por km de autoestrada de acordo com o ambiente de propagação, resultando para ambiente urbano mínimo de 108 Mbps e máxima de 2.82 Gbps. E para ambiente rural mínima de 42 Mbps e máxima de 1.1 Gbps. Simulando a capacidade da rede esta mostrou-se ser maior consoante maior a largura de banda principalmente com a utilização da

modulação de 256QAM. Posteriormente, a carga de tráfego foi simulada de acordo com a taxa de dados total mínima e máxima requerida por km de autoestrada multiplicada pela máxima distância gNB-veículos calculada durante o planeamento pela cobertura. A carga de tráfego apresentou-se ser maior quanto maior o raio de célula ou distância em UL, porém para ambiente rural LOS DL este apresentou-se ter menor carga de tráfego do que ambiente urbano LOS DL devido ao menor número de veículos. Racio de célula foi aplicado comparando a carga de tráfego com a capacidade da rede, com o intuito de indicar os pontos em que o planeamento é limitado pela cobertura ou pela capacidade e assim recalcular a máxima distância gNB-veículos. Assim, novo número de sites foi simulado após análise das limitações das células, onde resultados mostram que para 100 MHz de largura de banda e mínima taxa de dados exigida, a rede apresenta-se ser apenas limitada pela cobertura e ter condições de prover recursos rádio para todos os veículos, mas quando máxima taxa de dados é exigida quase todos os cenário são limitados pela capacidade devido às longas distâncias, principalmente em DL e para modulações mais baixas. Apenas MIMO 4x4 256QAM e MIMO 8x8 64QAM e 256QAM são limitados pela cobertura.

Palavras-chave: 5G-NR, veículos autónomos e conectados, V2X, planeamento rádio.

Table of contents

List of Figures

List of Tables

List of Acronyms

3GPP	3rd Generation Partnership Project
5GAA	5G Automotive Association
5G-NR	Fifth Generation New Radio
5G-PPP	5G Infrastructure Public Private Partnership
5GS	5G System
ADS	Automated Driving System
AI	Artificial Intelligence
AWGN	Average White Gaussian Noise
BER	Bit Error Rate
BS	Base Station
BSS	Basic Service Set
CAM	Cooperative Awareness Message
CAV	Connected and Autonomous Vehicles
CCAM	Cooperative, Connected and Autonomous Mobility
C-ITS	Cooperative ITS
COTS	Commercial Off-The-Shelf
CP	Cyclic Prefix
CSMA/CA	Carrier Sensing Multiple Access with Collision Avoidance
C-V2X	Cellular-V2X
DCC	Decentralized Congestion Control
DFT-s-OFDM	OFDM with Discrete Fourier Transform precoding
DL	Downlink
DSRC	Dedicated Short-Range Communication
eMBB	Enhanced Mobile Broadband
eNB	LTE (4G) base station
EN-DC	E-UTRAN-NR Dual Connectivity
en-gNB	E-UTRAN NR base station
EPC	Evolved Packet Network
ETSI	European Telecommunications Standards Institute

EU	European Union
E-UTRAN	Evolved Universal Terrestrial Access Network
EVM	Error Vector Magnitude
FDD	Frequency Division Duplex
FR1	Frequency Range 1
FR2	Frequency Range 2
GB	Guard Band
GP	Guard Period
HD	High Definition
IEEE	Institute of Electrical and Electronics Engineers
IoT	Internet of Things
ISD	Inter-Site Distance
ISI	Inter Symbol Interference
ITS	Intelligent Transportation System
KPI	Key Performance Indicators
LOS	Line of Sight
LTE	Long-Term Evolution
MAC	Medium Access Control
MAPL	Maximum Allowed PL
MCS	Modulation and Coding Scheme
MIMO	Multiple-Input Multiple-Output
mMTC	Massive Machine-Type Communications
mm Wave	Millimetre Wave
MNO	Mobile Network Operator
MU- MIMO	Multiple Users MIMO
MVNO	Mobile Virtual Network Operators
NF	Network Functions
NFV	Network Function Virtualization
NG-RAN	New Generation RAN
NLOS	Non-Line of Sight
NR	New Radio
NSA	Non-Standalone

NYU	New York University
OCB	Outside the Context of a Basic service set
OFDM	Orthogonal Frequency Division Multiplexing
PAPR	Peak-to-Average Power Ratio
PATH	Partners for Advanced Transportation and Technology
PBCH	Physical Broadcast Channel
PDCCH	Physical Downlink Control Channel
PHY	Physical
PL	Path loss
QAM	Quadrature Amplitude Modulation
QoS	Quality of Service
R&D	Research and Development
RAN	Radio Access Network
RAT	Radio Access Technology
RB	Resource Blocks
RE	Resource Element
RF	Radio Frequency
RMa	Rural Macro cell
RSS	Received Signal Strength
RSU	Roadside Units
SA	Standalone
SAE	Society of Automotive Engineers
SC-FDMA	Single Carrier Frequency Division Multiplexing Access
SCI	SL Control Information
SCS	Subcarriers Space
SDN	Software Defined Networking
SFI	Slot Format Indicator
SINR	Signal-to-Interference Noise Ratio
SL	Side Link
SN	Secondary Node
SNR	Signal-to-Noise Ratio
TB	Transport Blocks

TDD	Time Division Duplex
UE	User Equipment
UL	Uplink
UMa	Urban Macro cell
URLLC	Ultra-Reliable and Low-Latency Communications
USA	United States of America
UT	User Terminal
V2I	Vehicle-to-Infrastructure
V2N	Vehicle-to-Network
V2P	Vehicle-to-Pedestrian
V2V	Vehicle-to-Vehicle
V2X	Vehicle to Everything
WLAN	Wireless Local Area Network

List of Symbols

$\alpha^{(j)}$	Normalized scaling factor for TDD mode.
σ	Standard deviation.
μ	Numerology.
$v_{Layers}^{(j)}$	It is the maximum number of supported layers in UL and DL for MIMO configurations.
X	Shadowing.
BW	Bandwidth [MHz].
c	Propagation speed in free space.
CR	Cell-ratio.
d_{3D}	Distance between UT and BS on the air.
d_{2D}	Distance between UT and BS on the floor.
d_{BP}	Break point distance. Refers to the distance where the first Fresnel ellipsoid touches the floor.
d'_{BP}	Break point distance for UMa LOS.
D_{rate}	Maximum supported UE data rate [Mbps].
h_{UT}	User Terminal height.
h'_{UT}	Effective UT antennas heights.
f	Central frequency [Hz].
f_c	Central frequency [GHz].
$f^{(j)}$	Scaling factor.
G_{TX}	Transmitted gain [dB].
G_{RX}	Receiver gain [dB].
G_d	Diversity gain [dB].
h_{BS}	Base Station height.
h_{UT}	User Terminal height.
H	Average building height.
h'_{BS}	Effective BS antennas heights.
h_E	Effective environment height.
I_m	Interference margin [dB].
J	It is the number of aggregated component carriers in a band or band combination.
L_{feed}	Cable losses [dB].
LNF_{margin}	Log-normal fading margin.
N_{symbol}^{slot}	Number of OFDM symbols per slot.
$N_{\mathrm{sc}}^{\mathrm{RB}}$	Number of subcarriers per resource block.
$N_{RB}^{BW(j),\mu}$	Number of resource blocks.

NF	Noise Figure [dB].
$N_{s/5km}^{c}$	Number of sites for the entire stretch by coverage.
$N_{cells/km}^{c}$	Number of cells per kilometre by coverage.
$N_{v/cell}^{c}$	Number of vehicles per cell by coverage.
$N_{v/km}$	Number of vehicles per kilometre.
N_{v}^{s}	Number of vehicles per service supported by the network.
$OH^{(j)}$	Overhead.
$PL(d_{2D})$	Average path loss [dB].
P_{RX}	Received power [dBm].
P_{TX}	Transmitted power [dBm].
$Q_{m}^{(j)}$	It is the maximum supported modulation order in UL and DL.
RF_{margin}	Rayleigh fading margin.
RL	Road length that is being simulated.
R_{max}	Maximum coding rate.
S	Sensitivity.
SNR	Signal to noise ratio [dB].
SCS	Subcarrier Space [kHz].
T_{s}^{μ}	OFDM symbol duration.
T_{CP}	CP duration.
TL_{cell}	Traffic load per cell per kilometre.
TU	Total user data rate per km.
U_{v}^{s}	Minimum and maximum user data rate per vehicle, per service.
W	Average street width.

1. Introduction

1.1. Motivation

The telecommunications networks are under constant development. Lately, with fifth generation new radio (5G-NR) technology being deployed around the world many other emerge technologies are being studied to be deployed massively thanks to 5G, as internet of things (IoT), smart cities, virtual reality, augmented reality, and connected and autonomous vehicles (CAV). Currently, services of wi-fi mobile broadband for vehicles are already provided by mobile network operators (MNO), and autonomous vehicles sales have been increasing each year. According to [1], market predictions indicate that 20% of all vehicles sold by 2020 in Europe will have a certain level of automation and [2] affirm that 100% of the new passengers' cars will be connected by 2025, significantly impacting the telecommunications networks. Also, with the CAV's development, new types of services will show up to guarantee the vehicles to everything (V2X) pillars that are: road safety, traffic and resources efficiency and energy savings, and thus more data and reliability will be required from networks infrastructures. It is expected that with the intelligent transportation system (ITS) roll out, other sides will get affected or will need to undergo some development to follow the penetration of CAV in society. According to [3], one in each five miles travelled in UK could be automated by 2030, and roads around the world will need to pass through changes for CAV be deployed massively. The consequence is the amount of data and extreme low latency that will be required from all the vehicles, at the same time, to perform different types of tasks, with high variation of user data rates, demanding more than ever the flexibility from 5G-NR air interface to manage them and provide the best quality of service (QoS) as possible. According to [4], cars manufacturers will be required to continuously increase bandwidths (BW) for both point-to-point data pipes and distributed network structures to meet new data demands, and the highest automated cars' level will send 25 gigabytes of data to the cloud every hour. Figure 1.1 presents some examples of CAV service data rates.

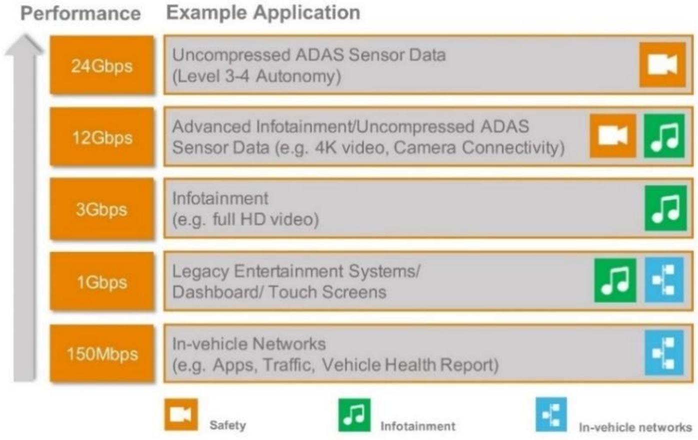

Figure 1.1 – Example of CAV service data rates (extracted from [4]).

1.2. Objectives

As explained on the previous section, the market forecast foresees that CAV will increase in the incoming years, followed by its required service data rates. Currently, the MNO are beginning to make this service available around the world, where user data rates for common mobile applications are much lower than for CAV usages, as can be seen on Figure 1.1. The goal of this thesis is study the user data rate of CAV services considered on 5G-MOBIX project from Horizon 2020 program of European Commission, and perform radio planning by coverage and capacity, aiming to calculate relevant key performance indicators (KPI) as the final number of sites necessary to provide enough radio resources for all vehicles in a highway in diverse propagations environments, and network configurations, comparing the results for when these vehicles require minimum and maximum user data rates for each service.

1.3. Document structure

The structure of this document is presented as five chapters, followed by references and annexes. The first and current chapter provide the introduction to the problem that aim to be solved, motivations and objectives. The second chapter presents the subject state of the start and presents the technology and its applications. The third chapter present the model which involve parameters and definitions. In the fourth chapter results analysis regarding the simulations are performed. In chapter five final conclusions are presented.

1.4. Published articles

While the development of this thesis, were performed, submitted, and accepted total of three scientific essays, which are listed below.

- Serrador A., Teixeira G., Lima M., Fernandes R., “Autonomous Vehicles Impact on 5G Network Base Station Inter-Site Distance”. European Conference on Networks and Communications (EUCNC), Dubrovnik, Croatia, June 2020. (Presented)
- Serrador A., Teixeira G., Lima M., Fernandes R., “Autonomous Vehicles Impact on 5G Network Inter-Site Distance”. Virtual ITS European Congress, November 2020. (Presented)
- Teixeira G., Serrador A., “5G NR Performance and Implementation in highway scenarios”. 9º Congresso Luso-Moçambicano de Engenharia, Maputo, Moçambique, August 2021. (Accepted).

2. State-of-the-art

2.1. 5G and autonomous vehicles worldwide

As an important part of the ITS, the CAV are becoming one of the most powerful business units around the world, and naturally plenty pilots and projects have been deployed or are just kicking off. Over the past five years, almost 1 billion euros were invested by European Commission in 5G-related projects, where 6% of them faces Cooperative, Connected and Autonomous Mobility (CCAM), as presented on Figure 2.1, [5]. The 5G Infrastructure Public Private Partnership (5G-PPP) phase three, part two, launched in 2018 three projects focused on testing and implementing 5G for CCAM on different use cases, applied on cross-border corridors: i) 5GCROCO, ii) 5GCARMEN, iii) 5GMOBIX, summing more than 49 million euros.

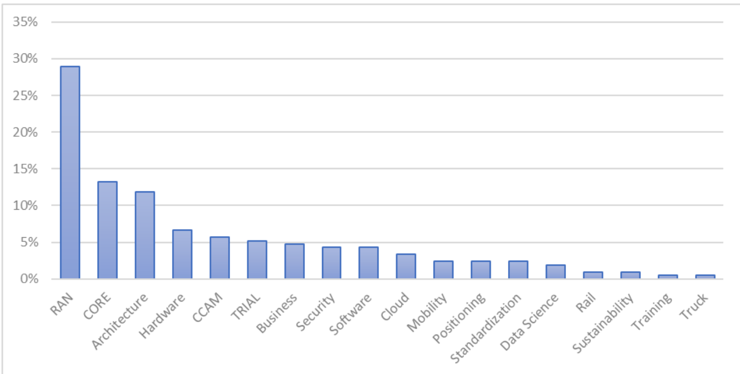

Figure 2.1 – 5G related projects funded by European Commission from 2015 to 2019.

Along several research ongoing projects, many technologies for CCAM were identified and will be deployed, tested and validated in Europe. 5GCROCO, besides identifying business opportunities and models on the application of these technologies, aims validate three CCAM scenarios: Tele-operated driving, High definition (HD) map generation and distribution for automated vehicles and Anticipated Cooperative Collision Avoidance. The main services that will be tested are: 5G features as new radio, MEC-enabled distributed computing, predictive QoS, network slicing, and improved positioning systems. The 5GCARMEN project is deploying four scenarios: cooperative manoeuvring, situation awareness, green driving, and infotainment, for level three and four of automation, aiming to provide a platform to support different kind of services from different Mobile (Virtual) Network Operators (M(V)NOs). Besides, it will also support short- and long-range communications, in other words, a combination of cellular and meshed networks and back-end solutions into the same platform, [6]. Regarding the 5GMOBIX project, it will apply CCAM test beds on cross-border corridors and in urban trial sites, aiming to identify business opportunities and contribute for standardizations and spectrum allocation. The use cases are classified into five categories: Advanced Driving, Platooning, Extended Sensors, Remote Driving and Vehicle quality of Service Support [7].

In China are expected 428 million 5G connections by 2025, but despite the numbers China faces a slow roll-out with 5G, comparing with the aggressive data rate high-demand on 4G [8]. However, China will construct 12 pilot small-scale cities to test use-cases in many vertical markets as autonomous vehicles, and it has been pushing hard to win the 5G race. The country hosts the biggest car manufactures in the world, and this is one of the main reasons why the promises to develop the 5G for autonomous vehicles stands for. All main MNOs such as China Mobile, China Telecom and China Unicom are being part of big projects to launch a mature technology from 2020 as China Mobile’s 5G Joint Innovation Centre and Baidu’s Apollo open-source software platform for autonomous driving. Also, private companies as Tencent with Smart transportation applying artificial intelligence, HD maps, simulation platforms, social network, mobile payments, network security, and other avenues, [9].

In South Korea, the Yonsei University and Korea Telecom are partners of Europe in the Primo-5G project to develop an end-to-end 5G video streaming system, millimeter wave (mm Wave) access, core network and artificial intelligence (AI)-assisted communications. Is also in South Korea where is the K-City, the 320 000 square meter city created to test autonomous vehicles and smart cities applications, was built and funded by Ministry of Land, Infrastructure and transport. Many other projects are getting more mature involving private big companies, MNOs and Original Equipment Manufacturers.

In United States of America (USA), there are many industrial and research and development (R&D) poles focused in 5G for autonomous vehicles. It is possible to highlight some of them as Society of Automotive Engineers (SAE), that had standardized the level of vehicles automation, now reference for 3rd Generation Partnership Project (3GPP) standardization body in Europe. USA Department of Transportation, Partners for Advanced Transportation and Technology (PATH) at University of California, Wireless Networking & Communications Group at University of Texas, NYU Wireless Industrial Affiliates Program at New York University.

2.2. Driving automation levels

One of the first steps done by the standardization bodies was to define the driving automation levels, once it affects network performance requirements and it will mean different approaches while the development. Driving automation levels were defined by SAE, which is a global professional organization that has been fostering worldwide collaboration to advance transportation technology since 1905 [10], to help the automotive industry on the development of different features and increase its capacity. And was considered by 3GPP TS 22.186, Release 16, “Enhancement of 3GPP support for V2X scenarios”, Stage 1 [11]. The levels are from 0 to 5, where the first 3 categories (0-2), refers to tasks when the human driver needs to make part of the driving procedures. And the other 3 categories (3-5), the human driver does not need to take control of the vehicle, leaving the automated driving system (ADS) carry out of all the tasks in reliable mode.

2.3. Vehicular communications

Road safety, traffic efficiency and energy savings are the biggest reasons why wireless vehicular communications have been getting more attention lately. When vehicles share information about themselves and around it, it is easier to prevent any accident or other event, beside to allow the system to make smarter decisions. The term V2X communications is used to refer generically to methods for passing information flows in different applications of ITS related to traffic safety and efficiency, automated driving, and infotainment [12]. V2X Service is further divided into Vehicle-to-Vehicle (V2V) Service, Vehicle-to-Pedestrian (V2P) Service, Vehicle-to-Infrastructure (V2I) Service, and Vehicle-to-Network (V2N) Service [7]. The standarization of V2X communication using wireless technologies, evolved and divided into Wireless Local Area Network (WLAN)-based and cellular-based, resulting in different families of standards. Here are the most relevant examples, Dedicated Short-Range Communication (DSRC) was defined in USA by Institute of Electrical and Electronics Engineers (IEEE). Cooperative ITS (C-ITS/ITS-G5) by European Telecommunications Standards Institute (ETSI) and Cellular-V2X (C-V2X) by 3GPP, both in Europe. DSRC and C-ITS are based on IEEE 802.11p (i.e. WLAN-based) access layer developed for vehicular networks [3], which is a short-range technology for V2V communications. And 3GPP's C-V2X (i.e. cellular-based) specifications, include short-range V2V communications, as well as wide-area V2N communication, that allows vehicles to communicate with the base station (BS) [6]. The following sections are presented their main characteristics.

2.3.1. IEEE 802.11p

Used as a basis for DSRC and C-ITS, the IEEE 802.11p protocol is an evolution of IEEE 802.11a standard with some amendments on Medium Access Control (MAC) and Physical (PHY) layers to address the vehicular environment, allocated on 5.9 GHz spectrum. Regarding to the PHY layer, it uses Orthogonal Frequency Division Multiplexing (OFDM) combined with a convolutional code [13] and 10 MHz channels instead of the 20 MHz channels used in IEEE 802.11a to address the increased root-mean-squared delay spread in the vehicular environment [12], resulting in a data rate up to 27 Mbps. Also, more rigorous receiver performance requirements in adjacent channel rejections and new spectrum masks are introduced to deal with cross-channel interference [12]. On the MAC layer, there is no need to establish a basic service set (BSS), once it is based on the Outside the Context of a Basic Service Set (OCB) operation mode which is well suited for rapid broadcast of short messages and a high level of mobility [12]. Furthermore, it is used carrier sensing multiple access with collision avoidance (CSMA/CA) that allows a fully distributed and uncoordinated access to the wireless channel, with no need for a resource allocation procedure. On the other hand, however, it implies in a resource waste due to frequent collisions as the channel use increases and arises concerns about its reliability under heavy traffic conditions [14]. With an increasing number of transmitters, in fact, the channel access latency and the probability of data packet collision increase being solved partially by Decentralized Congestion Control (DCC) reducing the transmission rate of Cooperative Awareness Message (CAM) [12].

2.3.2. 3GPP C-V2X

The first 3GPP C-V2X definition was included in the Release 14 of the long-term evolution (LTE) standard in 2016. As explained before, C-V2X involves such short-range as long-range communication, where the architecture is based on LTE-Uu, reference for V2X-enabled User Equipment (UE) and Evolved Universal Terrestrial Access Network (E-UTRAN), and PC5 reference for V2X-enabled UE for V2V, V2I, and V2P Services, independently for transmission and reception [15]. The LTE-Uu based architecture is called mode 3, where the V2V communication occur by the cellular management, providing the subchannels for each V2V transmission. And the PC5 based architecture is the mode 4, that doesn’t require the cellular network iteration, and autonomously choose the subchannel or radio resources for its V2V transmission [16]. On the PHY layer C-V2X is based on Single Carrier Frequency Division Multiplexing Access (SC-FDMA) and supports 10 or 20 MHz channels, where each channel is divided into sub-frames, Resource Blocks (RBs), and sub-channels [17]. Following the LTE structure, the channel is divided in 1ms sub-frames and RBs with 180 kHz each. Depending on the packet size, the number of RB in each sub-channel can vary according to the Modulation and Coding Scheme (MCS) [16].

Compared to IEEE 802.11p, C-V2X provides more flexibility in terms of configuration: occupied BW, modulation and coding scheme can be selected at physical layer (PHY) as well as set of parameters at medium access control (MAC) layer. This allows to adapt transmission according to the surrounding conditions e.g., adapting the transmission to available resources, or to the congestion level [17]. Regarding the comparison between the two technologies, an important study made by 5G Automotive Association (5GAA) shows that LTE-V2X (PC5) outperforms 802.11p in reducing fatalities and serious injuries on the EU’s roads. This is due to a combination of the superior performance of LTE-V2X (PC5) at the radio link level for ad hoc/direct communications between road users, and the market led conditions which better favour the deployment of LTE-V2X in vehicles and in smartphones and include a clear evolutionary path towards 5G-V2X [18].

2.4. 5G Network

Defined by 3GPP in TR 21.915 (Release 15), the fifth generation of mobile communication also called 5G System (5GS) [19], has been promising important changes on the digital world's transformation, as well as ambitious services and use cases as (i) enhanced mobile broadband (eMBB), (ii) ultra-reliable and low-latency communications (URLLC) and (iii) massive machine-type communications (mMTC) [10]. To achieve these high-level goals, 5GS intend to create an entire and flexible interface to join the several kinds of verticals (e.g., eHealth, energy, automotive, manufacturing, etc.), where each one has its own requirement defined by 5GPP.

According to [19], 5GS involves two types of architecture, Non-Standalone (NSA), where 5GMOBIX project is focused, and Standalone (SA). NSA layout involves 5G radio access network (RAN) and its new radio (NR) interface connected to already existing LTE infrastructure, such as radio access E-UTRAN and core network called Evolved Packet Network (EPC). It supports only LTE services but taking advantages of NR capacities (e.g., low latency, etc). SA architecture is based on the connection of 5G core network (5GC) and new generation RAN (NG-RAN) without need any part of LTE.

Due to the challenge of make all hardware working together and optimizing KPIs, some new technologies are also developed in the core network. NFV is the concept of transferring NFs from dedicated hardware appliances to software-based applications running on commercial off-the-shelf (COTS) equipment [21]. The basic principles of SDN are separation of control and data planes (also called infrastructure layer or user planes), logical centralization of network intelligence and abstraction of physical networks from the applications and services by standardized interfaces [20]. This means that the control messages will have a different path from data messages. While control messages pass through control plane, the data messages pass through user plane. With the management from

SDN framework, 5G-enabled vehicular network can make the best of the idle resource in data centres and achieve complex but efficient network management functionalities [22].

Another important feature on core level, is the logical network slicing. In the pass, the MNOs could point manually the types of services provided to the users (i.e., voice, mobile broadcast, SMS). Lately, with the increasing of verticals requirements, it became necessary to provide a set of services facing each vertical reality. According to [23], network slicing considers the ability to create end-to-end slices on the same infrastructure for heterogeneous services. Therefore, each slice will be comprised with the modules of the core network and each module will have the necessary functions to implement the vertical requirements. So, the internal functions of the modules in each slice, can be modified [24]. As one of the verticals, V2X scenarios faces many kinds of use cases and situations that needs to be considered, (i.e., lane merge, overtaking, HD streaming, safety, etc) and each one has different service requirements, which can take considerable advantages from network slicing. Table 2.1 presents some categories defined in [25] and proposed by [26] for slices of V2X that could be implemented, as well as its requirements.

Table 2.1 - V2X categories and main requirements (adapted from [29]).

V2X category	Communication type	RAT settings	Latency [ms]	Data rate
Safety and traffic efficiency	V2V, V2P	-	100	Not a concern
Autonomous driving	V2V, V2N, V2I	4G/5G NR	1	10 Mbps (DL/UL)
Tele-operated driving	V2N	4G/5G NR, 802.11 OCB	20 (end-to-end)	25 Mbps for video and sensors data (UL) 1 Mbps for application-related control and command (DL)
Vehicular Internet V2N and infotainment	V2N	4G/5G NR, 802.11 OCB	100 (for web browsing)	0.5 Mbps (web browsing) Up to 15 Mbps for UHD video streaming
Remote diagnostics and management	V2I, V2N	4G/5G NR, 802.11 OCB	Not a concern	Not a concern

2.4.1. 5G Air interface

Considering that this thesis will study the network's behaviour regarding the air interface, is very important to highlight some concepts. 5G air interface inherits many features from the legacy technology (4G) and was standardized in [27] and [28]. The studies regarding the application of 5G on V2X services were standardized in [29] and [30] that are still under development.

According to [19], the NR spectrum is divided in frequency range 1 (FR1) and frequency range 2 (FR2), where FR1 goes from 410 MHz to 7125 MHz, and FR2 goes from 24 250 GHz to 52 600 GHz, and for both ranges were defined a set of channel BWs, as shown on Table 2.2. The goal of wide spectrum is to embrace numerous use cases that 5G aims to cover. 5G pioneer bands identified at EU level are 700 MHz, 3.6 GHz (3.4-3.8 GHz) and 26 GHz (24.25-27.5 GHz) frequencies, [6], where 20.1% opted for the second one. Therefore, this thesis will consider studying and analysis only FR1 and its supported channel BWs. According to [31], the bands referred as n41, n77, n78 and n79 (i.e., 2496-2690, 3300-4200, 3300-3800 and 4400-5000 MHz) could be good choices once they enable the use of the highest channel BWs and consequently fits better for this study. But, considering that EU is focused on n78 band (3 300-3 800 MHz), this will be the approach of this thesis.

Table 2.2 - Frequency range and channel BW for NR architecture (extracted from [19]).

Frequency range	Frequency range [MHz]	Supported channel bandwidth [MHz]
FR1	410 – 7125	5, 10, 15, 20, 25, 30, 40, 50, 60, 80, 90, 100
FR2	24250 – 52600	50, 100, 200, 400

Like 4G, 5G-NR uses scalable OFDM with Cyclic Prefix (CP) (CP-OFDM) as the DL waveform, once that, enable many subcarriers share the spectrum without interfere each other thanks to their orthogonality in the frequency domain, and thanks to the cyclic prefix between symbols in the time domain. In contrast to 4G, OFDM can also be used in the NR UL direction. As a complement waveform with lower peak-to-average power ratio (PAPR), that indicates if an alternate signal presents high peaks according to its average, to improve UL coverage, OFDM with

Discrete Fourier Transform precoding (DFT-s-OFDM) can be used in the uplink although limited to single-layer transmission only [19].

To support different services and being more flexible, 5G-NR frame structure introduced the term “numerology” and for FR1, the SCS into the OFDM spectrum, can be 15, 30 and 60 kHz [31]. Thus, in the same BW, it is possible to have different subcarriers frequencies for different services. The different numerologies are referred as (µ) and the SCS’ are multiple of 15 kHz, as shown on Table 2.3.

Table 2.3 - Numerologies for OFDM spectrum (adapted from [32]).

µ	SCS [kHz]	T_s^{μ} [µs]	Type CP	T_{CP}[µs]	Total time slot [µs]
0	15	66.66	Normal	5.21/4.69	1000
1	30	33.33	Normal	2.60/2.34	500
2	60	16.66	Normal	1.30/1.17	250
			Extended	4.16	250

For the transmission based on OFDM, the frame’s structure is shown on Figure 2.2. Each frame has 10 ms, and a set of 10 subframes with 1 ms each. Depending on the numerology, the subframes are split in 1 or more slots, as shown in Table 2.4. Each slot conveys a different number of OFDM symbols ($N_{\text{symb}}^{\text{slot}}$) depending on the CP configuration [32]. For normal CP overhead (OH), are transmitted 14 symbols, and 12 symbols when the CP OH is extended (used by cells with high delay spread and need to reach low latency). On Table 2.3, T_s^{μ} represents the symbol duration and T_{CP} the CP duration, highlighting that the first CP is bigger. So, for µ=0, only one slot is allocated into one subframe of 1 ms, which this slot has 14 symbols. For this example, the entire time slot is the sum of the first CP OH period which is 5.21 µs, and the others (for the 13 slots) are 4.69 µs, plus the 14 symbols of 66.66 µs each, totalizing 1ms or 1000 µs, as shown on Table 2.4.

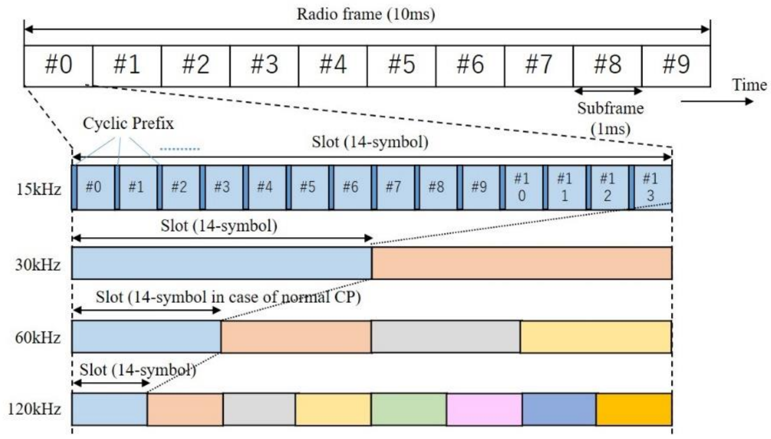

Figure 2.2 – 5G-NR Frame structure (extracted from [19]).

Table 2.4 - Number of OFDM symbols and slots for normal and extended cyclic prefix (adapted from [27]).

μ	Type CP	$N_{\text{symb}}^{\text{slot}}$	$N_{\text{slot}}^{\text{frame},\mu}$	$N_{\text{slot}}^{\text{subframe},\mu}$
0	Normal	14	10	1
1	Normal	14	20	2
2	Normal	14	40	4
	Extended	12	40	4

According to [27], for each numerology and carrier, a resource grid, is defined. There is one set of resource grids per transmission direction (UL, DL, or side link (SL)). Each element in the resource grid for antenna port and SCS configuration μ is called a resource element, that fit a subcarrier in frequency domain and an OFDM symbol in time domain. And a set of 12 consecutive subcarriers ($N_{\text{sc}}^{\text{RB}} = 12$) is called resource block (RB) in the frequency domain. RBs are the smallest amount of data that is transmitted, and it changes according to the numerology, for example, for SCS=15kHz, one RB is 15kHz*12=180kHz, SCS=30kHz, one RB is 360 kHz and for SCS=60kHz, one RB is 720 kHz. Thus, for each numerology and channel BW is defined a different number of RB ($N_{RB}^{BW(j),\mu}$) following the Equation 2-1, according to the percentages of spectrum utilization, defined in [33], meaning that the number of RB available on 5G-NR are the same for UL and DL.

$$N_{RB}^{BW(j),\mu} = \frac{BW_{[MHz]}}{SCS_{[kHz]} * N_{\text{sc}}^{\text{RB}}} * [\%] \qquad \text{Equation 2-1}$$

$N_{RB}^{BW(j),\mu}$ → Number of resource blocks attributed for each BW and numerology.

$BW_{[MHz]}$ → Bandwidth available for each numerology [MHz].

$SCS_{[kHz]}$ → Subcarriers spacing [kHz].

N_{sc}^{RB} → Number of subcarriers per resource block.

Table 2.5 - Maximum transmission bandwidth configuration (adapted from [31]).

	Bandwidth [MHz]										
SCS [kHz]	**10**	**15**	**20**	**25**	**30**	**40**	**50**	**60**	**80**	**90**	**100**
15	52	79	106	133	160	216	270	N/A	N/A	N/A	N/A
30	24	38	51	65	78	106	133	162	217	245	273
60	11	18	24	31	38	51	65	79	107	121	135

Table 2.6 - Minimum guard band for each UE channel bandwidth and SCS (adapted from [31]).

	Bandwidth [MHz]										
SCS [kHz]	**10**	**15**	**20**	**25**	**30**	**40**	**50**	**60**	**80**	**90**	**100**
15	312.5	382.5	452.5	522.5	592.5	552.5	692.5	N/A	N/A	N/A	N/A
30	665	645	805	785	945	905	1045	825	925	885	845
60	1010	990	1330	1310	1290	1610	1570	1530	1450	1410	1370

Using $N_{RB}^{BW(j),\mu}$ from $N RB BW(j),\mu$ → Number of resource blocks attributed for each BW and numerology.

$BW_{[MHz]}$ → Bandwidth available for each numerology [MHz].

$SCS_{[kHz]}$ → Subcarriers spacing [kHz].

N_{sc}^{RB} → Number of subcarriers per resource block.

Table 2.5, is possible to understand Table 2.6, where is presented the minimum guard band (GB) that needs to be considered for each UE channel BW and SCS. In an OFDM transmission, is important to take into consideration a reasonable GB to mitigate the inter symbol interference (ISI), regarding the multipath delay spread. In case of multiple numerologies are multiplexed in the same symbol, as presented on Figure 2.3, the minimum GB on each side of the carrier is the GB applied at the configured channel BW for the numerology that is received immediately adjacent to the guard. If multiple numerologies are multiplexed in the same symbol and the UE channel BW is >50 MHz, the minimum GB applied adjacent to 15 kHz SCS shall be the same as the minimum GB defined for 30 kHz SCS for the same UE channel BW [31]. It means that the GB can be asymmetric and is calculated following the Equation 2-2.

$$GB = \frac{BW_{[MHz]} * 1000\ (kHz) - N_{RB}^{BW(j),\mu} * SCS_{[kHz]} * N_{sc}^{RB}}{2} - \frac{SCS_{[kHz]}}{2} \quad \text{Equation 2-2}$$

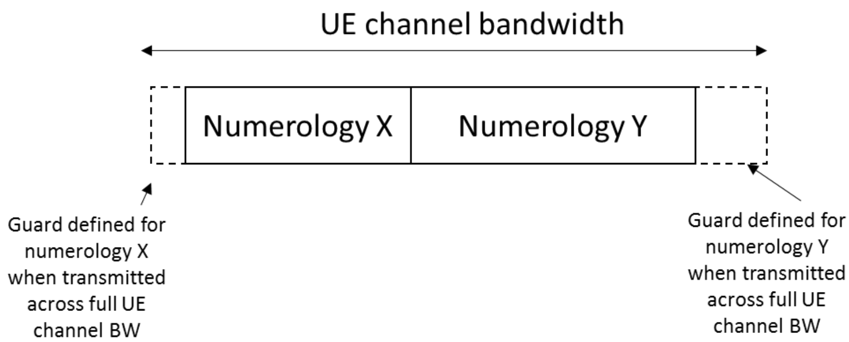

Figure 2.3 - Guard band definition when transmitting multiple numerologies.

Duplex modes

5G-NR supports both frequency division duplex (FDD) and time division duplex (TDD) operation with the same frame structure. In the case of TDD, and as to allow for flexible traffic adaptation, each OFDM symbol in a slot can be classified as ‘downlink’, ‘uplink’ or ‘flexible’ (i.e., either downlink or uplink). This can be configured semi-statically or it can change dynamically as part of the scheduling decision [19]. TDD is also the duplex mode used by n78 band, which is going to be the focus of this study.

Supported modulation schemes

Sub-channels are used to transmit data and control information. The data is transmitted in Transport Blocks (TBs) and the control information (i.e., modulation coding scheme (MCS), RBs, resource reservation interval) in SL Control Information (SCI) messages [17]. To transmit the data over the air interface is necessary modulate the radio frequency signals. Regarding the modulation, QPSK, 16QAM, 64QAM and 256QAM schemes are supported for UL and DL, excluding π/2-BPSK in UL, that was not considered for NR V2X, as presented on Table 2.7, and defined in [27] and [31]. The limit values for the average error vector magnitude (EVM) level, refer to the NR frequency band that will be used for NR V2X. According to the modulation scheme, the number of bits per symbol and number of symbols can change, variating latency, data rate, bit error rate (BER) and EVM. This parameter will be important to reach the good quality of service of the network in the software simulation.

Table 2.7 - Supported modulation schemes (adapted from [27] and [31]).

Transmission	Modulation scheme	Modulation order ($Q_m^{(j)}$)	Average EVM Level [%]
UL/DL	QPSK	2	17.5
UL/DL	16QAM	4	12.5
UL/DL	64QAM	6	8
UL/DL	256QAM	8	3.5

Massive Multiple Input Multiple Output factor

Another important feature in radio planning for autonomous vehicles is multiple-input multiple-output (MIMO), introduced by LTE on release 8 and evolved to massive MIMO on release 14. It refers to the utilization of many antennas to multiplex messages for several users on the same time-frequency resource (referred to as spatial multiplexing), and/or to focus the radiated signal toward the intended receivers and inherently minimize intra-cell and inter-cell interference [20], aiming to boost mainly the cell capacity and coverage. On 5G-NR, MIMO is defined in [19], and it supports multi-layers data transmission for a single UE, being the maximum of eight in DL and four in UL. For multiple UEs, it supports twelve layers in DL and UL. To explain what these layers are, is going to be used the reference [34], from a commercial mobile network operator, that says layers are data streams, from one transmitting array to a single user, or simultaneously sends different layers in separate beams to different/multiple users (MU-MIMO), increasing the throughput for the user and the network capacity. Once, for example, if the MIMO is 2x2, thus the number of streams will be 2. This could be an important advantage when computing the link budget on highways, in V2X scenarios, once there will have different services, requiring different features from the network. To achieve the increase in capacity for MU-MIMO depends on the signal-to-interference noise ratio (SINR) on each layer, that will be impacted also by the number of vehicles. That is why, the number of layers is fixed and determined.

2.5. 5G-NR V2X Services requirements

Vehicular environments present to be very complex, once several types of situations are susceptible to happen in a short period of time, requiring more reliable infrastructure to provide highest level of safety on the roads. In this matter, 3GPP defined a set of network requirements to support V2X applications presented by [11]. Each V2X application has a specific requirement, being studied many use cases to extract the target KPIs, which are presented by [25]. The use cases categories of 5G-MOBIX project, were defined based on last 3GPP definitions, making that all its use cases stories and consequently its use cases scenarios fall into one of the categories. The categories explanation is according to [30], and their expected user data rates are presented by Table 2.8, according to 5G-MOBIX deliverable 2.5 in [35], considering the minimum and maximum data rates for UL and DL along all the stories.

- **Vehicles Platooning** enables the vehicles to dynamically form a group travelling together. All the vehicles in the platoon receive periodic data from the leading vehicle, to carry on platoon operations. This information allows the distance between vehicles to become extremely small, i.e., the gap distance translated to time can be very low (sub second). Platooning applications may allow the vehicles following to be autonomously driven.

- **Advanced Driving** enables semi-automated or fully automated driving. Longer inter-vehicle distance is assumed. Each vehicle and/or roadside units (RSU) shares data obtained from its local sensors with vehicles in proximity, thus allowing vehicles to coordinate their trajectories or manoeuvres. In addition, each vehicle shares its driving intention with vehicles in proximity.

The benefits of this use case group are safer traveling, collision avoidance, and improved traffic efficiency.

- **Extended Sensors** enables the exchange of raw or processed data gathered through local sensors or live video data among vehicles, RSUs, devices of pedestrians and V2X application servers. The vehicles can enhance the perception of their environment beyond what their own sensors can detect and have a more holistic view of the local situation.

- **Remote Driving** enables a remote driver or a V2X application to operate a remote vehicle for those passengers who cannot drive themselves or a remote vehicle located in dangerous environments. For a case where variation is limited and routes are predictable, such as public transportation, driving based on cloud computing can be used. In addition, access to cloud-based back-end service platform can be considered for this use case group.

- **Vehicle QoS Support** enables a V2X application to be timely notified of expected or estimated change of quality of service before actual change occurs and to enable the 3GPP System to modify the quality of service in line with V2X application's quality of service needs. Based on the quality-of-service information, the V2X application can adapt behaviour to 3GPP System's conditions. The benefits of this use case group are offerings of smoother user experience of service.

Table 2.8 - User data rates per service (adapted from [35]).

	Minimum data rate [Mbps]		Maximum data rate [Mbps]	
Service	**UL**	**DL**	**UL**	**DL**
Vehicle platooning	100	50	200	100
Advanced driving	0.2	0.2	100	100
Extended sensors	10	10	200	200
Remote driving	1	1	200	100
Vehicle QoS support	4	8	500	100

3. Models and simulation tool

This chapter approaches and explain all formulations necessary to describe the model used for simulating channel fading and consequently the network behaviour as radio resources availability for connected and autonomous vehicles services. Planning a radio network, where autonomous vehicles stand for, require a special study mainly in air interface. Requisites of QoS, coverage and capacity appear as the main scope of differentiation in many studies as for railways, highways and roads and is also the focus of this thesis. Several scenarios were simulated, and radio parameters analysed when the users are exclusively CAV. MATLAB software has been used to develop a tool to simulate these scenarios intending to compute different KPIs that will be important for analyse the radio parameters in different network configurations and propagation environments enabling to create a QoS model of 5G-NR network when used by CAV. The simulation is divided into two blocks of radio planning: Coverage and Capacity. The final output of the simulation in both blocks is the number of cells necessary to cover the entire chosen stretch of roads on different scenarios. It is taken into consideration the propagation environments, network parameters and the set of services requirements, defined on section 2.5. The methodology used in the simulation is shown in the flowchart presented by Figure 3.1.

The simulation is based in deterministic model, where deterministic models do not have random variables, only average values, or input data from the own system.

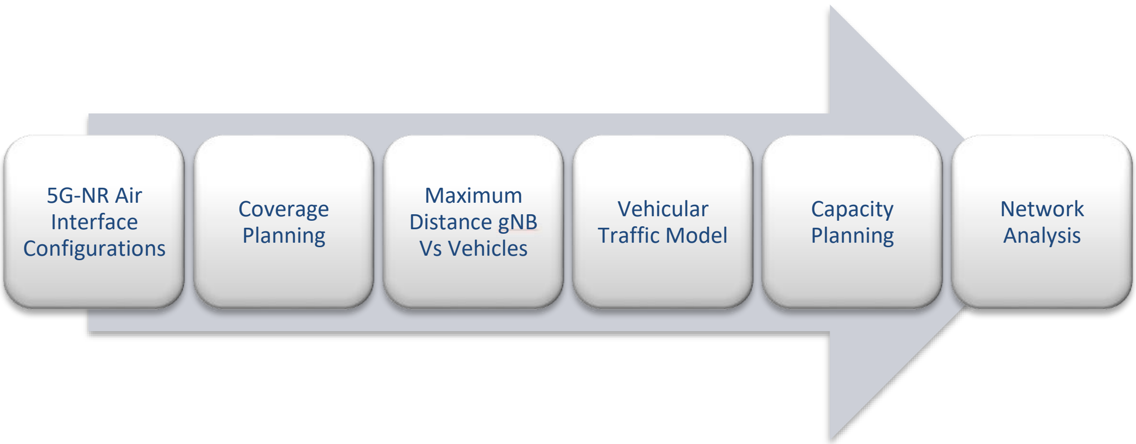

Figure 3.1 – Tool development methodology flowchart.

3.1. Considerations

The 3.5 GHz frequency band is considered, which is the band n78 with TDD duplex mode. In this mode the various slots in a frame can have different formats (e.g., UL, DL or flexible), according to [36]. This information is provided by the network to the UE, and if it is not, is considered as flexible by default. In this thesis, formats 0 and 1, first one entirely DL, and second one entirely UL, will be simulated separately.

3.2. Coverage planning

It is a rule that on radio planning by coverage, the main concern is always the QoS. Of course, that in a real radio project is considered coverage and capacity, some situations with less relevance than others. What is also true, is that when the network it is planned for CAVs both are extremely important specially because of the requested level of reliability of the services. The approach of this thesis on coverage planning is presented on Figure 3.2, where are calculated the average of path loss (PL), the received signal strength (RSS). A fixed value for SNR is defined and then calculated, the gNB and vehicles sensitivity, the maximum allowed path loss (MAPL), cell-range in UL and DL, inter-site distance (ISD), the number of cells and finally the number of vehicles covered.

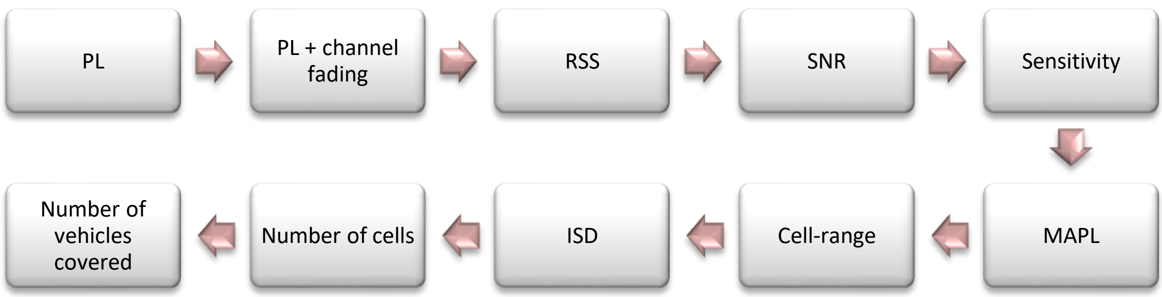

Figure 3.2 - Coverage planning flowchart.

3.2.1. *Path loss models*

The radio mobile channel faces many issues to reach good QoS on wireless communications systems. The path variation between the transmitter and the receiver can be very complex including obstructions like buildings, mountains, rivers, forest and so on, turning the radio channel extremely hard to model. Modelling the radio channel has historically done in a statistical fashion, based on measurements made specifically for an intended communication system or spectrum allocation [37]. Most of these models are based on empirical or/and theoretical methods, simulating the propagation environment, and adapting it for another transmission frequency, considering different channel effects as large-scale PL propagation models, that intend to estimate the mean RSS for long distances being able to predict the coverage area of a transmitter. The PL models are very useful to predict these obstacles and calculate the radio link budget as close as possible to the reality, and like this, provide the best QoS to the vehicle's connection.

The PL models used in this thesis are the defined by 3GPP, [38]. This parameter is log-normally distributed, followed by a specific standard deviation (σ) with zero-mean average, for each propagation environment. As higher is σ, more multipaths (higher signal variations amplitude) are present, and more obstructed the signal is.

Regarding the propagation environment, rural macro cell (RMa) and urban macro cell (UMa), in line-of-sight (LOS) and non-line of sight (NLOS) are considered. As the characteristics of the propagation channel changes according to the distance between the user terminal (UT) and the BS, is also defined by the scheme presented in Figure 3.3, the trigonometry draw that represents this distance. The Equation 3-1 presents the formula for the distance in three dimensions (d_{3D}), while include the distance in 2 dimensions (d_{2D}), that is the one which will be used for the cell-range computation. UT is considered as the vehicles, and the BS as the gNBs.

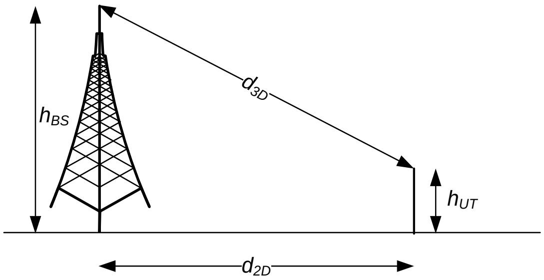

Figure 3.3 - Definition of d2D and d3D for outdoor UTs (extracted from [38]).

$$d_{3D} = \sqrt{{d_{2D}}^2 + (h_{BS} - h_{UT})^2} \quad \text{Equation 3-1}$$

h_{BS} → Base Station height [m].

h_{UT} → User Terminal height [m].

d_{2D} → Distance between UT and BS on the ground [m].

d_{3D} → Distance between UT and BS on the air [m].

The PL models for the different propagation environments are presented below.

Rural macro line of sight (RMa LOS)

$$PL_{RMa-LOS} = \begin{cases} PL_1 & 10m \leq d_{2D} \leq d_{BP} \\ PL_2 & d_{BP} \leq d_{2D} \leq 10km \end{cases} \quad \text{Equation 3-2}$$

$$PL_1 = 20\log_{10}(40\pi d_{3D}\frac{f_c}{3}) + \min(0.03h^{1.72}, 10)\log_{10}(d_{3D}) - \min(0.044h^{1.72}, 14.77) + 0.002\log_{10}(h)d_{3D} \quad \text{Equation 3-3}$$

$$d_{BP} = 2\pi h_{BS}h_{UT}\frac{f}{c} \quad \text{Equation 3-4}$$

The value of shadowing standard deviation (σ) for PL_1 is 4 dB.

d_{BP} → Break point distance. Refers to the distance where the first Fresnel ellipsoid touches the ground [m].

f_c → Central frequency [GHz].

f → Central frequency [Hz].

h → Average building height [m].

c → Propagation speed in free space, defined as (3.0×10^8 m/s).

$$PL_2 = PL_1(d_{BP}) + 40\log_{10}(\frac{d_{3D}}{d_{BP}}) \qquad \text{Equation 3-5}$$

The value of shadowing standard deviation (σ) for PL_2 is 6 dB.

Rural macro non line of sight (RMa NLOS)

$$PL_{RMa-NLOS} = \max(PL_{RMa-LOS}, PL'_{RMa-NLOS}) \quad \text{For } 10\text{m} \le d_{2D} \le 5\text{ km} \qquad \text{Equation 3-6}$$

$$PL'_{RMa-NLOS} = 161.04 - 7.1\log_{10}(W) + 7.5\log_{10}(h) - (24.37 - 3.7(\frac{h}{h_{BS}})^2)\log_{10}(h_{BS}) + (43.42 - 3.1\log_{10}(h_{BS}))(\log_{10}(d_{3D}) - 3) + 20\log_{10}(f_c) - (3.2(\log_{10}(11.75h_{UT})))^2 - 4.97) \qquad \text{Equation 3-7}$$

The value of shadowing standard deviation (σ) for $PL'_{RMa-NLOS}$ is 8 dB.

W → Average street width [m].

Urban macro line of sight (UMa LOS)

$$PL_{\text{UMa-LOS}} = \begin{cases} PL_1 & 10m \le d_{\text{2D}} \le d'_{\text{BP}} \\ PL_2 & d'_{\text{BP}} \le d_{\text{2D}} \le 5\text{km} \end{cases} \qquad \text{Equation 3-8}$$

$$PL_1 = 28 + 22\log_{10}(d_{3D}) + 20\log_{10}(f_c) \qquad \text{Equation 3-9}$$

$$PL_2 = 28 + 40\log_{10}(d_{3D}) + 20\log_{10}(f_c) - 9\log_{10}((d'_{BP})^2 + (h_{BS} - h_{UT})^2) \qquad \text{Equation 3-10}$$

$$d'_{BP} = 4h'_{BS}h'_{UT}\frac{f}{c} \qquad \text{Equation 3-11}$$

The value of shadowing standard deviation (σ) for PL_1 and PL_2 is 4 dB.

d'_{BP} → Break point distance for UMa LOS [m].

The calculation for break point in this case, follow the effective antennas heights $h'_{BS} = h_{BS} - h_E$ and $h'_{UT} = h_{UT} - h_E$. Both parameters depend on the h_E, which is the effective environment height, that for UMa h_E=1m, with a probability equal to 1/ (1+C (d_{2D}, h_{UT}) and chosen from a discrete uniform distribution. With C (d_{2D}, h_{UT}) given by Equation 3-14. As in this study the UTs are all vehicles, $h_{UT} =$ 1.5 m, C (d_{2D}, h_{UT}) is 0, thus the probability will be always 100%, and consequently $h_E = 1$.

$$C(d_{2D}, h_{UT}) = \begin{cases} 0 & , h_{UT} < 13m \\ \left(\frac{h_{UT} - 13}{10}\right)^{1.5} g(d_{2D}) & , 13m \leq h_{UT} \leq 23m \end{cases}$$ Equation 3-12

Urban macro non line of sight (UMa NLOS)

$$PL_{UMa-NLOS} = max(PL_{UMa-LOS}, PL_{UMa-NLOS}) \quad for\, 10m \leq d_{2D} \leq 5km$$ Equation 3-13

$$PL'_{UMa-NLOs} = 13.54 + 39.08 \log_{10}(d_{3D}) + 20 \log_{10}(f_c) - 0.6(h_{UT} - 1.5)$$ Equation 3-14

The value of shadowing standard deviation (σ) for $PL'_{UMa-NLOS}$ is 6 dB.

3.2.2. Link budget computation

The link budget computation englobes calculate the RSS in UL and DL, for all propagation environments, enabling service deliver to all vehicles on the highways even when the vehicles are at the cell edge, reaching the required high reliability. According to the BS categorization of [39], gNBs on rural environment are considered as “wide area” BS, and on urban environment as “local area” BS. To calculate RSS, PLs were simulated for all propagation environments considering its standard deviations and the following distance limit ranges: RMa LOS, 10 km; RMa NLOS, UMa LOS and UMa NLOS, 5 km. PL is necessary to predict the RSS, once it’s considered as received power ($P_{RX_{[dBm]}}$), even in DL or UL, balancing all gains and losses, according to the direction of the radio signal and It is represented by Equation 3-15.

$$P_{RX_{[dBm]}} = P_{TX_{[dBm]}} + G_{TX_{[dB]}} + G_{RX_{[dB]}} - L_{feed_{[dB]}} - (PL(d_{2D}) + X_{\sigma})_{[dB]} \qquad \text{Equation 3-15}$$

$P_{TX_{[dBm]}}$ → Transmitted power [dBm].

$G_{TX_{[dB]}}$ → Transmitter gain [dB].

$G_{RX_{[dB]}}$ → Receiver gain [dB].

$L_{feed_{[dB]}}$ → Cable losses [dB].

$PL(d_{2D}) + X_{\sigma}$ → Path loss models and its standard deviation calculated according to the section 3.2.1, [dB].

Calculating the minimum value of $P_{RX_{[dBm]}}$, the sensitivity ($S_{[dBm]}$) of the receiver can be estimated, in DL and UL. The sensitivity, in another words, is the minimum input power at the receiver, that from the vehicle's perspective it is the minimum received power to keep the vehicles performing the services applications, and from the gNB, to keep providing coverage and capacity. As lower is the sensitivity, higher is the gNB range and the vehicles can be covered even further. As higher is the sensitivity, closer the vehicles need to be from the gNB to receive a good QoS. As well as more power it is necessary to the transmission, maintaining the same desired QoS. According to [33], the sensitivity can be calculated as presented on Equation 3-16, and the same formula can be used in UL and DL.

$$S_{[dBm]} = -174 + 10\log_{10}\left(N_{RB}^{BW(j),\mu} * SCS_{[kHz]} * N_{SC}^{RB}\right) + NF_{[dB]} + SNR_{[dB]} + I_{m_{[dB]}} - G_{d_{[dB]}} \qquad \text{Equation 3-16}$$

$NF_{[dB]}$ → Noise Figure [dB].

$SNR_{[dB]}$ → Signal to noise ratio [dB].

$I_{m_{[dB]}}$ → Interference margin [dB].

$G_{d_{[dB]}}$ → Diversity gain [dB].

The value -174, is regarding the noise power which changes according to the temperature. The number of RB goes according to the BW and subcarrier spacing defined and presented by Table 2.5. The subcarrier spacing and definition is presented by Table 2.3. The number of subcarriers per resource block is standardized and defined as 12, as it is explained on section 2.4.3. The noise figure values are different in UL and DL and indicates the performance at the receiver. The diversity gain is the parameter that characterizes the number of layers of antennas ($v_{Layers}^{(j)}$) that the signal can be transmitted and received, and It is defined by Equation 3-17, according to [40]. The MIMO configurations that are going to be used in this thesis are: MIMO 2x2, 4x4 and 8x8. It means 2, 4 and 8 layers of antennas in both UL and DL respectively, and as higher is the number of layers of antennas, higher is the diversity gain. According to [40], the interference margin is considered as 2 dB. The SNR definition is explained on next section.

$$G_{d_{[dB]}} = 10 * \log_{10}(v_{Layers}^{(j)}) \qquad \text{Equation 3-17}$$

$v_{Layers}^{(j)}$ → Is the maximum number of supported layers in UL and DL for MIMO configurations.

3.2.3. Signal to noise ratio computation

For sensitivity calculation, is necessary to target SNR values. This is a very important parameter on radio planning, and it dictates how the channel is influencing on the traffic. It variates with the propagation environment, BW, data rate and the modulation order. Thus, in this thesis to reach SNR values, an average white gaussian noise (AWGN) ideal channel, with none coding scheme were simulated, referring the BER of each modulation scheme (QPSK, 16QAM, 64QAM, and 256QAM), as a function of Eb/N0 (i.e. Energy per bit to noise ratio), and defined by Equation A.1, Equation A.2 and Equation A.3, in Annex B. Eb/N0 and SNR are different parameters where both shows the difference between the signal and the noise levels. The first it is the ratio of energy per bit (Joule/bit) of the signal, and the noise density in 1 Hz, commonly expressed in dB, but also could be expressed in terms of time, once 1 Hz is 1 second on time. The second is the ratio of total signal power level to the density of noise presented in the entire bandwidth occupied, also commonly expressed in dB. To simplify, SNR values were considered as the ones of Eb/No in the AWGN simulation.

This is a theoretical approach to define the normalized SNR values, while AWGN channel is a very simple way to consider all the random multipaths from the propagation environments.

3.2.4. Maximum allowed PL

The sensitivity enables to compute how far the vehicles can be from the gNB to keep receiving a good signal level, in another words, the cell edge range, by computing the MAPL. This parameter could be also used to study and analyse handover distance, as well as the overlapping among gNBs, but out of the scope of this thesis. The MAPL computation is made by the Equation 3-18, considering the Equation 3-15, where $P_{RX_{[dBm]}}$is replaced into $S_{[dBm]}$, and the variable $PL(d_{2D})$ is isolated as MAPL. As the PL models are defined for 50% of coverage probability at the cell edge, to reach higher probability of coverage is necessary to add fading margins. Rayleigh margin is a fading margin used for macro cells, when the UE is in NLOS with the gNB, and there is no dominant component as in LOS, being necessary to increase the transmitted signal strength once it will just reach the UE by multipaths. It is defined as 3 dB as common value on radio planning. It is also added log-normal fading margin (LNF_{margin}), and it can be achieved using Jake's method, that implies on divide σ per coefficient of decay, and target a percentage of coverage reaching it at the cell edge. On this thesis, the values of the coefficient of decays are defined by [41] and multiplied by the standard deviations of each propagation environment, considered on the section 3.2.1. The LNF_{margin} values for 95 to 99% of coverage are presented by Table 3.1, for different types of propagation environments.

$$MAPL_{[dB](50\%)} = P_{TX_{[dBm]}} + G_{TX_{[dB]}} + G_{RX_{[dB]}} - S_{[dBm]} - L_{feed_{[dB]}} \qquad \text{Equation 3-18}$$

$$MAPL_{[dB](99\%)} = MAPL_{dB[50\%]} - LNF_{margin_{99\%}} - RF_{margin} \qquad \text{Equation 3-19}$$

LNF_{margin} → Log-normal fading margin [dB].

RF_{margin} → Rayleigh fading margin [dB].

Table 3.1 - Log-normal fading margins (adapted form [41]).

	RMa LOS	RMa NLOS	UMa LOS	UMa NLOS
$\boldsymbol{LNF_{margin_{95\%}}[dB]}$	6.56	13.12	6.56	9.84
$\boldsymbol{LNF_{margin_{96\%}}[dB]}$	7	14	7	10.5
$\boldsymbol{LNF_{margin_{97\%}}[dB]}$	7.56	15.12	7.56	11.34
$\boldsymbol{LNF_{margin_{98\%}}[dB]}$	8.2	16.4	8.2	12.3
$\boldsymbol{LNF_{margin_{99\%}}[dB]}$	9.32	18.64	9.32	13.98

3.2.5. Cell-range and maximum distance in uplink formulas definition

On section 3.2.1, where PL models were presented, is possible to see that on each propagation environment different PL equations were defined changing according to the distance vehicle-gNB, mostly until 5 or 10 km. This section defines the formulas used for the cell-range and for the maximum distance reached in UL calculation. The cell-range, also called as cell-radius, is the maximum distance that the gNB (in DL) can reach. And the maximum distance transmitter in UL will be called also as cell-range but in UL, considering the channel fading and the PL computed. Therefore, the cell-range in DL and UL can be compared, to compute the number of cells necessary to cover the highways considering the worse cases of coverage. If in DL and UL the $MAPL_{[dB](99\%)}$ is equal to PL, in the equations of PL models, thus, is possible to reach the maximum distance in 2D (d_{2D}) and 3D (d_{3D}) from the gNB and from vehicles, which equations for each scenario are presented from Equation 3-20 to Equation 3-23, and the definition of d_{2D} on Equation 3-24, derived from Equation 3-1.

RMa LOS

For rural macro line of sight scenario, the equation of PL model is PL_2, once isolating d_{3D} from PL_1 was going to reach an inequality. To simplify the simulation,

PL_2 from Equation 3-5 was changed for $MAPL_{[dB](99\%)}$ and, d_{3D} was isolated and its formula is presented on Equation 3-20.

$$d_{3D[km]} = \left(d_{BP} * 10^{\frac{MAPL_{[dB](99\%)} - \left(20\log_{10}\left(40\pi d_{BP}\frac{f_c}{3}\right) + \min\left(0.03h^{1.72}, 10\right)\log_{10}(d_{BP}) - \min\left(0.044h^{1.72}, 14.77\right) + 0.002\log_{10}(h)d_{BP}\right)}{40}}\right) \quad \text{Equation 3-20}$$

RMa NLOS

For rural macro non line of sight scenario, the equation of PL model is PL', from Equation 3-7, once it's the equation defined for this scenario, despite of the definition says that it must be the highest value between LOS and NLOS, but the probability of PL values on NLOS scenario is higher. The d_{3D} formula is presented on Equation 3-21.

$$d_{3D[km]} = 10^{\frac{MAPL_{[dB](99\%)} - \left(161.04 - 7.1\log_{10}(W) + 7.5\log_{10}(h) - \left(24.37 - 3.7\left(\frac{h}{h_{BS}}\right)^2\right)\log_{10}(h_{BS}) + 20\log_{10}(f_c) - \left(3.2\left(\log_{10}(11.75h_{UT})\right)^2 - 4.97\right)\right)}{\left(43.42 - 3.1\log_{10}(h_{BS})\right)} + 3} \quad \text{Equation 3-21}$$

UMa LOS

For urban macro line of sight scenario, the equation of PL model is PL_2, from Equation 3-10, once it is defined for situations where the vehicles are localized from distance of d_{BP} until 5 km, which is the distance of the highway that is studied, that will be explained ahead. The probability of the vehicle be in a distance smaller than d_{BP} is low, considering the current real situation. The d_{3D} formula is presented on Equation 3-22.

$$d_{3D[km]} = 10^{\frac{MAPL_{[dB](99\%)} - \left(28 + 20\log_{10}(f_c) - 9\log_{10}\left(\left(4h'_{BS}h'_{UT}\frac{f_c}{c}\right)^2 + (h_{BS} - h_{UT})^2\right)\right)}{40}} \quad \text{Equation 3-22}$$

UMa NLOS

The definition of PL equation on this scenario is like RMa NLOS. The equation is PL', from Equation 3-14, once is more likely the PL values on NLOS be higher than on LOS. As on this scenario the definition is what is higher, PL on UMa LOS or UMa NLOS. The d_{3D} formula is presented on Equation 3-23.

$$d_{3D[km]} = 10^{\frac{MAPL_{[dB](99\%)} - 13.54 - 20\log_{10}(f_c) + 0.6(h_{UT} - 1.5))}{39.08}} \qquad \text{Equation 3-23}$$

Distance in 2D

All the distances in 3D calculated follow the previous formulas were converted into 2D, enabling the computation of the number of cells necessary to cover the entire highway.

$$d_{2D} = \sqrt{{d_{3D}}^2 - (h_{BS} - h_{UT})^2} \qquad \text{Equation 3-24}$$

3.2.6. Cell's configuration and computation

The number of cells computation depend on the cell format definition. On this thesis, hexagonal format is considered, as well as tri-sectorized sites, which only two will cover the highway that is being studied, as can be shown in Figure 3.4. The distance between two hexagonal centres is ISD and is calculated by Equation 3-25. The early site' number is calculated dividing the whole length of the stretch for the ISD, when ISD is shorter than the road length. In case that the ISD is larger than the road length, is considered necessary one site for the entire stretch, the calculus definition is presented by Equation 3-26. The Equation 3-27 represents the calculation of number of cells per km. The number of cells necessary to cover the highway is considered as the number of sites calculated through the Equation 3-26 and multiplied per 2, once each tri-sectorized site has only two out of three cells covering the road, as can be seen by Figure 3.4.

$$ISD = \sqrt{3} * d2D \qquad \text{Equation 3-25}$$

$$N^c_{s/5km} = \begin{cases} \frac{RL_{[km]}}{ISD_{[km]}}, & ISD < Road\ Length \\ 1, & ISD \geq Road\ Length \end{cases} \qquad \text{Equation 3-26}$$

$$N^{c}_{cells/km} = \frac{1}{ISD_{[km]}} * 2 \quad \text{Equation 3-27}$$

$N^{c}_{s/5km}$ → Number of sites for the entire stretch by coverage.

$RL_{[km]}$ → Road length that is being simulated.

$N^{c}_{cells/km}$ → Number of cells per kilometre by coverage.

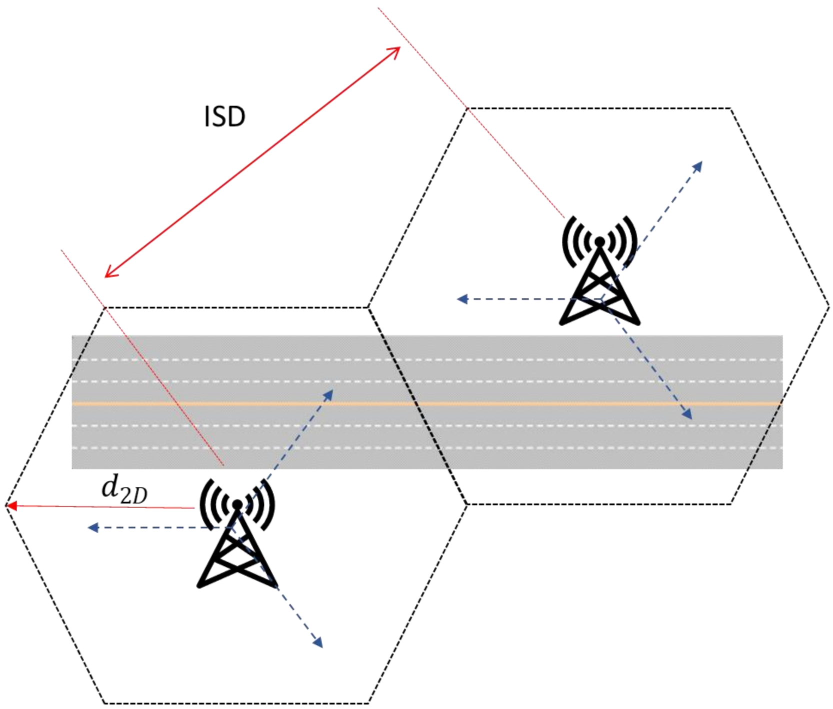

Figure 3.4 - Coverage planning configuration definition.

3.2.7. *Number of vehicles per cell*

Knowing the number of cells per kilometre (km) on the highway, and the number of vehicles per km that passes through the road, it is possible to estimate the vehicles density covered per cell, using the Equation 3-28.

$$N^{c}_{v/cell} = \frac{N_{v/km}}{N^{c}_{cells/km}} \quad \text{Equation 3-28}$$

$N^{c}_{v/cell}$ → Number of vehicles per cell by coverage.

$N_{v/km}$ → Number of vehicles per km.

3.3. Capacity planning

The cellular radio planning made on this thesis is divided into two blocks, coverage, and capacity, where the last one is necessary to compare the results from coverage-based planning. The cell breath occurs when it is necessary to shift between coverage and capacity. In the case of capacity planning, where the users are entirely vehicles, is extremely important providing enough resources, avoiding high latency, and guarantying the main V2X pillars as safety. To calculate the KPIs by capacity, the scheme of the Figure 3.5 is applied.

The main goal of capacity planning is estimating the amount of data that is being required from the vehicles and like this compare to the network capacity. Thus, vehicles density estimation is performed to compute the number of vehicles. Service data rate per vehicle is defined to calculate the total user data rate. Network capacity is computed for all scenarios, and the number of vehicles per service supported by the network capacity is simulated. Traffic load is computed, to calculate the total data rate required per cell considering the cell-range calculated by coverage. Thus, cell-ratio is computed, which is the comparison between the network capacity and the traffic load per cell, according to each scenario. The result must show if the cells are enabling the vehicles perform the services categories tasks or not. If yes, the cells are limited by coverage, if not, is limited by capacity and a new cell-vehicle-range is necessary to calculate.

Therefore, the new cell-vehicle range is computed and consequently the new ISD and the final number of cells necessary to cover the entire highways and provide capacity to all vehicles. The vehicles density estimation model, as well as the service data rate and total user data rate are scenarios defined and explained on section 4. The models to the rest of the blocks from Figure 3.5 is explained deeper on next sections, starting by network capacity model.

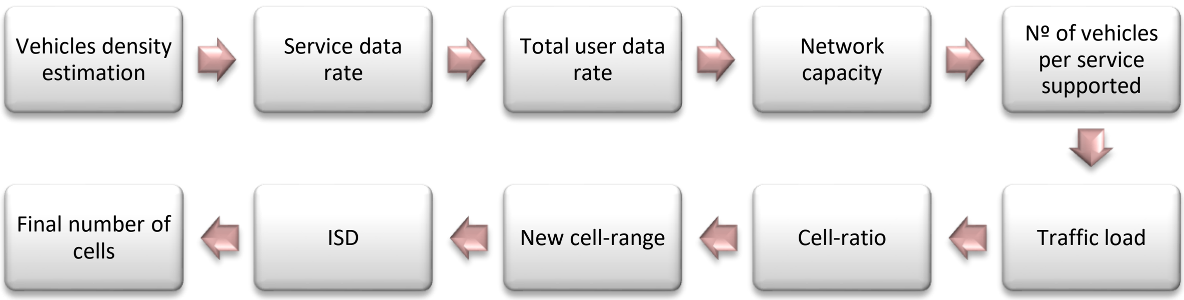

Figure 3.5 - Capacity planning flowchart.

3.3.1. *Network Capacity*

To simulate the cellular radio planning by capacity is necessary to compare data traffic demanded from the vehicles, with the gNBs capacity. The network capacity is calculated using the definition of maximum supported UE data rate according to [44] and [45] presented on Equation 3-29. The formula calculates the peak data rate supported by the UE in DL and UL by band or band combinations, as for example if the network is configurated the bands of 700 and 3300 MHz and, the first layer with 50 MHz and the second with 100 MHz of BW. In this thesis, only one band will be used (n78) as explained on section 2.4.3, as also, the simulation will consider only one carrier.

$$D_{Rate,[Mbps]} = 10^{-6} * \sum_{j=1}^{J} \left(\alpha^{(j)} * v_{Layers}^{(j)} * Q_m^{(j)} * f^{(j)} * R_{max} * \frac{N_{PRB}^{BW(j),\mu} * 12}{T_{s\ [sec]}^{\mu}} * \left(1 - OH^{(j)}\right) \right) \quad \text{Equation 3-29}$$

$$T_{s\ [sec]}^{\mu} = \frac{10^{-3}}{14 * 2^{\mu}} \quad \text{Equation 3-30}$$

$D_{Rate,[Mbps]}$ → Maximum supported UE data rate [Mbps].

J → Is the number of aggregated component carriers in a band or band combination.

$\alpha^{(j)}$ → Normalized scaling factor for TDD mode.

$v_{Layers}^{(j)}$ → Number of layers of antennas, defined by Equation 3-17.

$Q_m^{(j)}$ → It is the maximum supported modulation order in UL and DL, Table 2.7.

$f^{(j)}$ → Scaling factor.

R_{max} → Maximum coding rate.

$BW_{[MHz]}$ → Bandwidth available for each numerology [MHz], Table 2.5.

$SCS_{[kHz]}$ → Subcarriers spacing [kHz].

N_{sc}^{RB} → Number of subcarriers per resource block.

T_s^{μ} → OFDM symbol duration for numerology *μ,* explained on section 2.4.1 [sec].

$OH^{(j)}$ → Overhead.

As mentioned before, only one carrier is considered in this study, thus J will hold only the value 1. The MIMO configurations that will be simulated are MIMO 2x2, 4x4 and 8x8, considering like this the values 2, 4 and 8 for $v_{Layers}^{(j)}$. All modulation's orders are presented by Table 2.7, and all of them will be simulated, QPSK, 16QAM, 64QAM and 256QAM, making $Q_m^{(j)}$ gets the values of 2, 4, 6 and 8. The scaling factor $f^{(j)}$, is used to reflect different capabilities between baseband and RF for both SA and NSA UE. It is also used for scaling down the maximum throughput of NR UEs in EN-DC scenarios where there is LTE and NR hardware sharing. Their values can be 1, 0.8, 0.75, and 0.4, where only value 1 is going to be used for this simulation. The maximum coding rate R_{max} of each modulation scheme that are considered are presented by Table 3.2 and was defined on [46]. The coding rate refers to the useful number of bits in comparison to the transmitted bits. As higher the coding rate is more redundancy presents the data-stream. The T_s^{μ}, It's the average OFDM symbol duration in a subframe for numerology μ defined in the Table 2.3 and calculated by Equation 3-30, where this thesis assumes only normal CP. The overhead $OH^{(j)}$, is defined as 0.14 and 0.08 for UL and DL respectively in FR1 [44]. According to [28], the $OH^{(j)}$ is the average ratio of resource elements (RE) occupied by synchronization, physical broadcast channel (PBCH), physical downlink control channel (PDCCH), reference signals and guard periods, compared to the total number of REs available in the effective BW and a frame time product. According to [45], $\alpha^{(j)}$ is related to the proportion of resources used in the DL and UL ratio for the J component carrier. In FDD duplex mode its value is only 1, once the proportion is the same for UL and DL. In TDD mode, as for the whole stream it can take different percentage of DL and UL, $\alpha^{(j)}$ is calculated based on the frame structure of the Slot Format Indicator (SFI) as defined on section 2.4.3. In TDD DL, $\alpha^{(j)}$ considers the presence of GB, presented by Table 2.6, as part of the effective BW. Therefore, the impact of GP must be considered in the $OH^{(j)}$ calculation, but once the SFI used for this thesis simulation are format 0 and 1, that considers slot formats only for DL or UL, $\alpha^{(j)}$ will take only the value 1.

Table 3.2 - Defined coding rates for each modulation scheme (adapted from [46]).

MCS Index	$Q_m^{(j)}$	Target code Rate *R* x [1024]	R_{max}
4	2	602	3/5
10	4	658	2/3
19	6	873	6/7
27	8	948	1

3.3.2. Number of vehicles per service supported

Intending to analyse the network capacity towards and the minimum and maximum user data rate per service, was computed the number of vehicles per service that the network can provide radio resources, for each highway. This parameter helps the radio planning to analyse how prepared the network is to provide a minimum of service for CAVs. The Equation 3-31 was used to compute the number of vehicles per service supported by the network.

$$N_v^s = \frac{D_{Rate,[Mbps]}}{U_{v\,[Mbps]}^s} \qquad \text{Equation 3-31}$$

N_v^s → Number of vehicles per service supported by the network.

$U_{v\,[Mbps]}^s$ → Minimum and maximum user data rate per vehicle, per service.

The network capacity or maximum user data rate $D_{Rate,[Mbps]}$, is calculated regarding the definition from [44] and [45]. The minimum and maximum user data rate per vehicle and per service was defined on Table 2.8. N_v^s was calculated for each propagation environment and scenarios, considering all 5G-NR air interface configurations.

3.3.3. Traffic load calculation

Using the analysis from previous model, it is possible to reach the number of vehicles per service that the 5G network is enabled to provide radio resources enough enabling the vehicles to perform the tasks and manoeuvres from their services categories. Like this, is possible to reach a number and not the signal quality that is reaching the vehicles, opening a gap at capacity limitation. When a cell is enabled to provide capacity, the cell is limited by coverage. And when the cell reaches the capacity, the cell is limited by capacity. The next sections intend to identify these gaps and find out which are the 5G-NR air interface configurations that the cells are limited by coverage or capacity for CAVs services. The first step that needs to be taken is to calculate the whole amount of data rate that the vehicles are demanding for all scenarios. To reach this KPI, Equation 3-33 is applied, where the total user data rate per km is multiplied by the cell-range $d2D_{km}$. The variable total user data rate corresponds to the total amount of data from all vehicles per km. The result is a traffic load required from the vehicles to a cell, per km.

$$TL_{cell_{[Mbps]}} = \frac{TU_{[Mbps]}}{km} * d2D_{[km]} \qquad \text{Equation 3-32}$$

TL_{cell} → Traffic load per cell per km (Mbps/cell/km)

$TU_{[Mbps]}$ → Total user data rate per km (Mbps/km).

3.3.4. Cell-Ratio

As mentioned on the previous section, the intention of this section is to find the cell limits by coverage or capacity, to compute this cell-range reaching a reasonable coverage and capacity to provide a good QoS for CAVs, is required. Computing the KPI traffic load per cell per km is possible to analyse the amount of data required from vehicles on the highways to one specific cell, and it turns possible compare it to a cell capacity, reaching a new variable called cell-ratio (CR). Cell-ratio formula is presented on Equation 3-34, as a ratio between the cell capacity, $D_{Rate,[Mbps]}$, calculated by Equation 3-29, and the traffic load generated per cell, $TL_{cell,[Mbps]}$, calculated by Equation 3-32. Naturally, if the value of CR is higher than 1, the cell capacity is bigger than the traffic load, and the cell is limited by coverage. Instead, if the CR is lower or equal to 1, the traffic load is equal or higher than the network capacity and the cell is limited by capacity, being necessary to compute a new and shorter cell-range that reaches fewer vehicles, increasing cell capacity and decreasing cell coverage. The logic flowchart can be analysed by Figure 3.6.

$$CR = \frac{D_{Rate,[Mbps]}}{TL_{cell,[Mbps]}} \qquad \text{Equation 3-33}$$

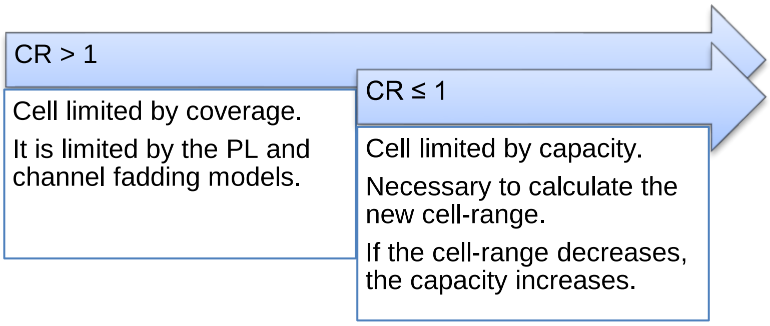

Figure 3.6 - Cell-ratio analysis flowchart.

3.3.5. New cell-range calculation

Analysing the cell-ratio calculated on previous section is possible to find the gaps where the cell is limited. For those scenarios where $CR \leq 1$, the cell is limited by capacity, thus is necessary to calculate the new cell-range that ensures coverage and capacity. When Equation 3-34 is analysed, whenever $CR \leq 1$, the cell is going to be limited by capacity. Avoiding that CR ≤ 1, and to find the cell-range that support the capacity, CR > 1 is necessary. Thus, if Equation 3-34 is > 1, and $d2D_{km}$ multiplies 1, Equation 3-35 is reached. For ensure that the cells are not saturated immediately, and the CR just reaches 1 when the cell is out of capacity, new cell-range is calculated considering 80% of the available radio resources. For this reason, 0.8 is multiplied by the network capacity $D_{Rate,[Mbps]}$, in Equation 3-35. Like this, the Equation 3-35, represents the maximum cell-range that enable $\frac{TU_{[Mbps]}}{km}$ doesn't overtake 80% of $D_{Rate,[Mbps]}$. So, for example, if $D_{Rate,[Mbps]}$ is 100 Mbps, and $TU_{[Mbps]}$ is 50 Mbps, per km, $d2D_{km}$ need to be less than $\frac{0.8*50}{120}$, which is 1.6 km. This parameter is calculated considering all scenarios previously explained, except the differentiation of LOS and NLOS, once the model for capacity analysis considers the network capacity in UL and DL, and the total user data rate per km in rural and urban propagation environments, reaching like this, results on both urban and rural environments in DL and UL. Being LOS and NLOS scenarios limited by coverage.

Analysing the new cell-range calculated by capacity, is possible to compute the ISD and the final number of cells desired for ensure coverage and capacity. The ISD by capacity is computed using the same logic from coverage planning, according to the Equation 3-25. And the final number of sites according to Equation 3-26.

$$CR \leq 1 \ \therefore \ \frac{D_{Rate,[Mbps]}}{\frac{TU_{[Mbps]}}{km} * d2D_{km}} \leq 1$$ Equation 3-34

$$d2D_{km} < \frac{0.8 * D_{Rate,[Mbps]}}{\frac{TU_{[Mbps]}}{km}}$$ Equation 3-35

4. Results Analysis

The objective of this thesis is to evaluate 5G-NR air interface performance when supporting connected and autonomous vehicles services categories defined by the 5G-MOBIX project. Radio cellular planning is performed aiming to compute the necessary number of sites that provides enough radio resources to support a good QoS for an estimated number of vehicles that passes through highways in rural and urban propagation environments. The radio planning is divided into two blocks: planning limited by coverage or by capacity, as so the results are going to be presented in this Chapter.

4.1. Planning limited by coverage

4.1.1. PL simulation

As explained on section 3.2.1, rural and urban propagation environments are considered and simulated in this thesis. As the objective is to analyse the network requirements when CAVs are considered, real highways were identified to be representative of both environments. Both cases the highways hold 3 lanes in each direction, totalizing 6 lanes, being better explained in section 4.2.1. For PL simulation, the parameters are defined and presented on Table 4.1, where the values for h_{BS} were chosen according to the default values presented in [19].

Table 4.1 - Variables definition for PL computation.

Variables	Value [m]
h_{BS}	35 (rural), 25 (urban)
h_{UT}	1.5
W	Highway with 6 lanes (6x4) → 24
h	5

Radio planning by coverage was performed using deterministic models. The PL models were simulated for rural and urban macro cells, in LOS and NLOS, and are presented in Figure 4.1. The average PL increases log-normally with distance significantly, reaching 125 dB in RMa LOS and 170 dB in UMa NLOS scenarios. All scenarios are limited at 5 km, except for RMa LOS, which the limitation (defined by Equation 3-2), it is 10 km. These first simulations are to analyse the PL models according to the distance, all scenarios were simulated until 5 km.

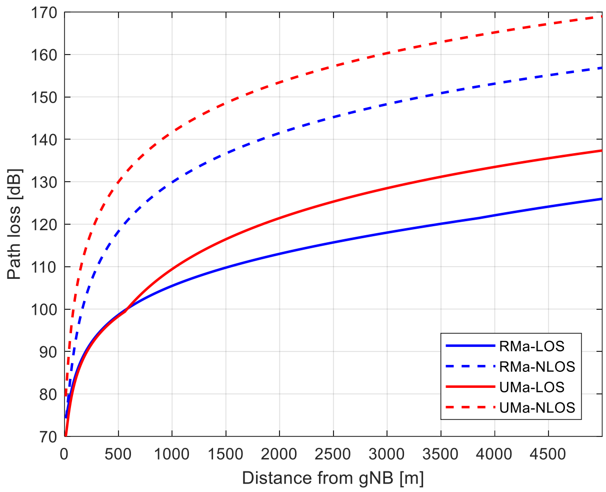

Figure 4.1 – a) Average PL model simulation; b) Variable PL model simulation

4.1.2. Received Signal Strength

Considering the gNBs categorization, the output/transmitter power is defined as 49 dBm considering directive antennas, once the application are highways. The noise figure is 5 and 13 dB for rural and urban environment, respectively. For UT (vehicles) parameters values, were considered the definitions from [33]. The UT is defined as class 3. Thus, the transmitter power is 23 dBm. Antenna gains and cables losses for both gNBs and vehicles, were considered common radio planning values, as presented by Table 4.2.

Using the standard deviation of each propagation environment defined on 3.2.1, the received power at UL and DL were simulated as RSS for the same scenarios, according to Equation 3-15 and Table 4.2, considering all gains and losses according to the communication direction between vehicle and gNB. Figure 4.2 a) presents the RSS simulations results for UL scenarios and Figure 4.2 b), presents the results of RSS for DL. It can be observed that, the lowest values of RSS are at the cell edge, reaching average of -95, -113, -94 and -126 dBm in UL, and -71, -89, -70 and -102 dBm in DL, for RMa LOS, RMa NLOS, UMa LOS and UMa NLOS, respectively. Naturally, for all scenarios presented, with the channel variation simulation, the RSS can reach even lower values at the cell edge, taking as example, the worst case in UMa NLOS in UL, the values of RSS go below -140 dBm. If vehicles sensitivity is around -110 dBm, which is a common value, vehicles will not receive good QoS at the cell edge, resulting in at least low throughput and delay, for this reason sensitivity is simulated as follow.

Table 4.2 - Radio parameters for link budget computation.

Parameter	gNodeB	User Terminal
Transmitter power [dBm]	49	23
Antenna gain [dBi]	18	2
Noise Figure [dB]	5 (rural), 13 (urban)	10
Cable loss [dB]	2	0

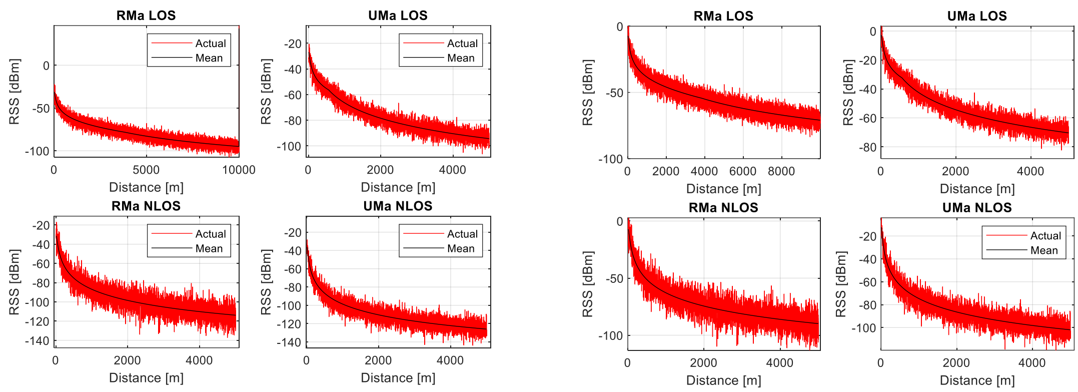

a) b)

Figure 4.2 - Received signal strength in a) UL and b) DL scenarios.

4.1.3. Signal to Noise Ratio

Sensitivity is an important parameter to calculate the link budget on radio planning, once targets the level of power at the transmitter that ensure delivering good signal strength even with all losses. To compute the sensitivity, SNR is required. An artificial AWGN channel was simulated considering all modulation orders, which the result is presented by Figure 4.3. As explained on section 3.2.3, the simulated AWGN channel presents the Eb/N0 values according to BER, and even Eb/N0 being a different parameter from SNR, they were considered the same to simplify the computation. Considering BER equal to 1%, and Eb/N0 values as SNR, it reaches 4, 8, 12 and 16 dB for, for QPSK, 16QAM, 64QAM and 256QAM, respectively.

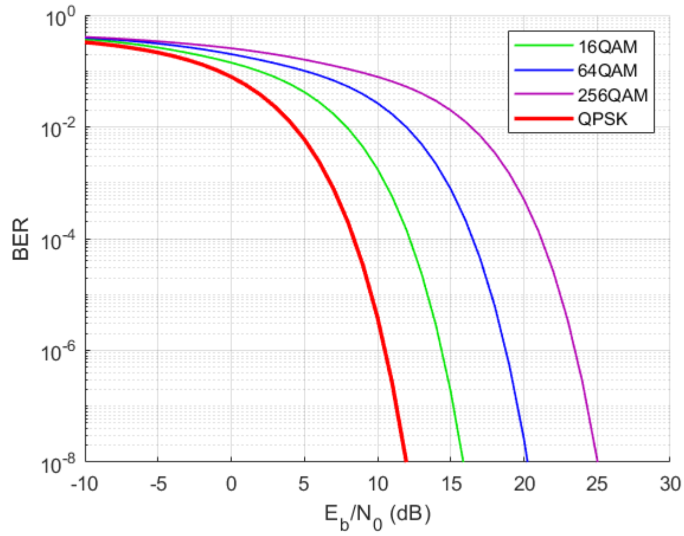

Figure 4.3 – AWGN channel simulation.

4.1.4. *Sensitivity*

Once SNR values are defined, it is possible to simulate the sensitivity for all propagation scenarios, according to Equation 3-16 and Table 4.3, applying different parameters to simulate rural and urban environments in UL, which represents the gNB sensitivity, and DL which represents the vehicles sensitivity, varying according to the modulation orders, BW, numerology and MIMO configurations applied. Figure 4.4 and Figure 4.5, present sensitivity simulations. From these figures, it is possible to analyse that the sensitivity increases significantly with the BW in both RMa and UMa scenarios. The different sensitivity values among numerologies in all scenarios are small, less than 1 dB for 10 MHz, and almost 0 dB in 100 MHz. Nevertheless, the differences among MIMO configurations are a bit more expressively, presenting to be 3 dB of difference between MIMO 2x2 and 4x4, as also between MIMO 4x4 and 8x8, and almost 7 dB between MIMO 2x2 and 8x8, this is regarding the MIMO gains added on the formula of 3, 6 and 9 dB, for MIMO 2x2, 4x4 and 8x8, respectively. This behaviour can be seen also on $MAPL_{[dB](99\%)}$, cell-range and ISD simulations, which the structure of the presented graphics is the same. It is also possible to analyse that the lowest values of sensitivity are presented for QPSK modulation, lower in UL than in DL. It means that as lower the modulation order, lower are the vehicles' sensitivity and less power is necessary to apply in the transmission for the signal received by vehicles. Higher modulation order requires higher sensitivity values, and more power are necessary in the transmission side. Being is possible to estimate the $MAPL_{[dB](99\%)}$, through the vehicles' sensitivity and thus the distance to the cell edge.

Table 4.3 - MIMO diversity gains.

Type	$v_{Layers}^{(j)}$	$G_{d\,[dB]}$
MIMO 2x2	2	3
MIMO 4x4	4	6
MIMO 8x8	8	9

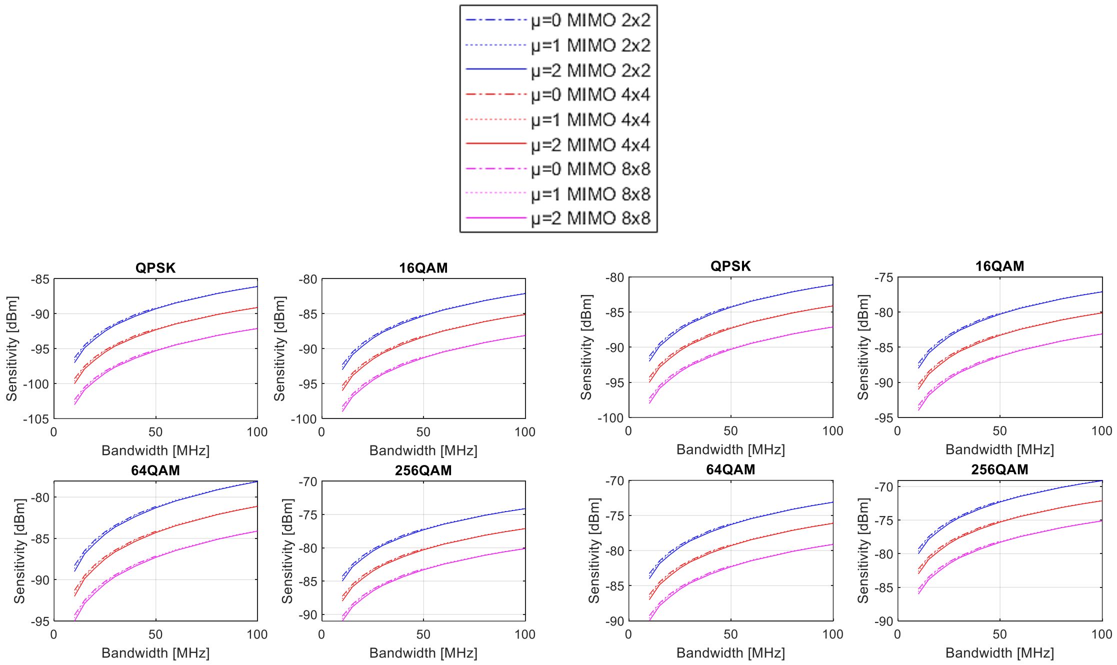

a) b)

Figure 4.4 - Sensitivity in RMa a) UL and b) DL scenarios.

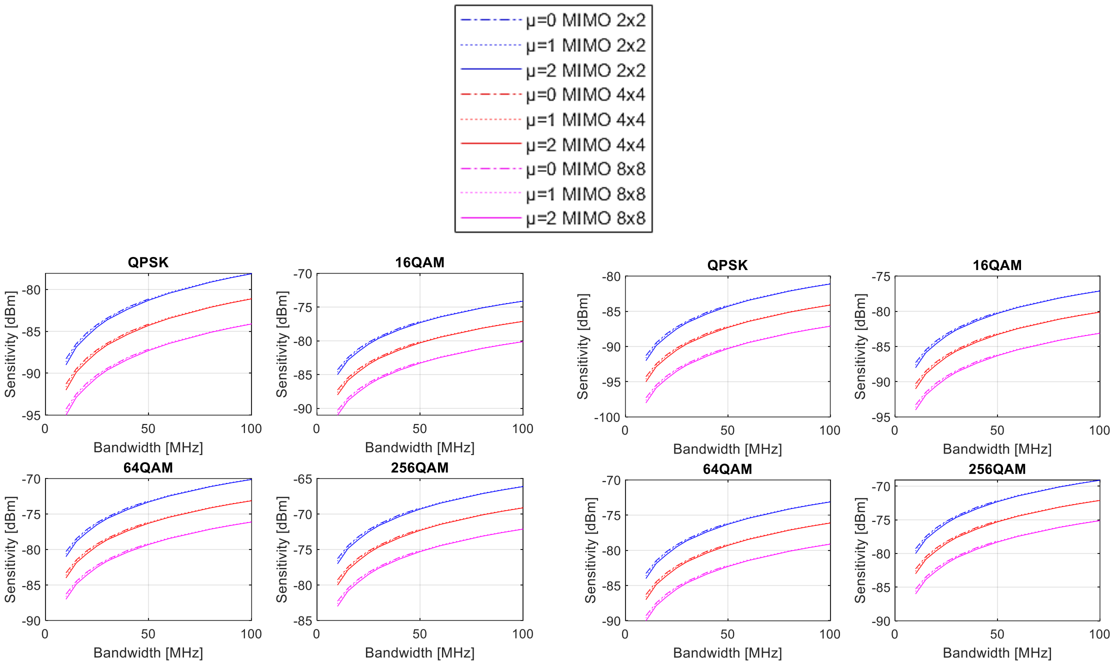

a) b)

Figure 4.5 - Sensitivity in UMa a) UL and b) DL scenarios.

4.1.5. Maximum allowed PL

The $MAPL_{[dB](99\%)}$ was simulated according to the explanation of section 3.2.4, and Equation 3-18, considering the PL models from section 3.2.1. The PL models are defined for 50% of probability of coverage at the cell edge, thus Rayleigh RF_{margin} and log-normal fading LNF_{margin} margins were added, using the Equation 3-19 to calculate $MAPL_{dBm[99\%]}$ for 99% of probability of coverage at the cell edge, for all scenarios. As explained before, RF_{margin}, was defined as 3 dB and LNF_{margin} according to the Table 3.1 for each scenario. $MAPL_{dBm[99\%]}$ simulations are presented in Annex C, by: Figure B.1, Figure B.2, Figure B.3 and Figure B.4. It is possible to analyse that $MAPL_{dBm[99\%]}$ simulations divide the results into LOS and NLOS, once it considers different values of LNF_{margin} in those scenarios, reaching highest values in DL as expected. Thus, $MAPL_{[dB](99\%)}$ values are equals in RMa LOS and UMa LOS, once it is used the same values of LNF_{margin} in these scenarios. It can be seen that $MAPL_{[dB](99\%)}$ is higher on QPSK modulations in all scenarios, reaching maximum of 152 dB in RMa LOS in DL for MIMO 8x8 and μ=2, Figure B.1 b), and minimum of 100 dB in UMa NLOS in UL for MIMO 2x2 and μ=0, Figure B.4 a). The differences in the values of $MAPL_{[dB](99\%)}$

regarding the MIMO configurations are due to the added MIMO gains (3 dB), and the differeces regarding the numerologies are not very significant in these simulations, varying less than 1 dB among them. The most expressively variation of $MAPL_{[dB](99\%)}$ values can be seen comparing them through the diferent channel BWs of 10 and 100 MHz and for all scenarios, is abaout 11 dB. This parameter ir very important to calculate the cell-range used to estimate the desired number of sites necessary to cover a certain region. In this simulation, it was possible to see that, the BW variation, while the network setup is crucial to determine the $MAPL_{[dB](99\%)}$, which can decrease until 10.9 dB its value, impacting the cell-range and the number of cells.

4.1.6. Maximum distance gNB-vehicles for downlink and uplink

The $MAPL_{[dB](99\%)}$ computation estimates the maximum reachable distance between gNB, and mobile terminals used by vehicles in downlink/uplink, also called as cell-range, using the methodology explained on section 3.2.5. Results are presented by Figure 4.6, Figure 4.7, Figure 4.8 and Figure 4.9, being possible to analyse that the distance decrease when the BW increases, numerology, MIMO configuration and modulation order, reaching maximum cell-range of 23.28 km as presented by Figure 4.6 b), that refers to RMa LOS DL scenario, for QPSK modulation, MIMO 8x8 with μ=2 configuration with 10 MHz of BW. And the minimum cell-range of 264 m, on Figure 4.9 b), in UMa NLOS DL scenario, for 256QAM modulation, MIMO 2x2 with μ=1 configuration and 100 MHz of BW. The maximum distance reached for gNB-vehicles in UL is 6.95 km for RMa LOS scenario, presented by Figure 4.6 a), for QPSK modulation, MIMO 8x8 with μ=2 configuration with 10 MHz of BW. And minimum of 42 m in UMa NLOS, presented on Figure 4.9 a), for 256QAM modulation, MIMO 2x2 with μ=1 and 100 MHz of BW. Results shows that the maximum distance gNB-vehicles can reaches very long distances in LOS and very short distances in NLOS. The QPSK case reach much longer distances than 256QAM, some cases overtaking 2x further as for example in UMa NLOS scenarios presented by Figure 4.9. For all configurations in RMa and UMa scenarios, the maximum distances in NLOS reach only 10% of the maximum distance calculated in LOS. It is also analysed that the numerologies are a differentiating factor and the own differentiation changes according to the

MIMO configuration, modulation orders and BW. For example, if RMa LOS DL QPSK MIMO 8x8 in 10 MHz is analysed, Figure 4.6 b), it can be seen that the distances interval between μ=2 and μ=1 is about 0.5 km, and that the interval between μ=1 and μ=0 is about 0.45 km, and smaller as higher is the modulation order, for example for the same scenario but 256QAM the difference is 0.25 and 0.23 km. This differentiation is very relevant when network configurations are being planned/installed, mainly for V2X network where coverage and capacity are very important parameters to enable vehicles perform the manoeuvres smoothly.

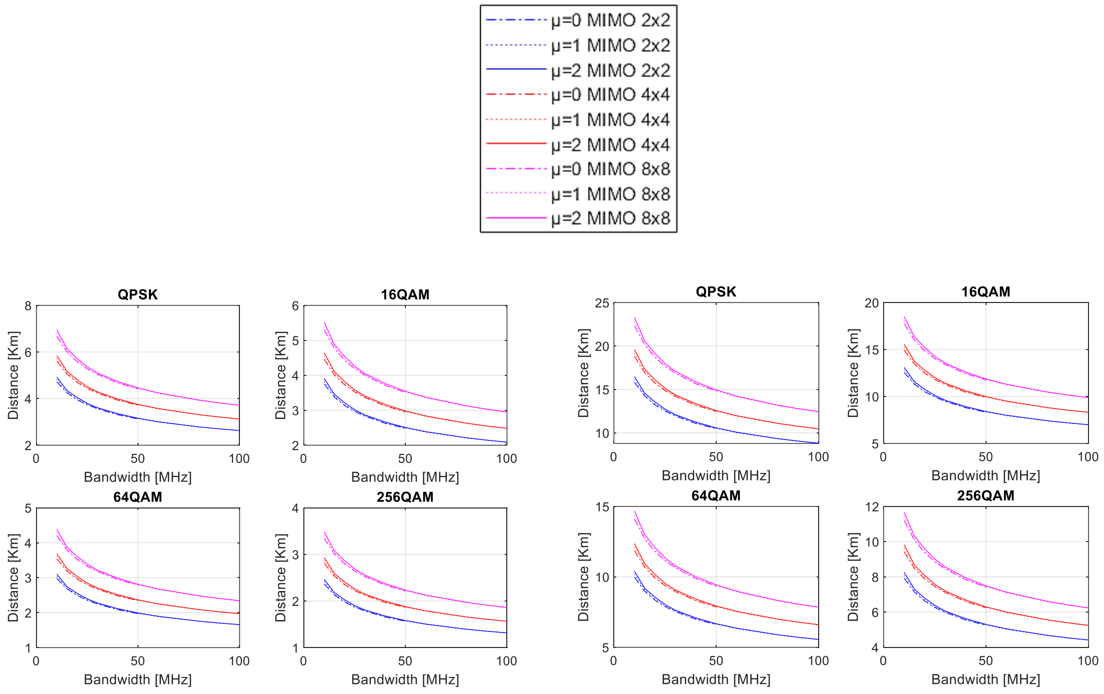

a) b)

Figure 4.6 - Maximum distance gNB-vehicles in RMa LOS a) UL and b) DL scenarios.

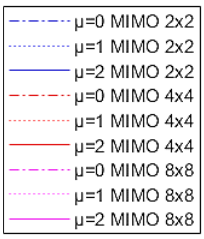

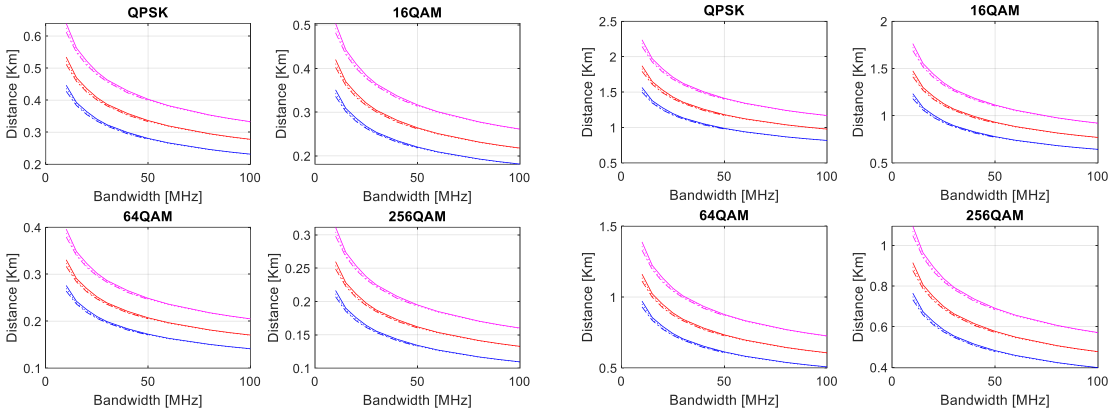

a) b)

Figure 4.7 - Maximum distance gNB-vehicles in RMa NLOS a) UL and b) DL scenarios.

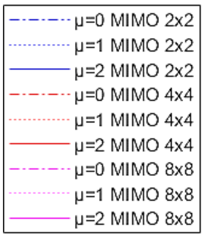

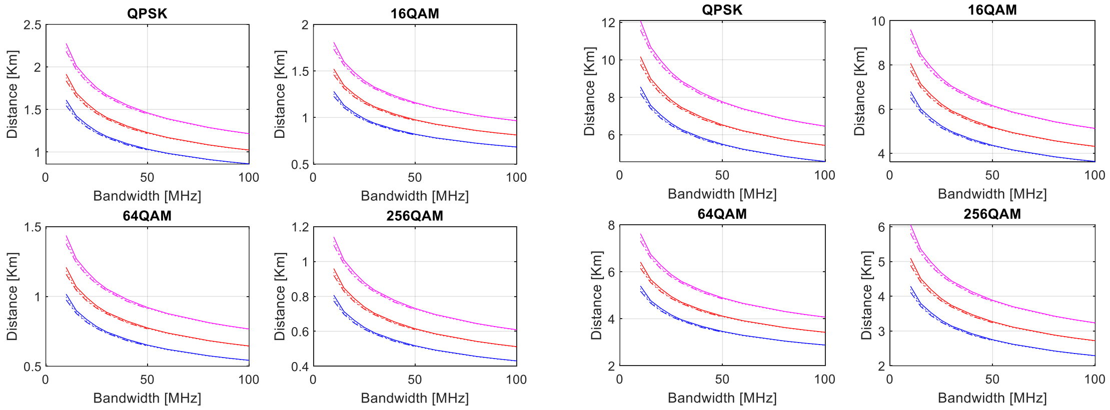

a) b)

Figure 4.8 - Maximum distance gNB-vehicles in UMa LOS a) UL and b) DL scenarios.

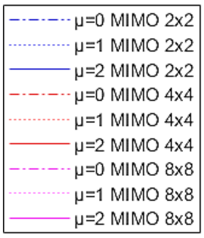

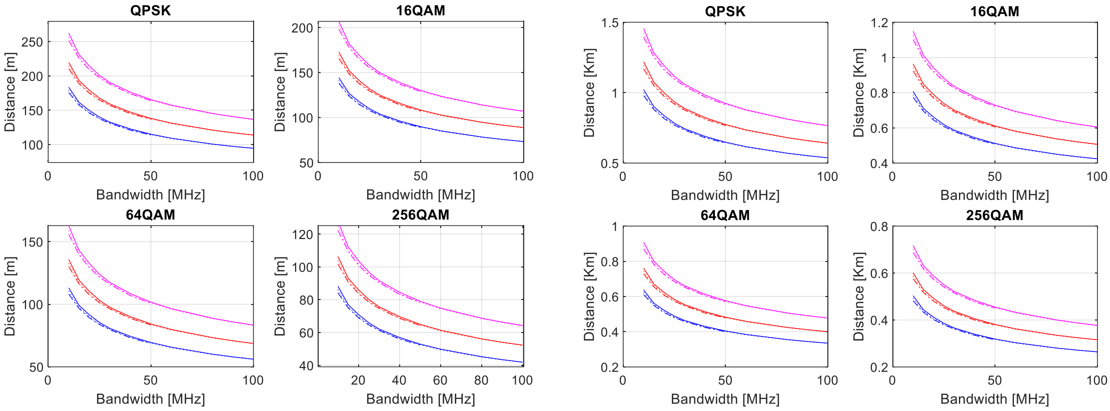

a) b)

Figure 4.9 - Maximum distance gNB-vehicles in UMa NLOS a) UL and b) DL scenarios.

4.1.7. *Inter-site distance*

Knowing the cell-range and vehicle-range, it is possible to compute the number of sites and cells necessary to cover the entire highway, for both propagation environments. ISD distance was calculate according to Equation 3-25, explained in the section 3.2.6, and the results are presented in Annex D, by Figure C.1, Figure C.2, Figure C.3 and Figure C.4. It is possible to analyse that the inter-site distance for RMa LOS scenarios reached very high values as maximum of 40 km in DL and 12 km in UL for QPSK modulation and MIMO 8x8 for μ=2 in 10 MHz BW. Instead, if the entire BW is used (100 MHz), the maximum reached ISD for the same scenarios are 21.55 km in DL and 6.43 km in UL, which corresponds to less than 1/3 of the previous distance. But, as the determining factors in this simulation are the scenarios in NLOS and UL, due to its very hostil environment propagation, RMa NLOS UL and UMa NLOS UL scenarios will be analysed. In the first one, the maximum ISD reached is 1.1 km for QPSK, MIMO 8x8, 10 MHz of BW and μ=2, and the minimum is 0.18 km for 256QAM, MIMO 2x2, 100 MHz of BW and μ=1. In the second one, the maximum ISD reached is 454.8 m for QPSK, MIMO 8x8, 10 MHz of BW and μ=2, and the minimum is 72.6 m for 256QAM, MIMO 2x2, 100 MHz of BW and μ=1, as can be seen in Figure 4.10; a) and b). Thus, as higher the modulation order, shorter is the cell and vehicle-range for higher BWs. MIMO gains bring the values upper in 3 dB each, and numerologies increase the distance as higher the subcarrier spacing but the differences are very small, few tens of meters and it is bigger as smaller the BW. For high BW configuration, smaller the difference in the distance ranges regarding the numerologies. Another important point analysed is that, from 10 to 50 MHz the difference among ISD values for different MIMO and numerologies configurations is higher than from 50 to 100 MHz.

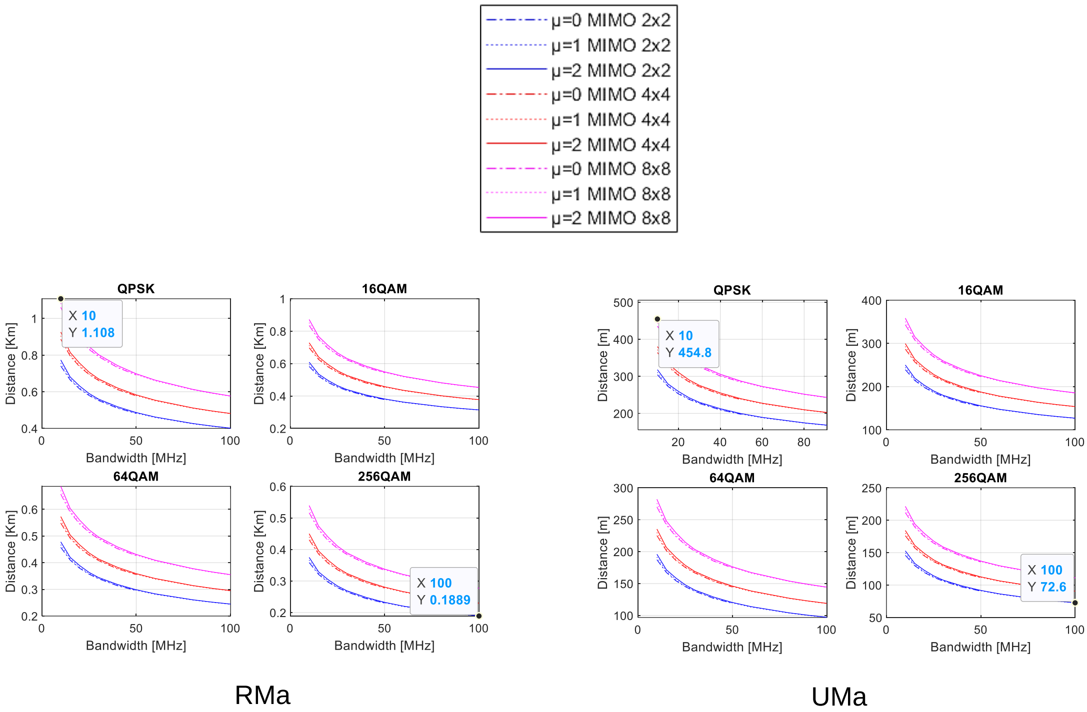

Figure 4.10 - Maximum and minimum ISD analysis in a) RMa NLOS UL and b) UMa NLOS UL scenarios

4.1.8. Number of sites

Using the ISD is possible to estimate the whole number of sites necessary to cover the highways assumed by this thesis. As it was defined on Equation 3-26, the total number of sites is calculated as the division of the road lentgh per ISD value. The results are presented in Annex E, and to analyse the number of sites to cover the highway stretch. In RMa LOS scenarios, as the ISD is above 5 km in UL and DL, the division of 5 km per its ISD reach only values below 1. For this reason, to present an integer number of sites in this scenario was considered the highest value of ISD (which is 40 km in RMa LOS DL, for QPSK modulation and μ=2 for 10 MHz), and divided 40 km per ISD, which result can be seen on Figure D.2. For the rest of the scenarios (RMa NLOS and UMa LOS and NLOS) the calculation of number of sites consideres the definition from Equation 3-26, and the results are presented by Figure D.3, Figure D.4 and Figure D.5. For UMa LOS DL scenario, for some network configurations the number of sites are presented below 1, once the ISD for this scenario is up to 20 km, thus the number of sites necessary in this scenario is 1 for the entire 5 km. It can be seen that the necessary number of sites increase with BW, modulation orders and MIMO configurations. In this methodology the numerologies do not result in major differences on the number of sites. The main issue is in NLOS UL scenarios, one conclude that if the entire BW is used (100 MHz) the number of sites necessary to cover the 5 km range from 13 to 25 sites in RMa and 20 to 70 sites in UMa, having impact the MIMO gains, and expressively according the modulation orders. Therefore, the number of cells would be 2 times the number of sites, reaching 140 cells for UMa NLOS UL scenario. The numbers can be analyse in Annex E.

4.1.9. Number of cells per km

The number of cells is considered as 2 times the number of sites, as explained on section 3.2.6. Thus, the number of cells per km was computed according to the Equation 3-27, except for RMa LOS UL and DL scenarios where the number of sites considered for the entire road length is 1, and the number of cells is 2. Results are presented in Annex F. For RMa NLOS scenario, Figure E.1, it can be seen an expressively increase in the number of cells per km if compared to RMa LOS, reaching 5 cells/km in QPSK, 100 MHz and MIMO 2x2, and more than 10 cells/km for 256QAM, once for this modulation the cell and vehicle-ranges are much shorter. In UMa LOS DL, Figure E.2 b), results presented values below 1, once the ISD in this scenario is mostly above 5 km and consequently the number of sites calculate is less than 1 for the 5 km stretch and for all network configurations as show in Figure D.4, except for 64QAM, MIMO 2x2, 100 MHz and 256QAM, MIMO 2x2, above 50 MHz and MIMO 4x4 above 80 MHz. Instead, for UMa LOS UL scenario, for QPSK it requires at least 1 cell per km and 2, at least the double for 256QAM in all MIMO configurations. For UMa NLOS scenario, as expected the number of cells per km is significantly higher, due to its high fading and consequently short range, reaching at least 2 in QPSK and 4 for 256QAM, 100 MHz in DL, which is the double of UMa LOS UL scenario. And for UMa NLOS UL when the whole BW is used, the results are up to minimum of 8 cells/km for QPSK ad MIMO 8x8, and maximum of 27 cells/km for 256QAM and MIMO 2x2. Urban environments and NLOS communications, the number of cells per km presents to be expressively higher than the other scenarios, due to the increased number of multipaths regarding the ambient and the channel fading.

Moreover, when using the PL models for macro cells, the final number of cells in the road is very high compared to normal macro cells, especially in UMa NLOS UL scenarios that present requiring the biggest number of cells, due to the higher frequency which implies to higher levels of interference increasing PLes, and the lower transmitting power level considered in UL.

4.1.10. Number of vehicles per cell

Knowing the number of cells per km and the number of vehicles per km, it is possible to predict the number of vehicles that are covered per each cell, being results presented in Annex G. The maximum number of vehicles per cell are computed for each scenario (RMa and UMa LOS DL).

4.2. Results by capacity

As explained on section 3.3, the radio planning by capacity was simulated according to the flowchart presented in Figure 3.5.

4.2.1. Vehicles density estimation

The first KPI required to calculate capacity, is the number of users, in this case connected vehicles. To compute this parameter, the most suitable model was used, to compute real numbers of vehicles at the highways in both propagation environments. This work was made using an online platform called “TomTom move traffic stats” [42], this platform shows plenty of statistics computations regarding the traffic road around the world, besides of current speed, time of travel and as more relevant for this study, number of vehicles. First, was chosen a highway stretch for urban and another one for rural environment, around Lisbon in Portugal, according to [43]. Figure 4.11 presents the highway for urban environment, and Figure 4.12, a highway for rural environment, both have 5 km of length, 6 lanes, 3 in each direction and maximum speed of 120 km/h.

According to [42], the busy hour in Lisbon is around 8 am and 6 pm, as presented by Figure 4.13. Considering the rush times, is necessary to know the number of vehicles on that periods. As the platform of traffic road was used on free trial version, the dates available to generate reports were from 01/04/2019 to 30/04/2019, all the time, all days, all weeks, so reports were generated for the respective routes in both directions, in both rush times. From the reports that were generated, the average number of vehicles that passes on the highways were computed and presented in Table 4.4 and Table 4.5. It was considered the number of vehicles in both directions, in-out Lisbon, in morning and afternoon, in urban and rural environments and computed the average number of vehicles in 5 km, in one hour. Having the average number of vehicles on the whole patch of 5 km in 1 hour and the average travel time, it is possible to estimate the number of vehicles per km per second, that convert the number of vehicles on the road in 1 hour into number of vehicles per second, and through the travel time (T) compute the total number of vehicles in one second in 1 km, which parameters are presented by Table 4.6 and Table 4.7. To the result, is applied a percentage of penetration, which refers to the vehicles with some relevant level of automation or connection to telecommunications network. To the urban highway is applied 80%, and to rural highway 40%, then both are divided per three, which correspond to the division though different telecommunications operators, the result is the final number of vehicles per km that will be used to compute the traffic load and is presented for both propagation environments by Table 4.8.

Figure 4.11 - Urban environment A1 highway stretch (extracted from [42]).

Figure 4.12 - Rural environment A9 highway stretch (extracted from [42]).

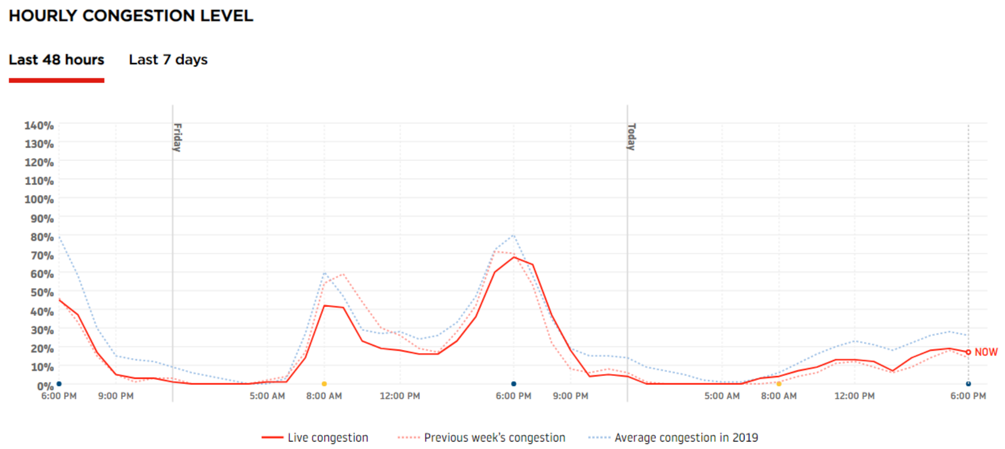

Figure 4.13 - Rush traffic time in Lisbon (extracted from [42]).

Table 4.4 – Average number of vehicles in 5 km in 1 hour for urban environment

Time	Outside -> Inside	Inside -> Outside
8:00-9:00	3672	2788
18:00-19:00	3724	3457
Average in one direction	3698	3122.5
Average Nº of vehicles in urban environment in 5 km in 1 h		6821

Table 4.5 – Average number of vehicles in 5 km in 1 hour for rural environment.

Time	Outside -> Inside	Inside -> Outside
8:00-9:00	3921	1671
18:00-19:00	2616	3393
Average in one direction	3268.5	2532
Average Nº of vehicles in rural environment in 5 km in 1 h		5801

Table 4.6 – Average number of vehicles per km on urban highway.

URBAN	Outside -> Inside	Inside -> Outside
Average travel time of 5 km (T) [sec]	254.15	173.50
Average Speed (km/h)	71.00	104
Average Nº of vehicles in 1 h	3698	3122.5
Average Nº of vehicles getting into the road per second	1.027	0.867
Average Nº of vehicles in 5 km	262	151
Average Nº of vehicles in 1 km (considering 3 lanes)	53	31
Average Nº of vehicles per km/sec including both directions		84 veic/km

Table 4.7 - Average number of vehicles per km on rural highway.

RURAL	Outside -> Inside	Inside -> Outside
Average travel time of 5 km [sec]	199.28	165.34
Average Speed (km/h)	91.00	109
Average Nº of vehicles in 1 h	3268.5	2532
Average Nº of vehicles getting into the road per second	0.907	0.703
Average Nº of vehicles in 5 km	181	117
Average Nº of vehicles in 1 km (considering 3 lanes)	37	24
Average Nº of vehicles per km/sec including both directions		61 veic/km

Table 4.8 - Final number of vehicles per km.

	$N_{v/km}^{cap}$	Percentage of CAV	Final Nº of vehicles per km
Urban highway	84	80%	23
Rural highway	61	40%	9

4.2.2. Service data rate and percentage definition

As explained on section 2.5 the vehicular services considered on this study are the ones defined by 5G MOBIX project. The services aim to involve a set of possible scenarios in low and high level of data traffic. As presented by Table 2.8, the values for user data rates were considered in a general perspective of the main use cases categories, without get into each user stories defined on the project.

In this section, the number of vehicles for each service is defined, used to compute the demanded data traffic on both proposed highways. From the final number of vehicles per km defined by Table 4.8, a percentage is attributed considering that no vehicle performs more than one category, and some of categories has bigger penetration than others according to their characteristics, aiming to compute the entire user data traffic load per km in both highways' paths pre-defined. As can be seen on Table 4.9, a percentage of 3% is defined for vehicle platooning, once it is not a service that will be common on the roads instead corporative vehicles running in platooning and as just the first vehicle will guide the others just that one will be requiring data from the network. To advanced driving category an 80% is applied, once it covers the most common types of services and manoeuvres that all type of vehicles will perform and most probably will be the majority service that will be used on the roads. For the extended sensors service 15% is applied, considering that this category includes live video stream and that only vehicles with high level of automation will be able to require this service. For remote driving and vehicle QoS support, 1% is applied, considering that only vehicles in specific situations will be performing these services, as shuttles and travel transports.

Table 4.9 – Proposed percentage attributed for each service category.

Services	Percentage attributed
Vehicle platooning	3%
Advanced driving	80%
Extended sensors	15%
Remote driving	1%
Vehicle QoS support	1%

The defined percentages of each service category from Table 4.9 is multiplied to the final number of vehicles per km for urban and rural environments from Table 4.8. As the user data rate for each service category is defined for minimum and maximum throughput in UL and DL on Table 2.8, a total user data rate per km is calculated for the final number of vehicles per km.

4.2.3. Total user data rate per km

The vehicles density was estimated as 23 and 9 vehicles per km, for urban and rural environment respectively, as can be seen on Table 4.8. The service percentages defined by Table 4.9 were multiplied to the previous numbers of vehicles per km (23 and 9) and reached a number of vehicles per service per km. The service user data rates defined by Table 2.8 as minimum and maximum data rates in UL and DL, were multiplied to the number of vehicles per service per km and reached the total user data rate per km presented by Table 4.10 and Table 4.11 . As can be seen, the minimum amount of data in UL of 5G-MOBIX services, considering the vehicles traffic in one urban road of Lisbon is 108.33 Mbps and maximum of 2.82 Gbps. And considering the rural road is about minimum of 42.39 Mbps and maximum of 1.1 Gbps. It is also possible to analyse that all services present very high difference between minimum and maximum data rates, for example, for Advanced driving category service from Table 4.10, presents the minimum data rate of 3.68 Mbps and maximum of 1840 Mbps, 500 times more, requiring much bigger amount of radio resources from the network if the peak data rate is reached, differing a lot the radio planning when the vehicles require minimum or maximum data rates. For this reason, the network capacity is simulated aiming to compare it to the total user data rate estimated.

Table 4.10 – User data rate per service per km on urban environment.

	Minimum [Mbps]		Maximum [Mbps]	
Services	**UL**	**DL**	**UL**	**DL**
Vehicle platooning	69	34.5	138	69
Advanced driving	3.68	3.68	1840	1840
Extended sensors	34.5	34.5	690	690
Remote driving	0.23	0.23	46	23
Vehicle QoS support	0.92	1.84	115	23
Total	108.33	74.75	2829	2645

Table 4.11 – User data rate per service per km on rural environment.

	Minimum [Mbps]		Maximum [Mbps]	
Services	**UL**	**DL**	**UL**	**DL**
Vehicle platooning	27	13.5	54	27
Advanced driving	1.44	1.44	720	720
Extended sensors	13.5	13.5	270	270
Remote driving	0.09	0.09	18	9
Vehicle QoS support	0.36	0.72	45	9
Total	42.39	29.25	1107	1035

4.2.4. Network capacity simulation

As defined by [44], the maximum supported UE user data rate, here called as network capacity was simulated according to Equation 3-29. Changing Bandwidth, numerology, modulation order, MIMO configurations, propagation environment and communication direction, one gnerates results presented by Figure 4.14, Figure 4.15 and Figure 4.16. As was explained on section 2.4.3, the number of RB available in 5G-NR in UL and DL are kept the same, variating only the $OH^{(j)}$, for this reason, the results presented below do not show major differences between UL and DL. Differences are more expressively as function of BW and the modulation order, for 256QAM, μ=1 in 100 MHz the difference is about 80 Mbps, and for 10 MHz is about 5 Mbps. As can be seen also, the peak data rate for MIMO 8x8 is around 5 Gbps (Figure 4.16) and 1.2 Gbps for MIMO 2x2 (Figure 4.14), separately UL of DL, where as the n78 band is TDD mode, and the slot formats 0 and 1 are used, that entire frame is used for each communication direction, reaching for example maximum of 5+5 Gbps. The influence of the numerology in the network capacity is according to the BW and the modulation order, it goes from 2 to 13 Mbps, to 10 and 100 MHz, respectively. For capacity analysis is necessary to compare the network capacity to the total user data rate required from the vehicles to the network, thus the total user data rate from previous section was multiplied per cell-range and computed traffic load of each cell, which is presented on the next section.

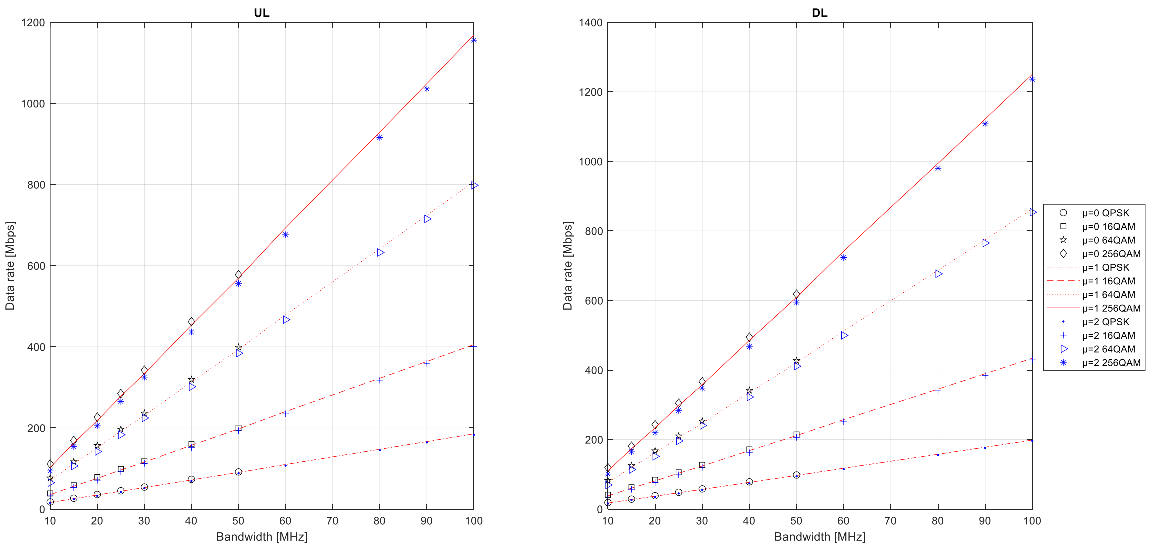

Figure 4.14 - Maximum supported user data rate for MIMO 2x2

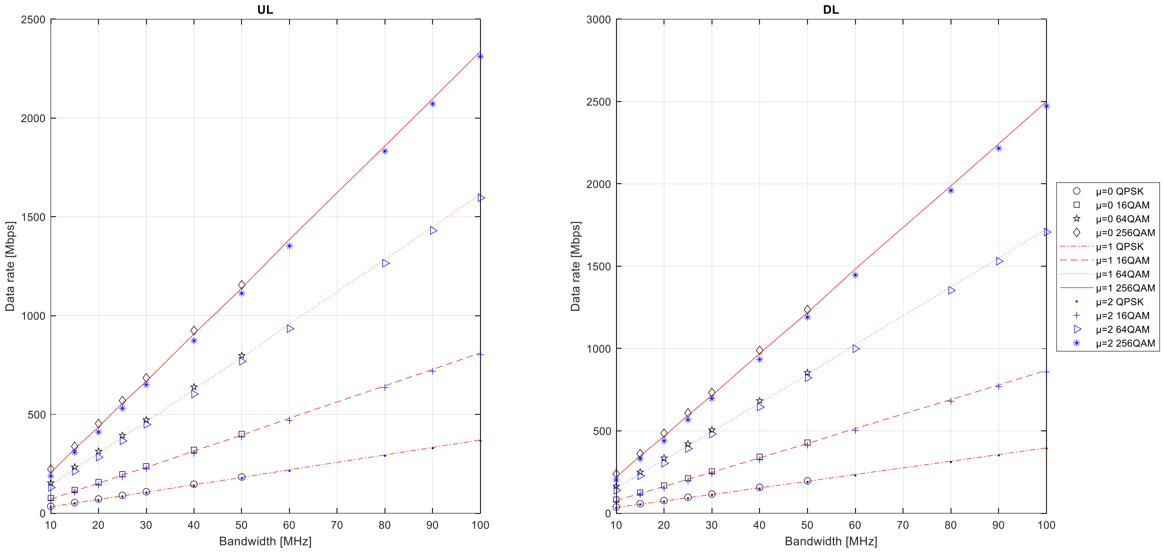

Figure 4.15 - Maximum supported user data rate for MIMO 4x4

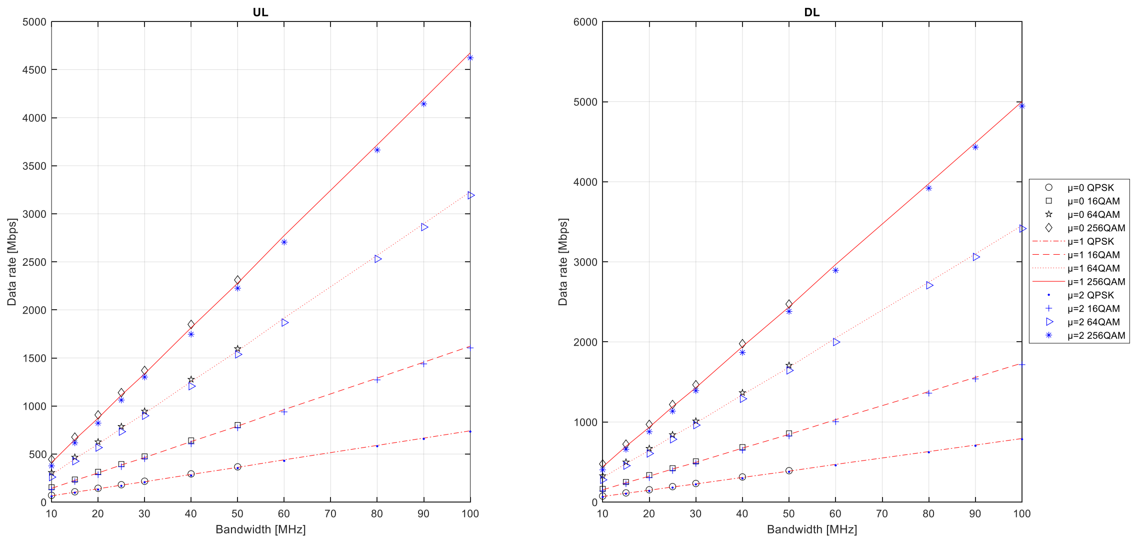

Figure 4.16 - Maximum supported user data rate for MIMO 8x8

4.2.5. Traffic load computation

The traffic load computation was made through the Equation 3-32 and explained on section 3.3.3, which results are presented on Annex H. The traffic load was computed when the vehicles require minimum and maximum data rates according to each scenario, thus, is possible to plan the network differently when the traffic density is in low data rate or high data rate and chose different network parameters and physical layer configurations. As can be seen in Figure G.1 to Figure G.8, the highest traffic load present itself when the cell presents highest cell-range, or in UL, when the vehicles present the highest vehicles-range, although the traffic load for RMa LOS DL is lower than for UMa LOS DL, this happens due to the number of vehicles per km in urban environment being higher than in rural environment. It can be seen also that the traffic load increase as lower the modulation order, once the range is longer. It increases as higher numerology and as higher the number of MIMO layers. The traffic load decrease with the BW once, as higher the number of RB, shorter is the cell-range or the vehicle range. Like this, is possible to analyse the amount of data that is required to the network in each case and chose the correct network configurations. To analyse case by case, next step is to divide the network capacity per cell, to traffic load per cell as follow.

4.2.6. Cell Ratio

Dividing the network capacity per traffic load per cell, cell-ratio is computed according to Equation 3-33Equation 3-34 and Figure 3.6, as explained on section 3.3.4. When the division's result is above number 1, it means that the network capacity is higher than the traffic load, and thus the cell is limited by coverage and can handle with the demanded data traffic from the vehicles. Instead, if the division's result is below or equal to 1, it means that the cell is working on the limit or it's up to its capacity, in another words is limited by capacity and a new cell-range and vehicles-range need to be calculated by decreasing the distance between gNB and vehicles and reach fewer number of vehicles, increasing network capacity's availability. The results of the cell-ratio simulation for each scenario are presented by Figure 4.17 to Figure 4.24. In all simulations a line was drawn through number 1 at cell-ratio axis and made zoom in showing where the graphics intercept that line, it means that for all scenarios where the graphics are below 1 the cell is limited by capacity and is going to be necessary to recalculate the cell and vehicles-range. For example, on Figure 4.17, for RMa LOS DL scenario, the cell-ratio calculated for maximum user data rate are all below 1, it means that for all those scenarios cell-range and vehicles-range is going to need being calculated again, instead, for this same scenario, but for the cell-ratio for minimum user data rate the results are not all below 1, for MIMO 2x2 and 256QAM is going to need being calculate a new cell-range until 20 MHz, in MIMO 4x4 64QAM only until 40 MHz and for MIMO 8x8 QPSK only until 60 MHz, as are indicated in the Figure 4.17 below. This methodology is applied in all simulations of cell-ratio presented as follow.

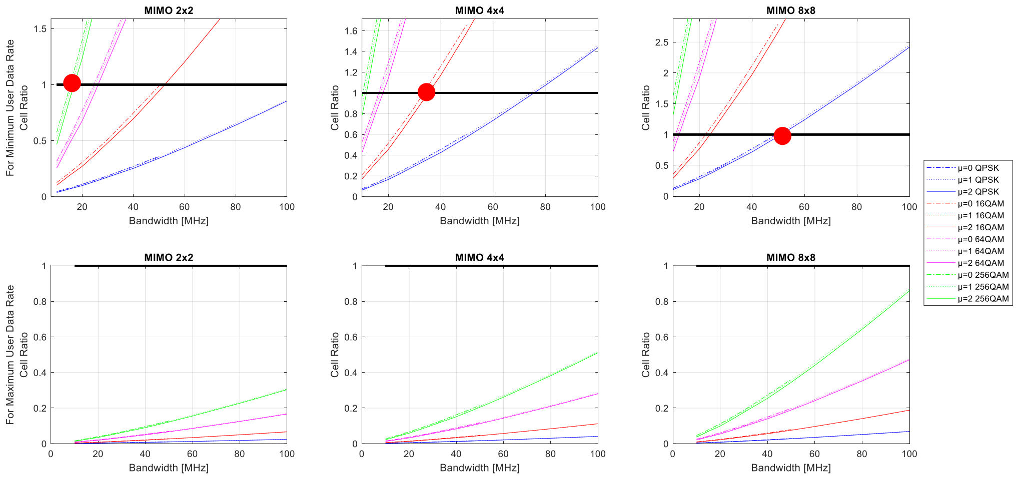

Figure 4.17 - Cell-ratio on RMa LOS DL scenario

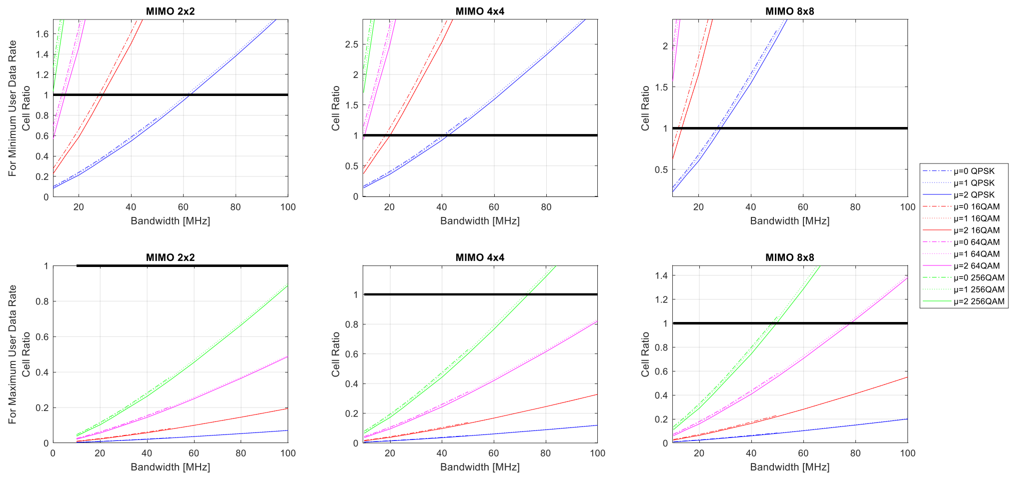

Figure 4.18 - Cell-ratio on RMa LOS UL scenario

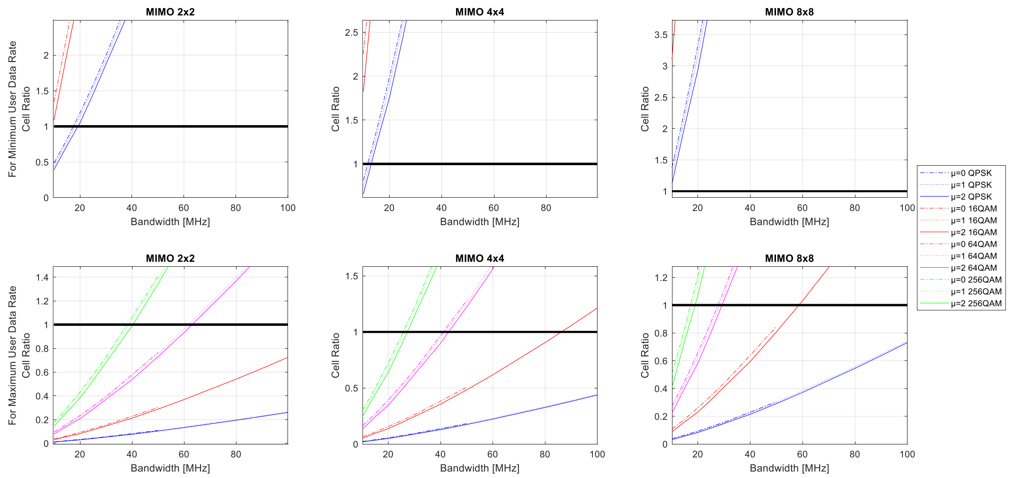

Figure 4.19 - Cell-ratio on RMa NLOS DL scenario

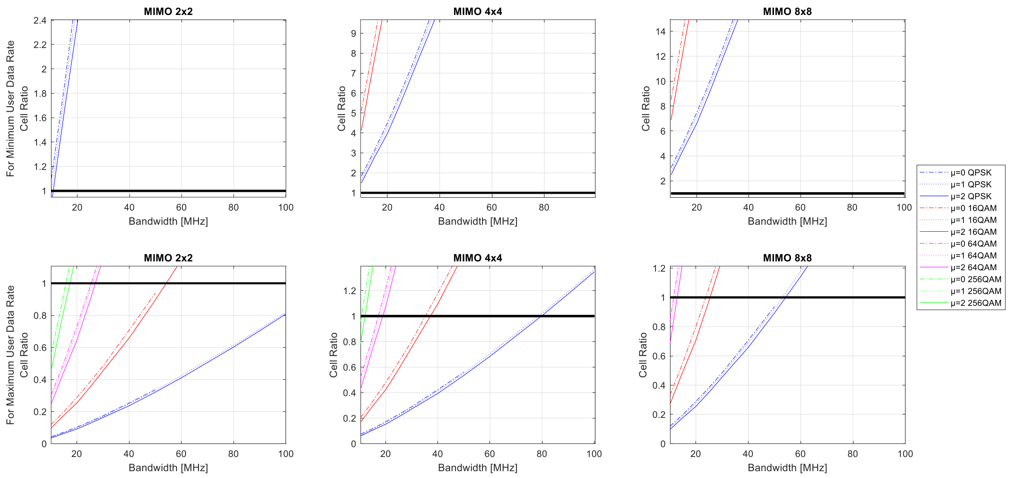

Figure 4.20 - Cell-ratio on RMa NLOS UL scenario

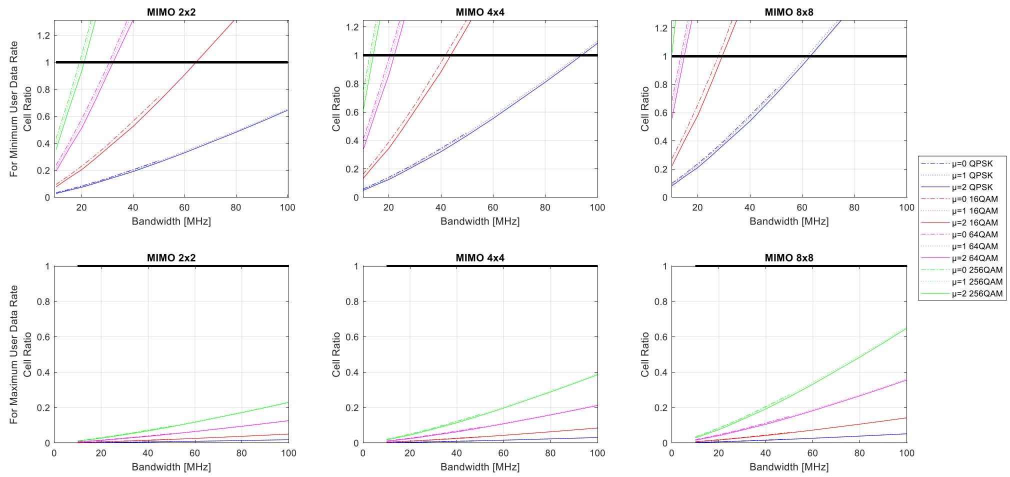

Figure 4.21 - Cell-ratio on UMa LOS DL scenario

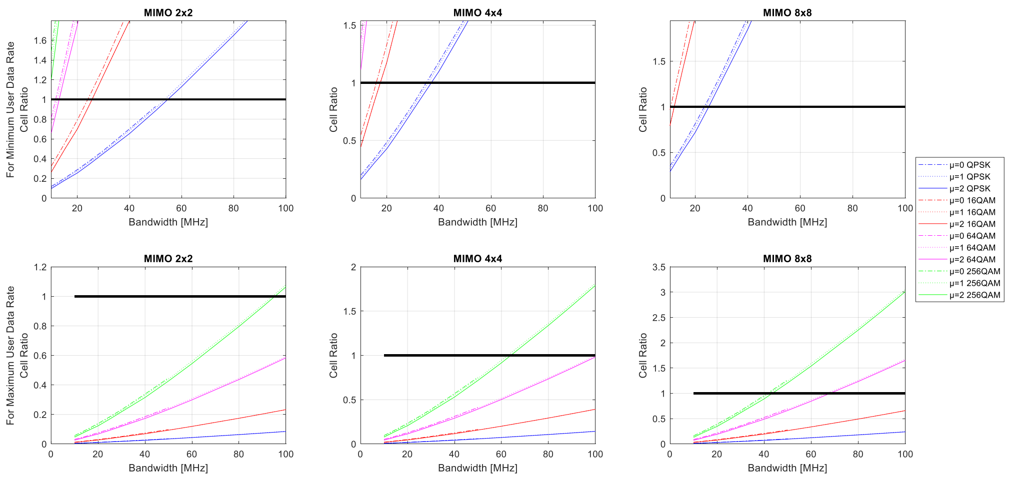

Figure 4.22 - Cell-ratio on UMa LOS UL scenario

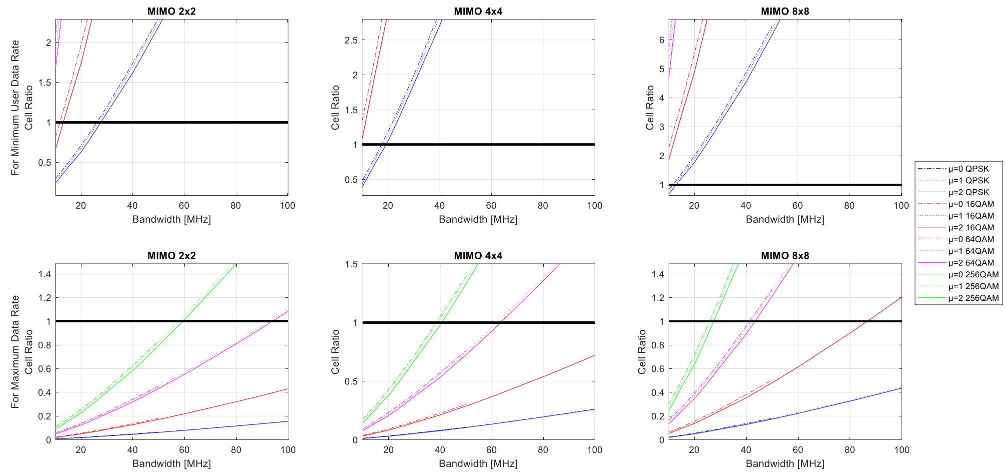

Figure 4.23 - Cell-ratio on UMa NLOS DL scenario

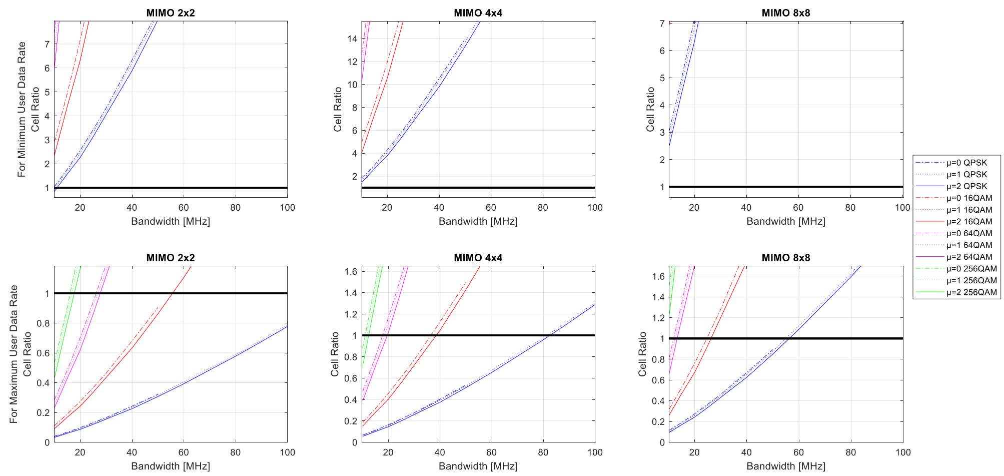

Figure 4.24 - Cell-ratio on UMa NLOS UL scenario

4.2.7. Cell-range and vehicles-range limit calculation

Analysing the cell-ratio computed for all scenarios previously was possible to analyse for each case where the cell was limited by capacity that become necessary to compute new cells and vehicles range. To simulate this new parameter the methodology is proposed in section 3.3.5. The results are presented by Figure 4.25, Figure 4.26, Figure 4.27 and Figure 4.28, for RMa and UMa, LOS and NLOS scenarios, for minimum and maximum user data rate. To simplify this methodology, the Equation 3-35 was applied for all scenarios, not only for those ones where the cell-ratio is below 1, and yes also for when cell-ratio is above 1. Like this, was necessary to approximate to the spots on those curves which require to calculate the new cell and vehicles-range considering the cell-ratios from LOS scenarios, once NLOS are mostly limited by coverage.

In Figure 4.25, cell-range is calculated for rural environment considering the cell-ratio of Figure 4.17, where for maximum user data rate the cell presented being completely limited by capacity, and for minimum user data rate, case by case is analysed. For MIMO 2x2, the modulations QPSK, 16QAM, 64QAM and 256QAM are limited on 100, 60, 30 and 20 MHz, as signalized by red circles, it means that these BWs are the limitations of the cell-range by capacity, and that the cell-range must be that distance or below. Above these BWs the cell-range must be considered the ones calculate by coverage methodology. Following the same logic, the limitations for all other scenarios are presented also as red circles in the respective figures. If any modulation order is not signalized it means that for that modulation, the limitation is entirely by coverage, as in MIMO 8x8 where 256QAM is not circled. As also on maximum user data rate curves, where none curve present red circles, due to the coverage limitation.

Is possible to analyse that the distances of the follow results are increasing with the BW regarding Equation 3-35, where the distances that are shown are the maximum communication distance to ensure that the total user data rate doesn't overtake 80% of the network capacity, thus when Figure 4.25 is analysed, for minimum user data rate, MIMO 2x2 and 256QAM, in 20 MHz it is limited between 6 and 7 km, and when confronted to Figure 4.6 b), which is the cell-range calculated by coverage method, for the same scenario the cell-range is between 10 and 11 km, overtaking the capacity limitation for this study. Thus, when 20 MHz BW, or lower, is used, the maximum cell-range that should be applied is from 3 to 7 km, according to the numerology. The same principle it is used when analysed QPSK modulation, instead of 256QAM. Still in Figure 4.25, for QPSK, the cell limit is on 100 MHz, it means that for this scenario, this modulation is completely limited by capacity, and the maximum cell-range acceptable is around 5 km, differently of 9 km from coverage planning. For all scenarios, the analysis is equal, and is possible to see that the majority cell and vehicles ranges limitations are for maximum user data rate and on low BWs for minimum user data rate. As higher the user data rate, more radio resources are required from the network and more the cell is going to be limited by capacity. If the amount of data does not overtake the network capacity, thus the cell is able to provide the correct amount of radio resources to connected vehicles. The 5G-NR is flexible to change its network configurations automatically according to the requests from the 5G vehicles' terminals. For example, if QPSK and MIMO 2x2 is used, in RMa LOS in DL to send control data, low BWs are enough to provide radio resources. For the video stream in 4K, higher BWs are necessary and 64 or 256QAM modulations can fit better the necessity. The results below show the distance limitations according to the amount of data that is required and the radio resources available to the vehicles, providing inputs for a future flexible and smarter radio planning. For example, if the vehicles' speed is known, it is possible to compute the distance to the gNB, and like this change the modulation order, numerology and BW according to the necessity.

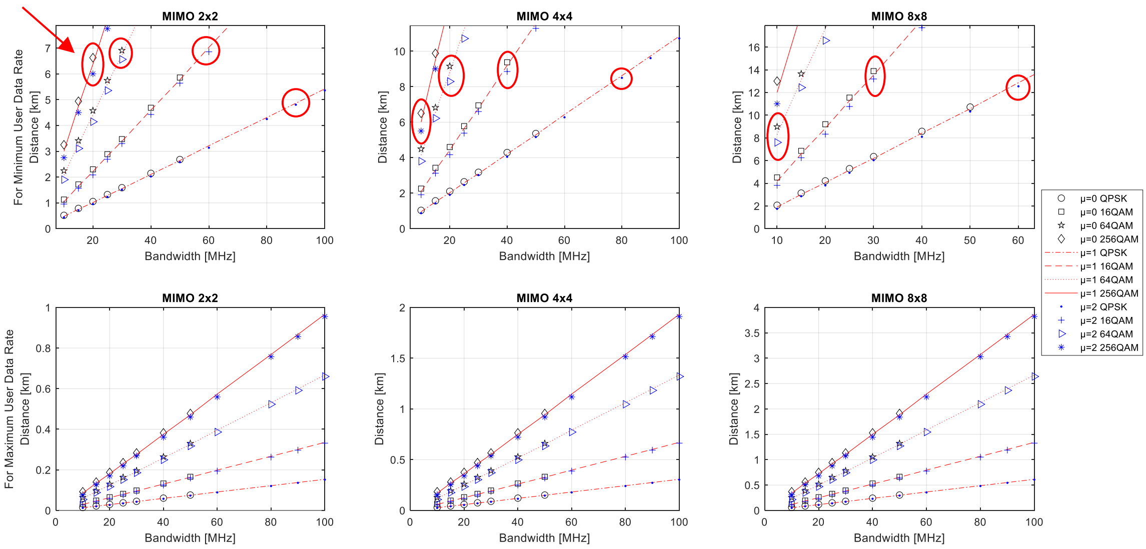

Figure 4.25 - Cell-range limited by capacity on RMa DL scenario

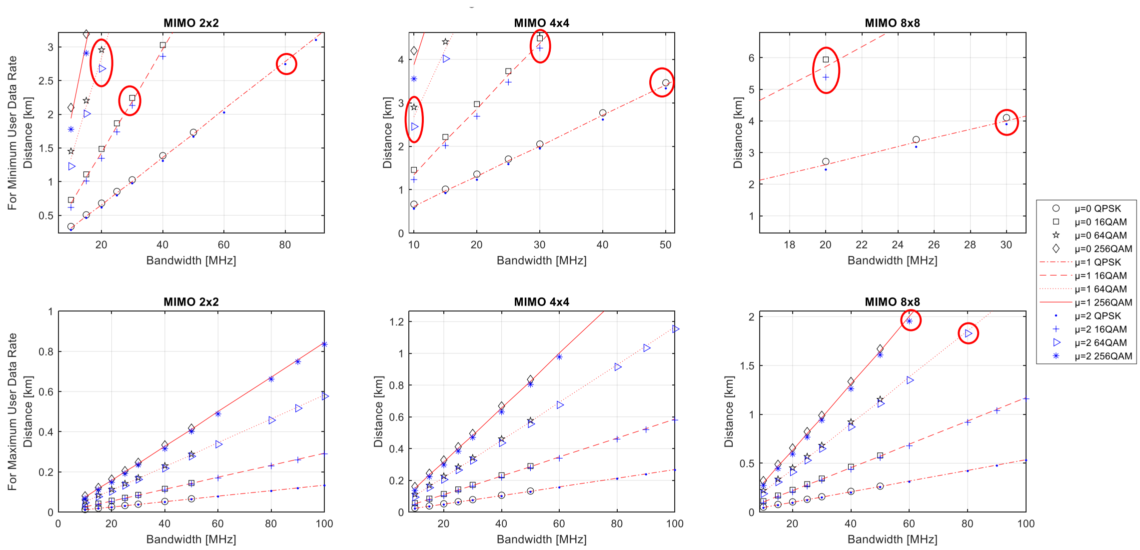

Figure 4.26 - Vehicles-range limited by capacity on RMa UL scenario

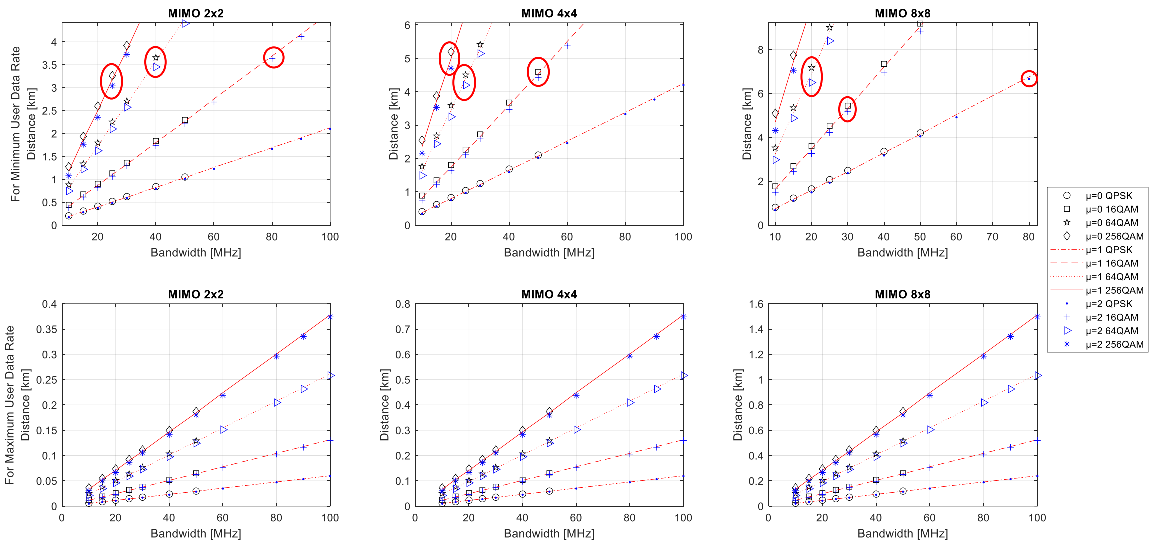

Figure 4.27 - Cell-range limited by capacity on UMa DL scenario

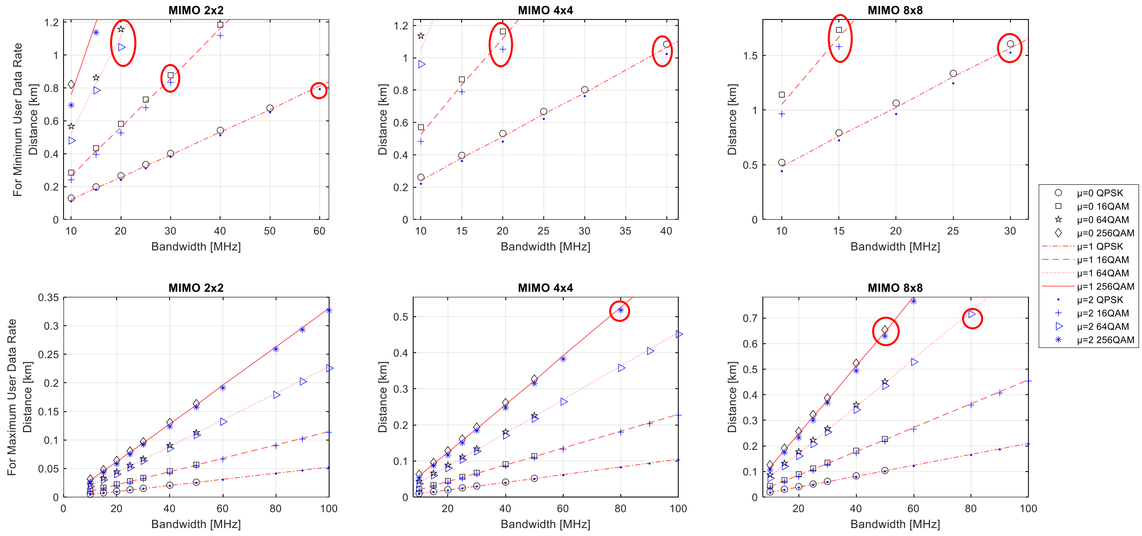

Figure 4.28 – Vehicles-range limited by capacity on UMa UL scenario

4.2.8. Final number of sites

As the new cell-range and vehicles-range were calculated and presented on previous section, the new ISD is also calculated following the same method. The results are presented in Annex J, by Figure I.1 to Figure I.4, for the same scenarios zoomed in on section 4.2.5. The results are the inputs to calculate the final and desired number of sites for the entire road stretch of 5 km. The minimum number of sites is computed for all scenarios (RMa and UMa, UL and DL), which results are presented by Figure 4.29, Figure 4.30, Figure 4.31 and Figure 4.32. As explained before, in the cell-range and vehicles-range limitation simulation, were highlighted in the graphics with red circles, where is the distance capacity limitation for each scenario, according to the user data rate (minimum and maximum), MIMO configuration, modulation order, numerology and BW considering the cell-ratio computation from section 4.2.6. The same is performed on the minimum number of sites computation results highlighted by black arrows, as can be seen. The normal simulations, without the arrows and no zoom in are presented on Annex K. The arrows signalize the BW where, for each modulation order and numerology, the cell is limited by capacity and it means that until that BW the cell can support the minimum or maximum user data rate. From that BW ahead the cell is limited by coverage and then the number of sites considered are the ones presented on section 4.1.8, always prevailing the greatest number of sites. Some simulations presented in this section doesn't show any arrow in the graphics due to the cell being totally limited by capacity, as can be seen in cell-ratio simulations graphics mainly for maximum user data rate. Some curves present values for the number of sites less than 1, regarding the range limitation being more than 5 km. For these results, 1 site for the entire 5 km is considered.

As can be seen in Figure 4.29, the number of sites were simulated for rural environment in DL scenario, considering the cell-range and vehicles-range limit calculation for the same scenario. When minimum user data rate is required, QPSK modulation is limited in 100, 80 and 60 MHz for MIMO 2x2, 4x4 and 8x8 respectively. As the results present values below 1, it means that is necessary at least 1 site to provide capacity to the entire 5 km. Thus, if these results are compared to the number of sites calculated by coverage methodology for the same scenario, in Annex E, the previous number of sites calculated was around 2~3 sites per 40 km for MIMO 2x2, 4x4 and 8x8, it means that 1 site per 5 km is necessary to provide coverage and capacity in RMa DL scenario, when QPSK, MIMO 2x2, 4x4 and 8x8 is used, and It can increase according to the BW applied, for example, for MIMO 4x4 if QPSK is used on 10 MHz, 3 sites are necessary to provide enough capacity for minimum user data rate and more than 100 for maximum user data rate. For V2X applications, for the network parameters must be used the flexibility provided from 5G-NR and change the radio resources according to the necessity. The results presented below show that the calculated number of sites can change abruptly with the required user data rate, thus, if the preferable number of sites is calculated for a scenario, when the scenario changes or purely the service, the number of sites will not be accurate, being impossible to estimate the best number, because this will depend on the vehicles traffic and consequently total data traffic. Therefore, for this study it is possible to conclude that RMa and UMa UL (using 100 MHz), are the most determining scenarios in radio planning due to the shorter range, being the more suitable number of sites presented in Table 4.12.

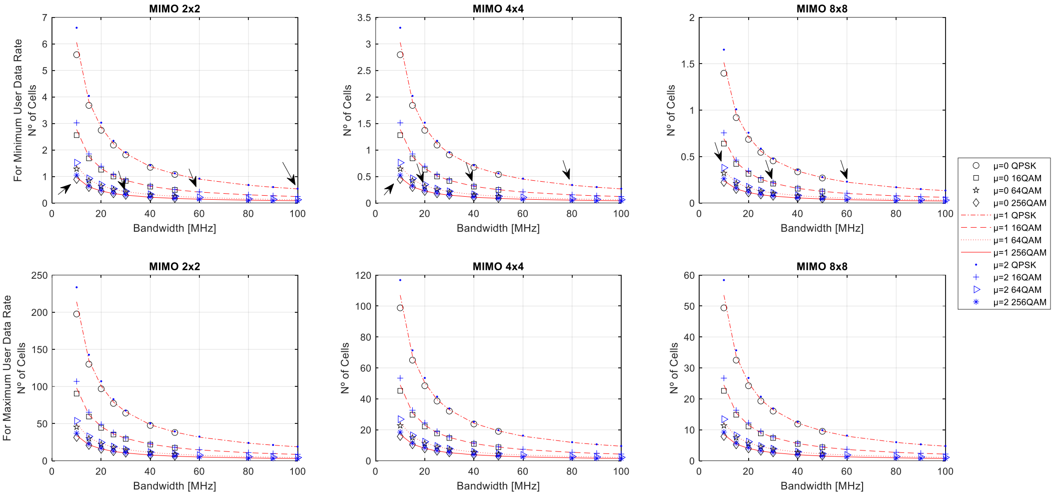

Figure 4.29 - Number of cells by capacity on RMa DL scenario

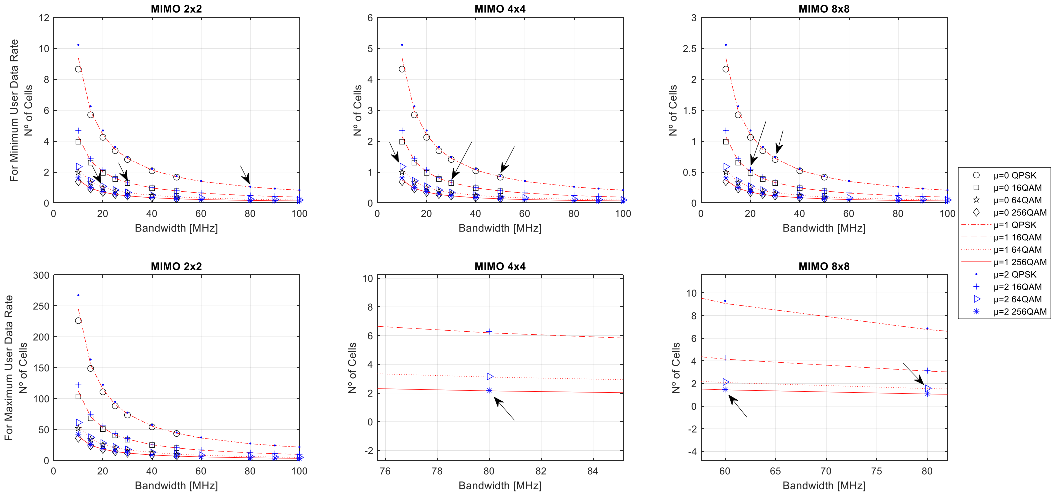

Figure 4.30 - Number of cells by capacity on RMa UL scenario

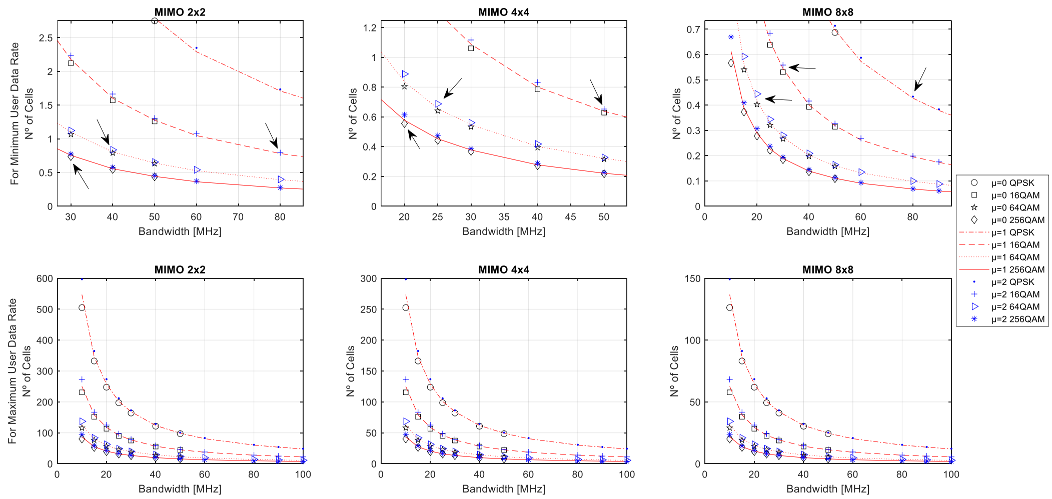

Figure 4.31 - Number of cells by capacity on UMa DL scenario

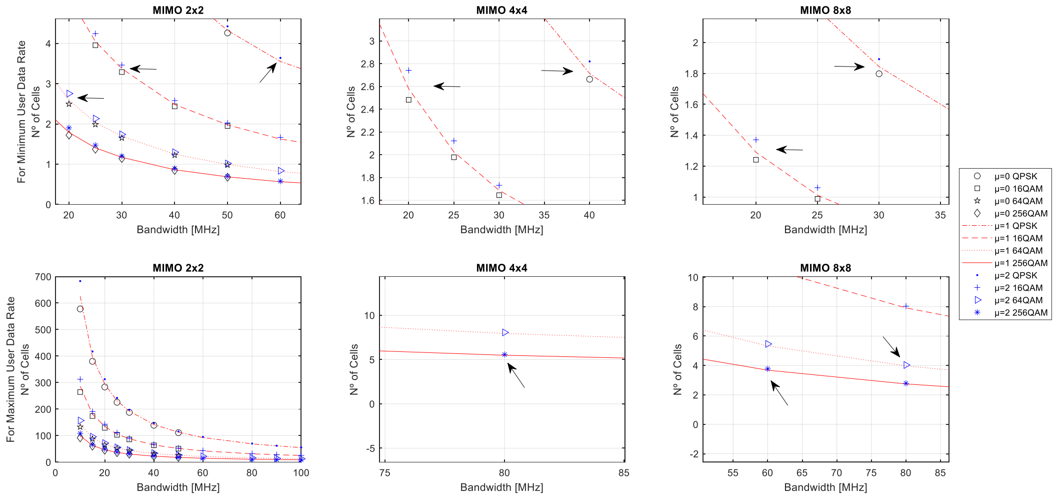

Figure 4.32 - Number of cells by capacity on UMa UL scenario

In Table 4.12, is presented the final number of sites analysed by coverage and capacity according to the methodology explained previously. It is highlighted, those values defined by coverage, and the rest of the values are defined by capacity method, following the cell-ratio calculated on section 4.2.6, and analysing the vehicles-range limitation. Thus, for 100 MHz, when minimum user data rate is required, the cells are limited entirely by coverage. This means that the total user data traffic generated by vehicles in both highways fits in 100 MHz and the network capacity can provide enough radio resources. Nevertheless, when maximum user data rate is required from the vehicles, only MIMO 4x4 256QAM and MIMO 8x8 64QAM and 256QAM are limited by coverage. For the rest of the network configurations the cells are limited by capacity, meaning that the network capacity is not able to provide enough radio resources for a certain defined distance to the entire amount of required data from the vehicles, and like this, they couldn't perform the V2X applications correctly as expectable. The number of sites for minimum user data rate increase as higher the modulation order and decrease as higher the number of MIMO antennas. However, the values for maximum user data rate decrease with modulation orders due to higher network capacity on 100 MHz. Instead, the defined by coverage highlighted results for maximum user data rate in RMa UL scenario, present higher number of sites than the logic sequence, demonstrating the consequence of the much higher network capacity of 64QAM and 256QAM in comparison to QPSK and 16QAM as can be seen on Annex E.

This simulation proves the complexity in 5G technology choosing a final number of sites considering CAV services once it presents a big gap between minimum and maximum user data rate, thus the worst-case scenario should be considered to guarantee that all vehicles are covered with enough V2X QoS.

Table 4.12 - Final number of sites by coverage and capacity for 100 MHz.

		QPSK	16QAM	64QAM	256QAM	
RMa UL	MIMO 2X2	9	11	14	18	For minimum user data rate
	MIMO 4X4	8	10	12	15	
	MIMO 8X8	7	8	10	13	
UMa UL	MIMO 2X2	4	5	6	7	
	MIMO 4X4	3	4	5	6	
	MIMO 8X8	3	3	4	5	
RMa UL	MIMO 2X2	22	10	5	4	For maximum user data rate
	MIMO 4X4	11	5	3	15	
	MIMO 8X8	6	3	10	13	
UMa UL	MIMO 2X2	56	26	13	9	
	MIMO 4X4	28	13	7	6	
	MIMO 8X8	14	7	4	5	

4.2.9. Number of vehicles per service

As can be seen on Table 2.8, the user data rate per service is quite diverse when analysed in UL and DL. Network capacity for V2X applications was analysed, comparing itself to the total user data rate generated by the vehicles considering all services together and considering that any vehicle performs more than one service simultaneously. This enables the radio network planning based on physical layer KPI. Nevertheless, in real life it is know that the autonomous vehicles will perform several types of services in parallel, due to this, the number of vehicles per service that the network is able to support was simulated and the results are presented on Annex I. As can be seen in Figure H.1 to Figure H.10, the services categories were simulated separately, computing the number of vehicles that could fit in each scenario. Table 2.8 show the service with highest user data rate is the Vehicle QoS Support in UL, with expected 500 Mbps. And the lowest, is the Advanced Driving with expected 0.2 Mbps in UL and DL. Analysing Figure H.10, MIMO 8x8, 256QAM modulation and 100 MHz BW, is possible to see that cells can support, for maximum user data rate, up to 9 vehicles, differing from 2 vehicles, if the same BW and modulation is used but with MIMO 2x2. Yet on MIMO 2x2 configuration, for maximum user data rate, the network can support only 1 vehicle. In the case that 64QAM and 256QAM modulations are used and if the vehicles are allocated from 50 MHz ahead. The same happen in the values for MIMO 4x4 and 8x8. If a line is cross 1, is possible to see that in all cases there will have a minimum configuration to enable the services to be provided. When the second scenario, Advanced Driving in DL is analysed in Figure H.3, as the user data rate is much lower than the previous service category, the number of vehicles that the network can support present to be higher. For minimum user data rate for this service, in MIMO 8x8, 256QAM and 100 MHz of BW the cells can support around 25 vehicles, and in the same case but MIMO 2x2, the minimum configuration to support at least 1 vehicle in this service is 20 MHz.

5. Conclusions

5G-NR is under development, enabling emerge technologies being deployed and becoming a reality to the society, as such CAV and V2X. Many market forecasts show the business opportunity over ITS development, ensuring more security, avoiding accidents, transforming the vehicular traffic as we know. The grown of CAV's market directly impacts the telecommunications infrastructures in a matter of data traffic, and consequently radio and core architecture. 5G-NR air interface brought plenty known features from the legacy technology 4G-LTE, as the conception of flexible and shared spectrum according to the service, the massive introduction of MIMO, high modulation orders mainly in DL, but with some differences as the introduction of the subcarrier spacings, highest available BWs, flexible spectrum in different duplex modes, different cyclic prefix and time slot usage, etc.

With the 5G evolution, European Commission has funded many projects to help CCAM development as 5G-MOBIX project. The service categories and their user data rates defined in this project were inputs for the simulation model in this thesis. Based on these inputs radio planning was performed by coverage and capacity, where KPIs were computed for minimum and maximum user data rates.

For radio coverage planning, the 3GPP PL model was used for RMa and UMa in LOS and NLOS scenarios. PL was used to calculate the RSS in UL and DL and the average results reached minimum of -95, -113, -94 and -126 dBm in UL, and -71, -89, -70 and -102 dBm in DL, for RMa LOS, RMa NLOS, UMa LOS and UMa NLOS, respectively. According to RSS variation by distance, sensitivity was simulated using SNR values from AWGN channel simulation using QPSK, 16QAM, 64QAM and 256QAM modulation orders, which 4, 8, 12 and 16 dB were considered respectively. The sensitivity simulation presented differentiation according to the BW, modulation order, MIMO configuration, and propagation scenario (RMa and UMa in LOS and NLOS). Sensitivity values increase with BW, modulation order and numerology reduction, decreasing as higher the number of layer of antennas in MIMO configuration and being higher in DL (vehicles) than in UL (gNB). In another words, the sensitivity itself is lower as the BW increase and it can be increased with more layers of antennas in MIMO configuration. $MAPL_{[dB](99\%)}$, was calculated considering log-normal fading margins for 99% of coverage at the cell-edge, reaching maximum of 152 dB in RMa LOS in DL for MIMO 8x8 and μ=2, and minimum of 100 dB in UMa NLOS in UL for MIMO 2x2 and μ=0. Another important parameter calculated was the maximum distance gNB-vehicles in DL (cell-range) and UL (vehicle-range), following the results from $MAPL_{[dB](99\%)}$ simulations in DL and UL. The results, present very high values in RMa LOS scenarios, and very short distances in UMa NLOS scenarios, reaching 23.28 km in RMa LOS DL for QPSK, MIMO 8x8 with μ=2, with 10 MHz of BW. And the minimum of almost 40 m in UMa NLOS UL, for 256QAM modulation, MIMO 2x2 with μ=1, and 100 MHz of BW. DL and UL coverage range were inputs to calculate ISD and the number of sites necessary to cover 5 km of highways in both RMa and UMa scenarios. In RMa LOS, as the ISD calculated was very high, the number of sites was calculated for 40 km, reaching 17 sites in UL, 256QAM, MIMO 2x2 and 100 MHz of BW. And 1 site, in DL, for QPSK, MIMO 8x8, μ=0 and 10 MHz of BW. By radio capacity planning vehicle traffic model was performed to compute the minimum and maximum total user data rate per scenario as the required vehicles throughput. Network capacity was simulated, considering all scenarios previously defined, in TDD duplex modes, considering slots formats 0 and 1 (i.e., DL and UL links separately). Thus, network capacity per cell was compared to the total user data rate reaching cell-ratio, which identified the scenarios where the cell was limited by capacity and coverage.

Results analysis of planning by capacity show that for the maximum user data rate, most scenarios required a new cell and vehicles range recalculation, once the cells presented themselves being completely limited by capacity, mainly in DL scenarios. As expected, lowest modulation orders are more limited by capacity. New cells and vehicles ranges were computed and signalized the limitations by capacity (using BW as reference) presented by cell-ratios. Results reveals that the maximum range reachable in a cell can provide radio resources to the entire number of vehicles without overtake 80% of the capacity. Using the ranges results, ISD and final number of sites were simulated, where the limitations were also signalized. The final number of sites shows that for 100 MHz, when minimum user data rate is required, the cells are limited entirely by coverage, it means that the total user data traffic generated by vehicles in both highways fits in 100 MHz and the network capacity can provide enough radio resources. Thus, for maximum user data rate, only MIMO 4x4 256QAM and MIMO 8x8 64QAM and 256QAM are limited by coverage, for the remaining cases cells are limited by capacity due to the longer range. As the last KPI, the number of vehicles per service supported were calculated, intending to analyse the network capacity facing the service categories minimum and maximum data rates, in DL and UL scenarios. Diverse number of vehicles per each service was presented, variating quite a lot regarding each BW.

5G-NR provides a useful and flexible air interface to develop CAV communications, enabling to reach tens of meters of cell-range in NLOS scenarios and kilometres in LOS scenarios. The cell capacity takes advantages of the modulation orders and numerologies providing enough resources when CAV require minimum user data rates, which scenarios were entirely limited by coverage, if the current vehicular traffic model is applied. In the other hand, if CAV require maximum user data rates the radio planning shows being limited by both coverage and capacity, being necessary recalculate the cell ranges in those scenarios where is limited by capacity, and thus the desired number of cells to provide the best QoS. The final result, shows that the number of sites calculated for 5 km and 100 MHz of bandwidth, is much higher when considering maximum user data rate than minimum user data rate, due to the cell capacity limitation. And UMa shows requiring the double of sites when comparing to RMa in UL, due to the higher vehicles traffic. Even using MIMO configurations, modulations orders and all 5G air interface features, the radio planning shows having different results when the data rates have so big gaps, and this can be an issue when radio planning is performed. Commonly, is find out a spot in the middle of all scenarios, that match the best situation, and chosen a final number of sites to cover and provide capacity to the highways. However, when V2X applications are considered, safety is the main concern, and there is no possibility of simply choose a final number of sites and leave shadows in the radio planning. For this reason, a more automatic, smart, versatile, and independent network is necessary, that can provide the 100% reliability to the CAV users.

Future work

As mentioned before, to solve the problem find out in this thesis, the network must suffer a development in a matter of dependence, to receive the CAV. Were presented numerous scenarios and situations which could be used as an input for programming software defined network in telecommunications field and radio planning for CAV and V2X. A few sites could be deployed intending only cover the highways, transferring the capacity responsibility to the side link networks. An algorithm could be implemented considering all network features and technologies considered in this thesis, adding beamforming to ensure the coverage to the CAV on highways. Also, radio layers of 100 MHz could be added to the sites, saving radio resources to the side link networks capacity without interfere in the coverage.

References

[1] European Commission, Horizon 2020, "Automated Road Transport – On the way to connected and automated mobility". Brussels, Belgium, March 2019.

[2] SBD, GSMA, "2025 Every Car Connected: Forecasting the Growth and Opportunity". February 2012.

[3] European Automobile Manufacturers Association (ACEA) accessed on 09/12/2019. (https://www.acea.be/press-releases/article/passenger-car-registrations-0.7-10-months-into-2019-8.7-in-october)

[4] IEEE Spectrum, "6 Key Connectivity Requirements of Autonomous Driving". Accessed on 01/12/2020. (https://spectrum.ieee.org/transportation/advanced-cars/6-key-connectivity-requirements-of-autonomous-driving)

[5] 5GMOBIX, Deliverable 6.1, "Plan and preliminary report on the deployment options for 5G technologies for CCAM". Accessed on 30/10/2020. (https://www.5g-mobix.com/assets/files/5G-MOBIX-D6.1-Plan-and-preliminary-report-on-the-deployment-options-for-5G-technologies-for-CCAM-v1.0.pdf)

[6] 5GPPP, "The European 5G Annual Journal 2019". Accessed on 28/02/2020. (https://5g-ppp.eu/annual-journal/)

[7] 5GMOBIX, Deliverable 2.1, "5G-enabled CCAM use cases specifications". Accessed on 28/02/2020, (https://www.5g-mobix.com/assets/files/5G-MOBIX-D2.1-5G-enabled-CCAM-use-cases-specifications-V2.0.pdf)

[8] GSMA Intelligence, "5G in China: Outlook and regional comparisons," 2017.

[9] GSMA Intelligence, "5G in China: the enterprise story," 2018.

[10] SAE MOBILUS. Accessed on 09/12/2019, (https://saemobilus.sae.org/content/J3016_201806/)

[11] 3GPP, Enhancement of 3GPP Support for V2X scenarios, Stage 1, TS 22.186, (Release 16), V16.2.0, June 2019.

[12] V. Vukadinovic et al., “3GPPP C-V2X and IEEE 802.11.p for Vehicle-to-Vehicle communications in highway platooning scenarios”, Ad Hoc Networks, vol. 74, no. March, pp. 17-29, 2018.

[13] R. Itu-r, “Radio interface standards of vehicle-to-vehicle and vehicle-to-infrastructure communications for intelligent transport system applications”, vol. 0, 2015

[14] Bazzi, A., Masini, B. M., Zanella, A., & Thibault, I. (2017). On the performance of IEEE 802.11p and LTE-V2V for the cooperative awareness of connected vehicles. IEEE Transactions on Vehicular Technology, 66(11), 10419–10432. https://doi.org/10.1109/TVT.2017.2750803

[15] 3GPP, Study on architecture enhancements for LTE support of V2X services TR 23.785, (Release 14), V1.1.0, July 2016.

[16] Molina-Masegosa, R., Gozalvez, J., & Sepulcre, M. (2018). Configuration of the C-V2X Mode 4 Sidelink PC5 Interface for Vehicular Communication. Proceedings - 14th International Conference on Mobile Ad-Hoc and Sensor Networks, MSN 2018, (December), 43–48. https://doi.org/10.1109/MSN.2018.00014

[17] V. Mannoni, V. Berg, S. Sesia, and E. Perraud, “A comparison of the V2X communication systems: ITS-G5 and C-V2X,” in IEEE Vehicular Technology Conference, 2019, vol. 2019-April.

[18] 5G Automotive Association. (2017). An assessment of direct communications technologies for improved road safety in the EU. (December), 1–80. Retrieved from http://5gaa.org/wp-content/uploads/2017/12/5GAA-Road-safety-FINAL2017-12-05.pdf

[19] 3GPP, Release 15 Description; Summary of Rel-15 Work Items, TR 21.915, (Release 15), V15.0.0, September 2019.

[20] Osseiran, A., Monserrat, J. F., & Marsch, P. (2016). 5G mobile and wireless communications technology. In 5G Mobile and Wireless Communications Technology. https://doi.org/10.1017/CBO9781316417744

[21] Hawilo, H., Shami, A., Mirahmadi, M., & Asal, R. (2014). NFV: State of the art, challenges, and implementation in next generation mobile networks (vEPC). IEEE Network, 28(6), 18–26. https://doi.org/10.1109/MNET.2014.6963800

[22] Yu, R., Ding, J., Huang, X., Zhou, M. T., Gjessing, S., & Zhang, Y. (2016). Optimal Resource Sharing in 5G-Enabled Vehicular Networks: A Matrix Game Approach. IEEE Transactions on Vehicular Technology, 65(10), 7844–7856. https://doi.org/10.1109/TVT.2016.2536441

[23] Architecture, G., & Group, W. (2017). View of 5G Architecture. (December), 140. Retrieved from https://5g-ppp.eu/wp-content/uploads/2018/01/5G-PPP-5G-Architecture-White-Paper-Jan-2018-v2.0.pdf

[24] I. Alexandre and R. Belchior, "Evaluation of 5G Cellular Network Implementation Over an Existing LTE One Thesis to obtain the Master of Science Degree in Supervisor : Prof. Luís Manuel de Jesus Sousa Correia," no. November 2018.

[25] 3GPP, Study on enhancement of 3GPP Support for 5G V2X Services, TR 22.886, (Release 16), V16.2.0, December 2018.

[26] C. Campolo, A. Molinaro, A. Iera, and F. Menichella, "5G network slicing for vehicle-to-everything services," *IEEE Wirel. Commun.*, vol. 24, no. 6, pp. 38–45, 2017.

[27] 3GPP, TS 38.211, NR; Physical channels and modulation (Release 16), V16.0.0. December 2019.

[28] 3GPP, TR 38.912, Study on New Radio (NR) access technology (Release 15), V15.0.0. June 2018.

[29] 3GPP, TR 38.885, NR; Study on NR Vehicle-to-Everything (V2X) (Release 16), V16.0.0. March 2019.

[30] 3GPP, TR 38.886, V2X Services based on NR; User Equipment (UE) radio transmission and reception; (Release 16), V16.0.0. June 2020.

[31] 3GPP, TS 38 101-1, NR; User Equipment (UE) radio transmission and reception; Part 1: Range 1 Standalone (Release 16), V16.3.0. March 2020.

[32] J. L. Carcel, B. Mouhouche, M. Fuentes, E. Garro, and D. Gomez-Barquero, “IMT-2020 Key Performance Indicators: Evaluation and Extension Towards 5G New Radio Point-to-Multipoint,” IEEE Int. Symp. Broadband Multimed. Syst. Broadcast. BMSB, vol. 2019-June, no. June 2019, 2019.

[33] 3GPP, TR 38 817-01, General aspects for User Equipment (UE) Radio Frequency (RF) for NR (Release 16), V16.1.0. September 2019.

[34] Ericsson, “Advanced antenna systems for 5G networks”. Accessed on 17/12/2020. (https://www.ericsson.com/en/reports-and-papers/white-papers/advanced-antenna-systems-for-5g-networks)

[35] 5GMOBIX, Deliverable 2.5, “Initial evaluation KPIs and metrics”. Accessed on 07/12/2020, (https://www.5g-mobix.com/assets/files/5G-MOBIX-D2.5-Initial-evaluation-KPIs-and-metrics-V1.4.pdf)

[36] 3GPP, TS 38 213, NR; Physical layer procedures for control (Release 16), V16.3.0. September 2020.

[37] Rappaport, “Rappaport - Wireless Communications Principles and Practice.” pp. 268–583, 2002.

[38] 3GPP, Study on channel model for frequencies from 0.5 to 100 GHz, TR 38.901, (Release 16), V16.1.0. December 2019.

[39] 3GPP, TS 38 817-02, NR; General aspects for Base Station (BS) Radio Frequency (RF) for NR (Release 15), V15.7.0. March 2020.

[40] N. Al-Falahy and O. Y. K. Alani, “Design considerations of ultra-dense 5G network in millimetre wave band,” *Int. Conf. Ubiquitous Future. Networks, ICUFN*, pp. 141–146, 2017.

[41] A. Kukushkin, Introduction to Mobile Network Engineering: GSM, 3G-WCDMA, LTE and the Road to 5G. 2018.

[42] Tom-tom move. Accessed in 26/09/2020. (https://www.tomtom.com/en_gb/traffic-index/lisbon-traffic/)

[43] Serrador A., Teixeira G., Lima M., Fernandes R., “Autonomous Vehicles Impact on 5G Network Inter-Site Distance”. Virtual ITS European Congress, November 2020.

[44] 3GPP, TS 38 306, NR; User Equipment (UE) radio access capabilities (Release 16), V16.0.0. March 2020.

[45] ITU, “FINAL EVALUATION REPORT FROM THE 5G INFRASTRUCTURE ASSOCIATION ON IMT-2020 PROPOSALS IMT-2020/ 14, 15, 16, PARTS OF 17”, Document 5D/50-E. February 2020.

[46] 3GPP, TS 38 214, NR; Physical layer procedures for data (Release 16), V16.1.0. March 2020.

Annexes

Annex A. BER Vs Eb/N0

The parameter SNR was reached simulating AWGN channel in MATLAB, where the results showed a graphic of BER in function of Eb/N0, varying according to each modulation scheme, which are based on Equation A.1 and Equation A.2.

1) QPSK

$$BER = Q\left(\sqrt{\frac{2E_b}{N_0}}\right) \qquad \text{Equation A.1}$$

2) 16QAM, 64QAM and 256QAM

$$BER = \frac{2}{\sqrt{M}\log_2\left(\sqrt{M}\right)} * \sum_{k=1}^{\log_2\sqrt{M}} \sum_{i=0}^{(1-2^{-k})\sqrt{M}-1} \left\{(-1)^{\left\lfloor\frac{i2^{k-1}}{\sqrt{M}}\right\rfloor}\left(2^{k-1} - \left\lfloor\frac{i2^{k-1}}{\sqrt{M}}+\frac{1}{2}\right\rfloor\right) Q\left((2i+1)\sqrt{\frac{6\log_2 M}{2(M-1)}\frac{E_b}{N_0}}\right)\right\} \qquad \text{Equation A.2}$$

Where k=log$_2$*M,* and *M* is the modulation order, which differ according to the modulation as on Table 2.7. The *Q* variable, is a mathematical probabilistic function presented on Equation A.3.

$$Q(x) = \frac{1}{2\pi}\int_x^\infty \exp\left(\frac{-t^2}{2}\right)\ dt \qquad \text{Equation A.3}$$

Annex B. MAPL

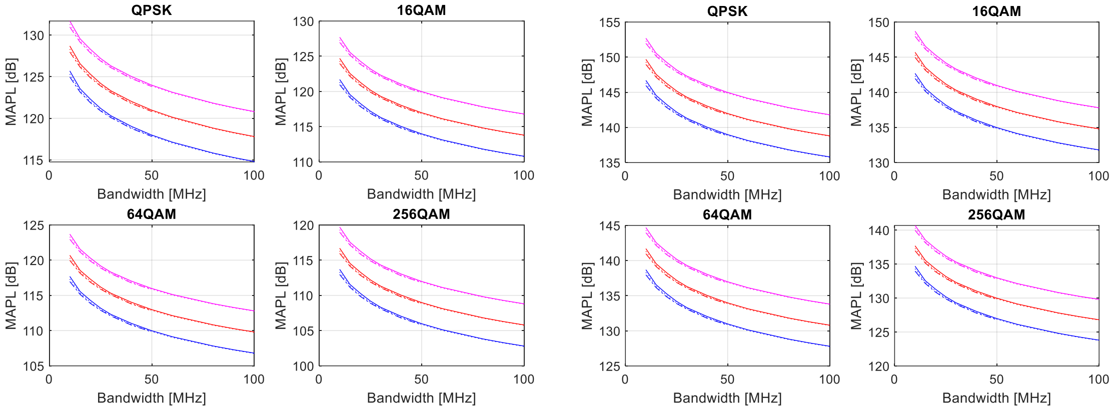

a) b)

Figure B.1 - MAPL in RMa LOS a) UL and b) DL scenarios.

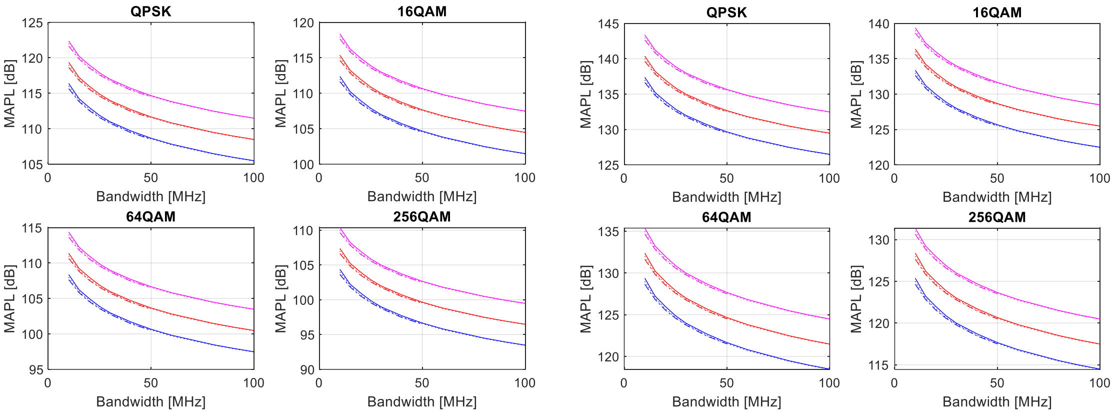

a) b)

Figure B.2 - MAPL in RMa NLOS a) UL and b) DL scenarios.

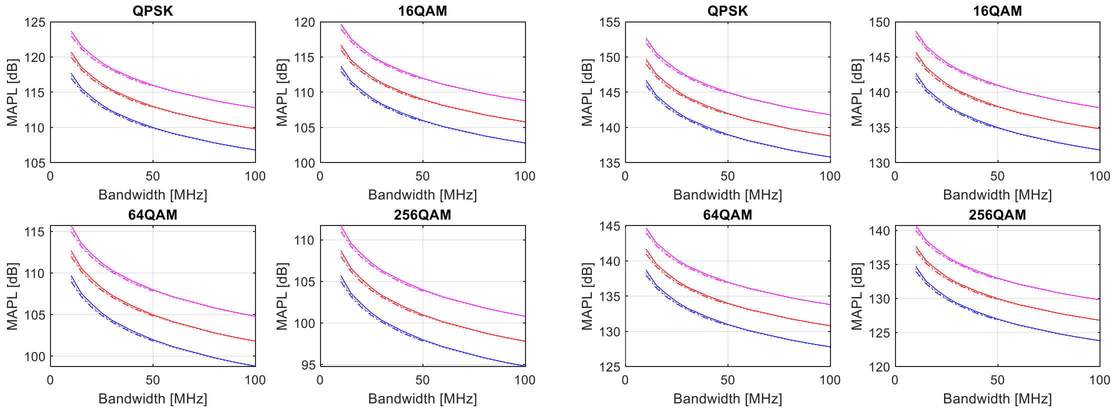

a) b)

Figure B.3 - MAPL in UMa LOS a) UL and b) DL scenarios.

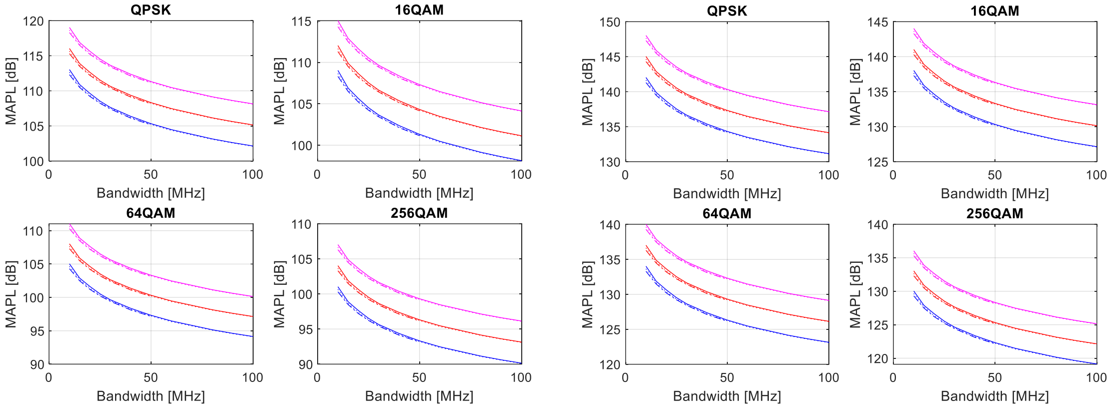

a) b)

Figure B.4 - MAPL in UMa NLOS a) UL and b) DL scenarios.

Annex C. Inter-site distance

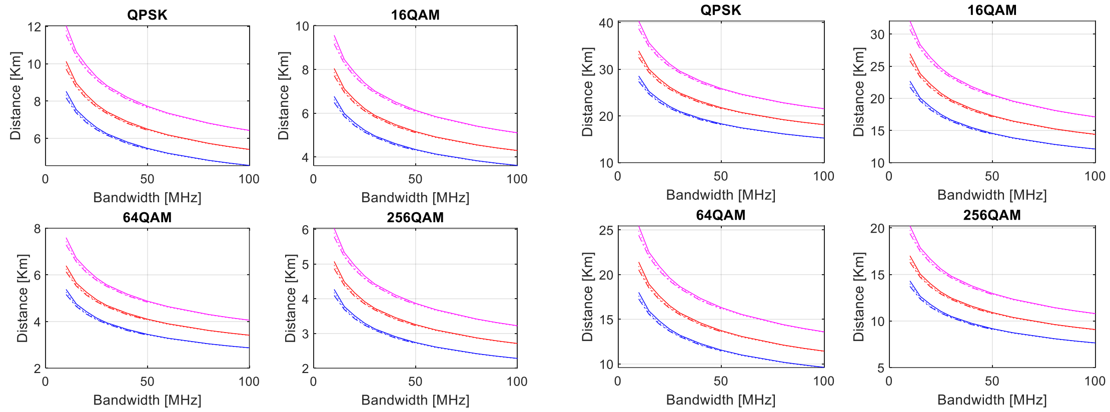

a) b)

Figure C.1 - Inter-site distance in RMa LOS a) UL and b) DL scenarios.

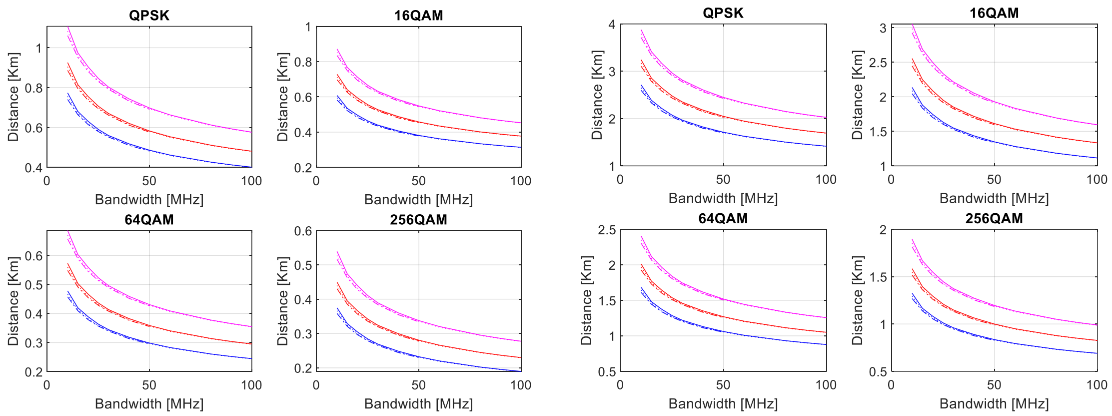

a) b)

Figure C.2 - Inter-site distance in RMa NLOS a) UL and b) DL scenarios.

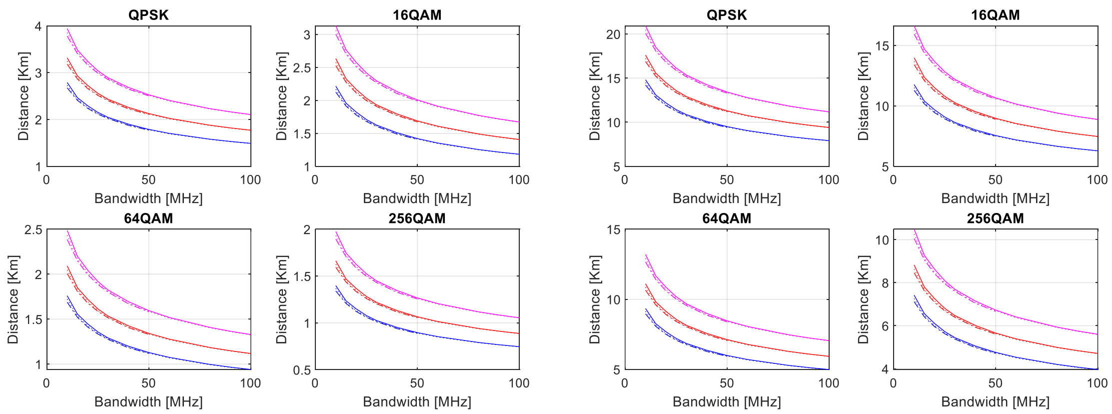

a) b)

Figure C.3 - Inter-site distance in UMa LOS a) UL and b) DL scenarios.

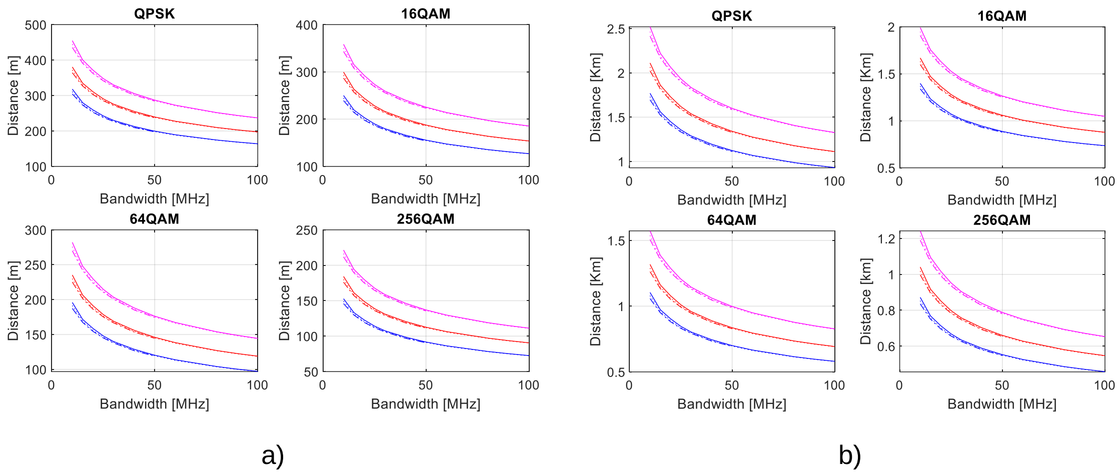

Figure C.4 - Inter-site distance in UMa NLOS a) UL and b) DL scenarios.

Annex D. Number of sites

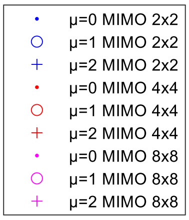

Figure D.1 - Legend to analyse number of sites by coverage simulation.

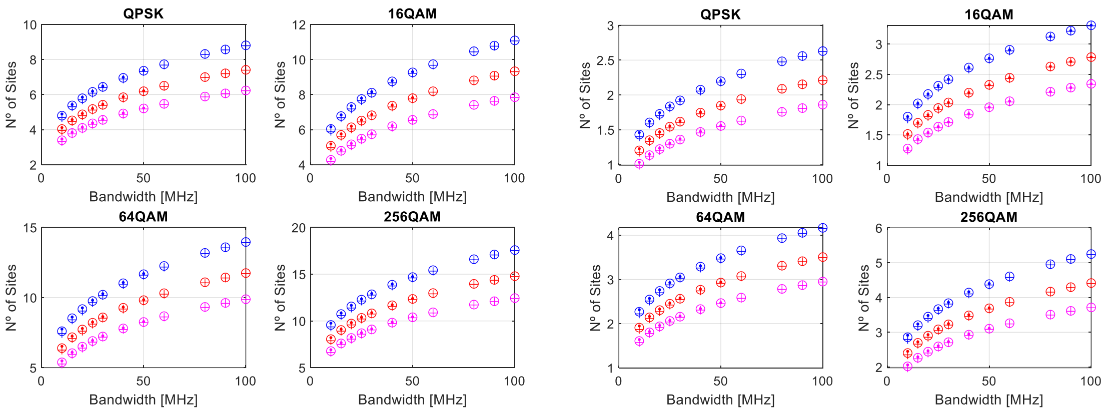

a) b)

Figure D.2 - Number of sites for 40 km in RMa LOS a) UL and b) DL scenarios.

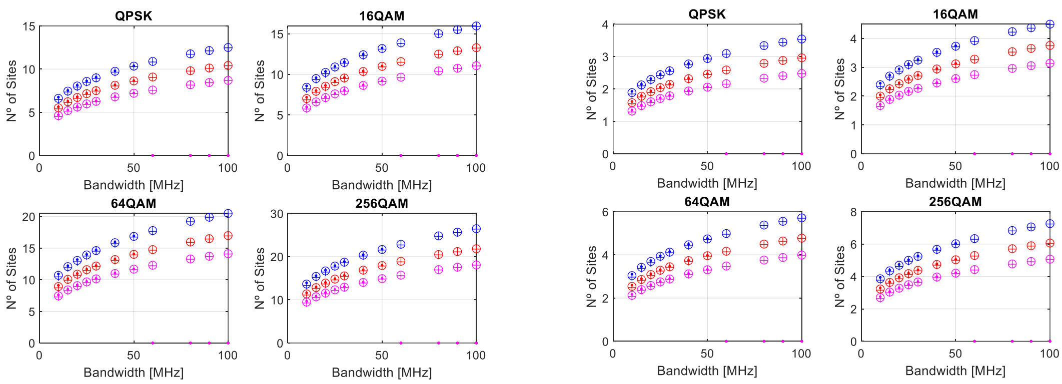

a) b)

Figure D.3 - Number of sites for 5 km in RMa NLOS a) UL and b) DL scenarios.

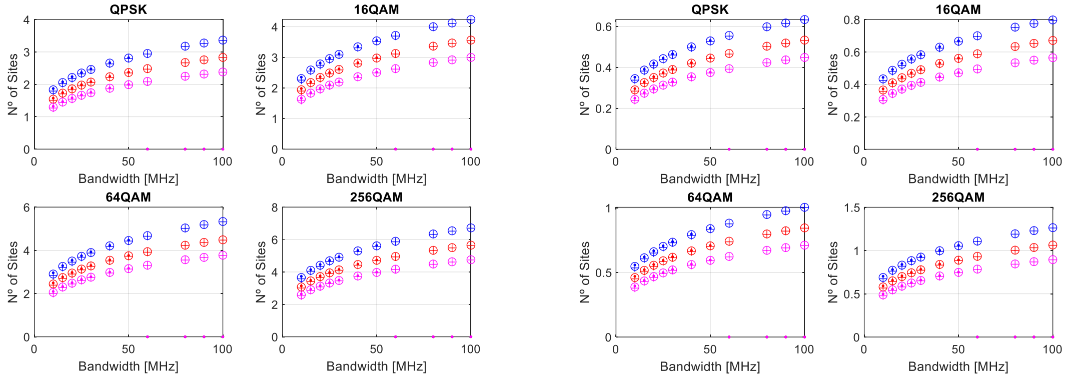

a) b)

Figure D.4 - Number of sites for 5 km in UMa LOS a) UL and b) DL scenarios.

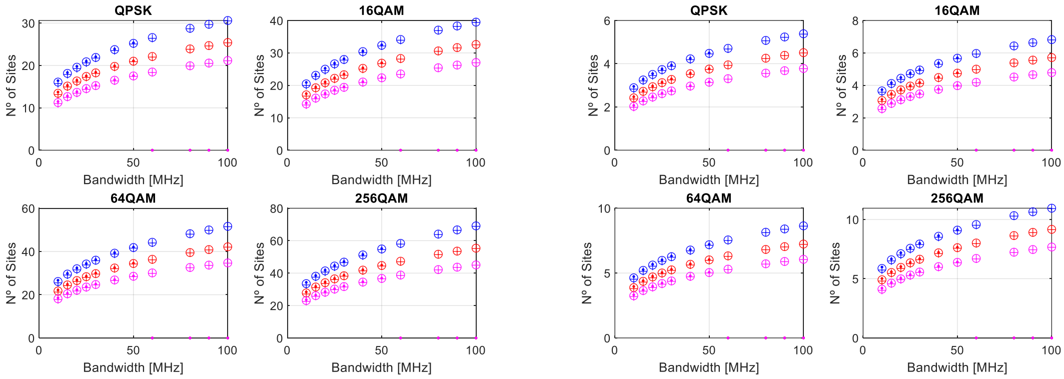

a) b)

Figure D.5 - Number of sites for 5 km in UMa NLOS a) UL and b) DL scenarios.

Annex E. Number of cells per kilometre

For RMa LOS UL and DL, the number of cells is considered 2 for the whole stretch.

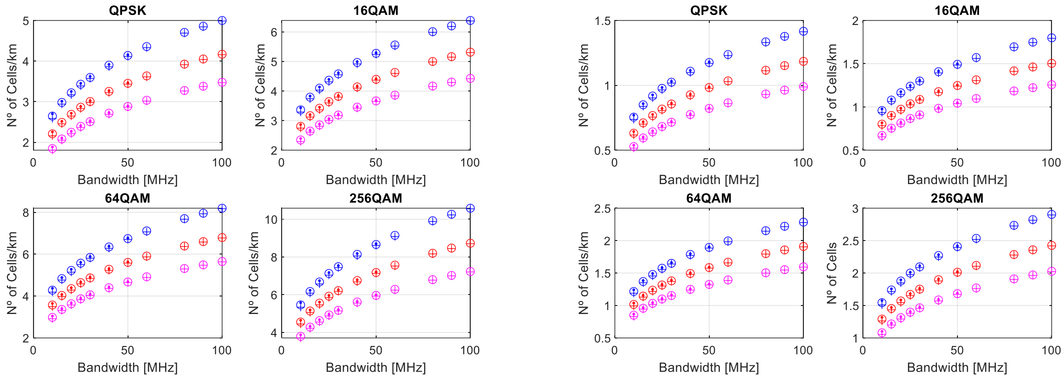

a) b)

Figure E.1 - Number of cells per km in RMa NLOS a) UL and b) DL scenarios.

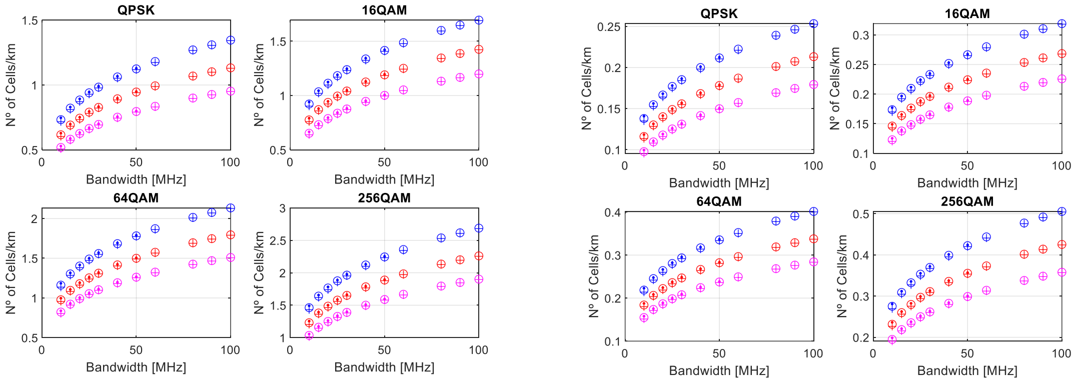

a) b)

Figure E.2 - Number of cells per km in UMa LOS a) UL and b) DL scenarios.

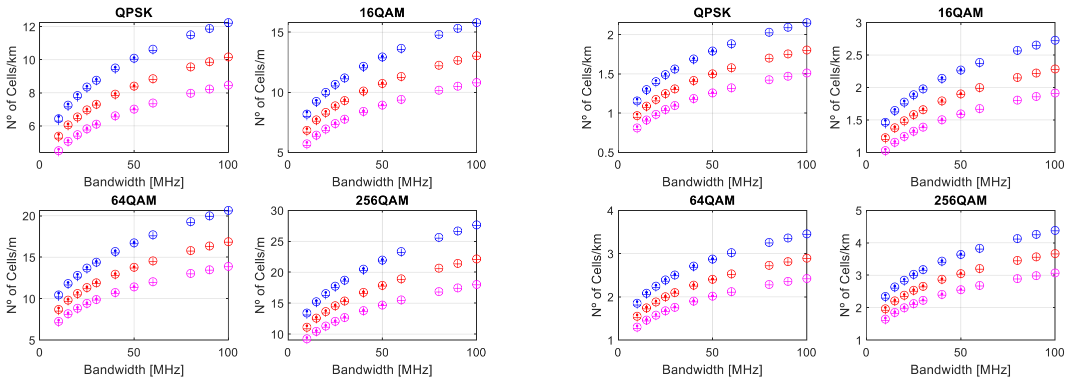

a) b)

Figure E.3 - Number of cells per km in UMa NLOS a) UL and b) DL scenarios.

Annex F. Number of vehicles per cell

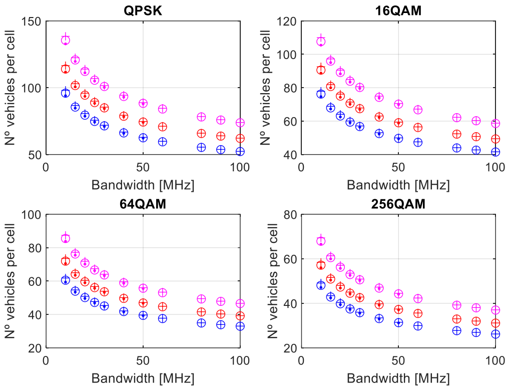

Figure F.1 - Number of vehicles covered per cell in RMa LOS UL scenario.

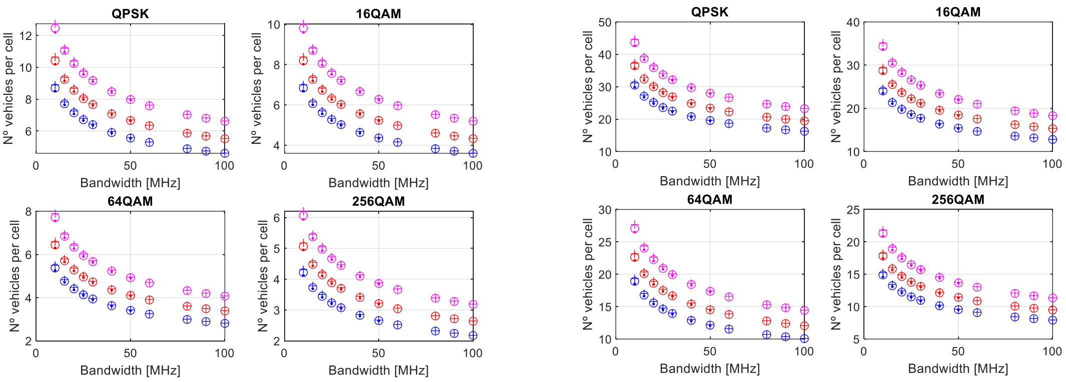

a) b)

Figure F.2 - Number of vehicles covered per cell in RMa NLOS a) UL and b) DL scenarios.

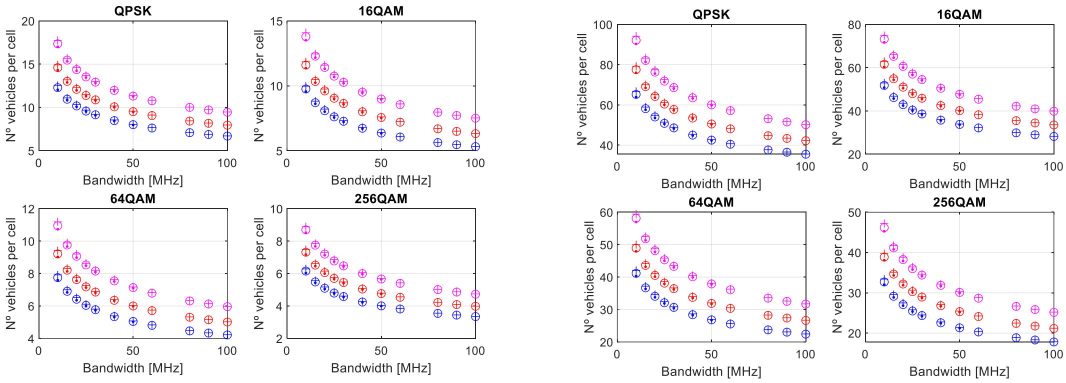

a) b)

Figure F.3 - Number of vehicles covered per cell in UMa LOS a) UL and b) DL scenarios.

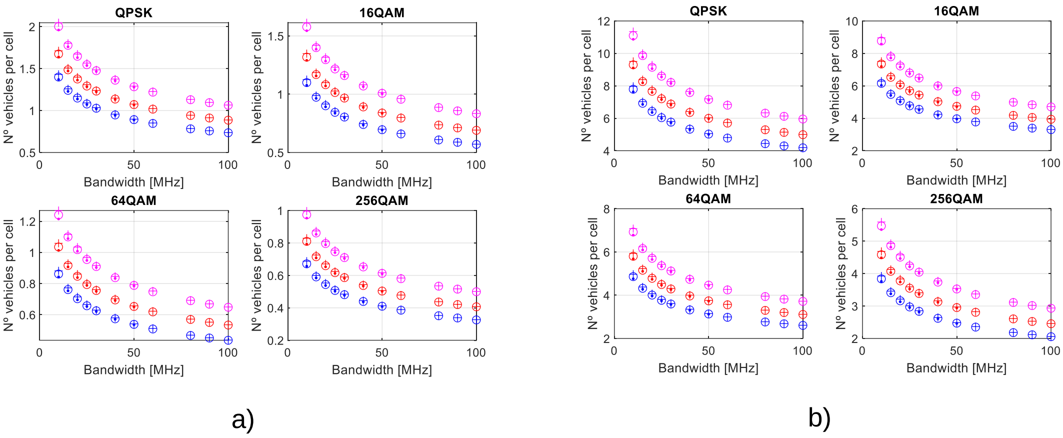

Figure F.4 - Number of vehicles covered per cell in UMa NLOS a) UL and b) DL scenarios.

Annex G. Traffic load computation

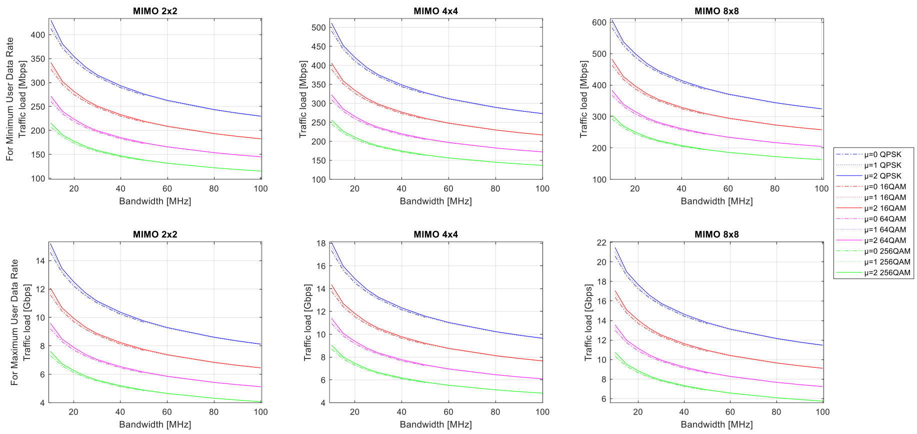

Figure G.1 - Traffic load on RMa LOS DL scenario.

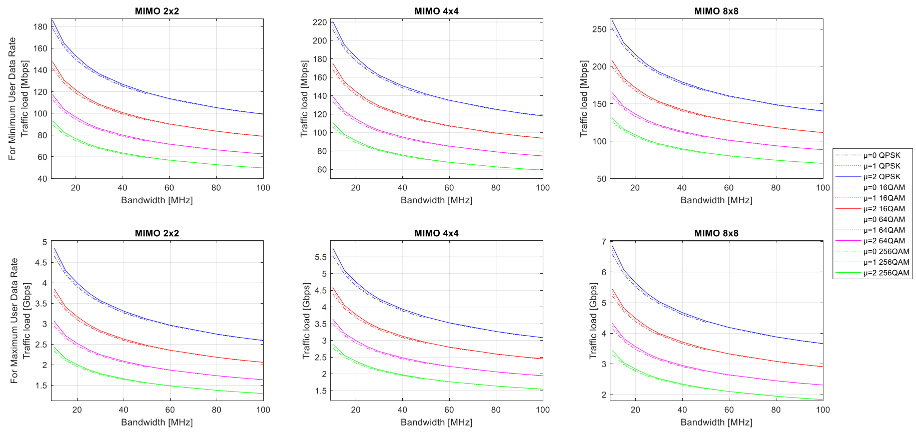

Figure G.2 - Traffic load on RMa LOS UL scenario.

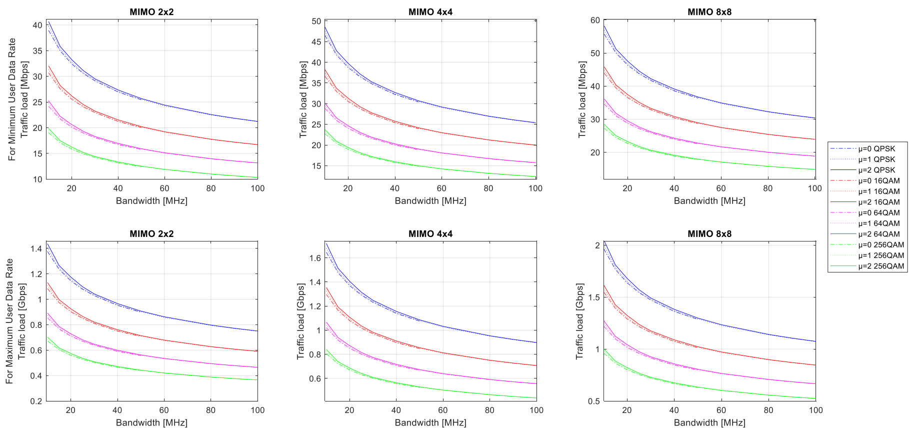

Figure G.3 - Traffic load on RMa NLOS DL scenario.

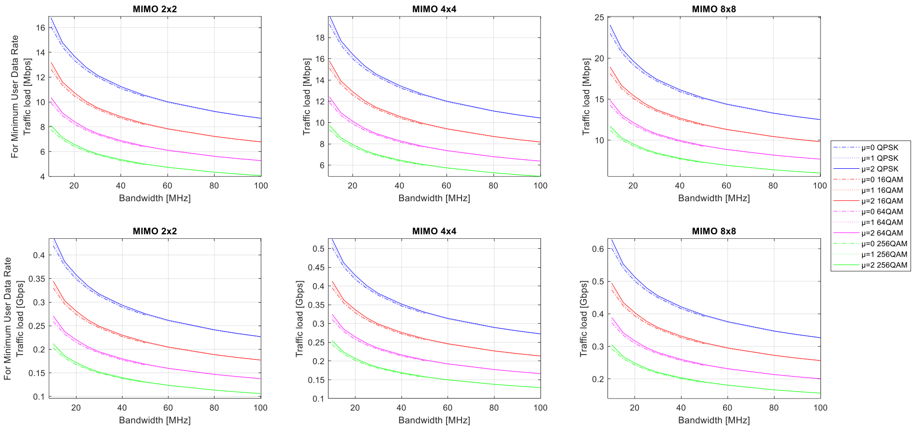

Figure G.4 - Traffic load on RMa NLOS UL scenario.

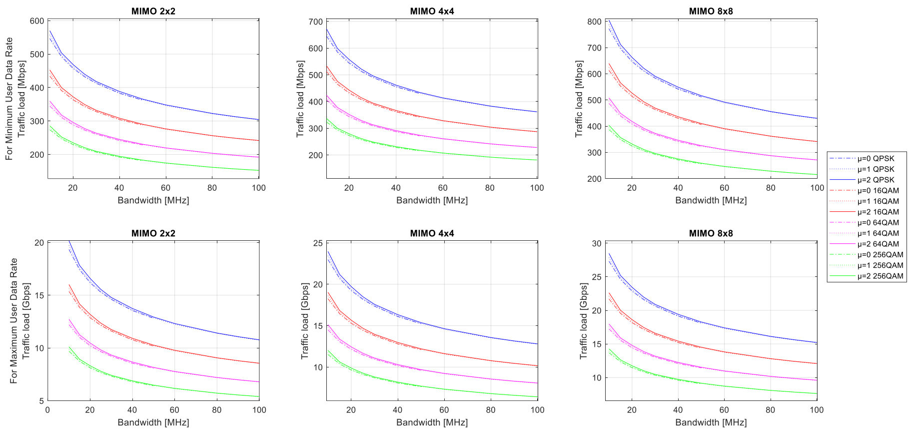

Figure G.5 - Traffic load on UMa LOS DL scenario.

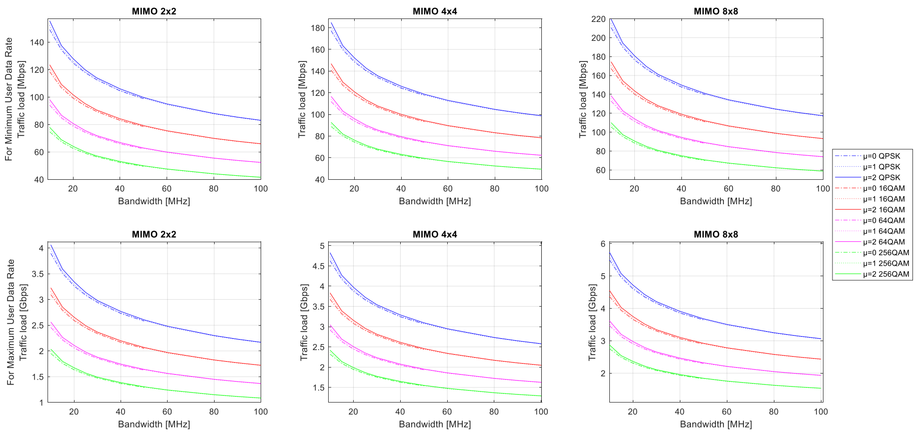

Figure G.6 - Traffic load on UMa LOS UL scenario.

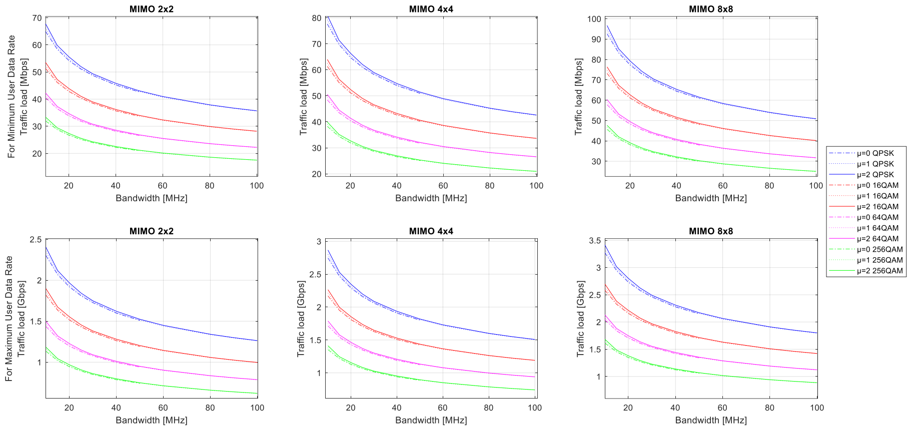

Figure G.7 - Traffic load on UMa NLOS DL scenario.

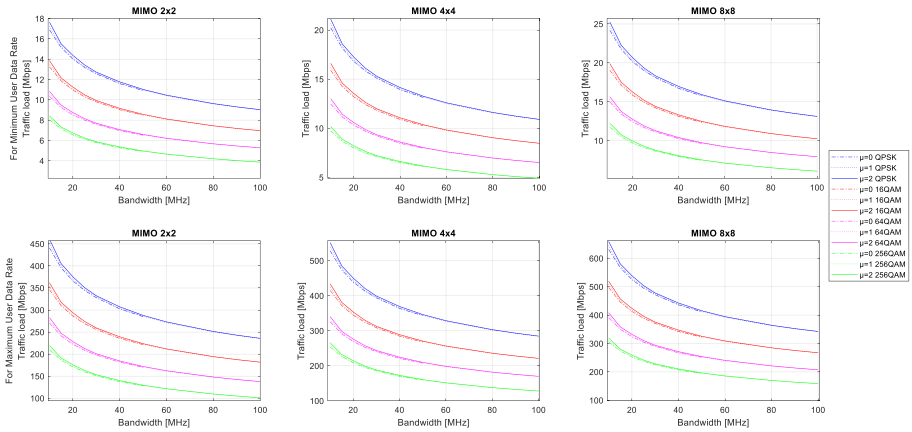

Figure G.8 - Traffic load on UMa NLOS UL scenario.

Annex H. Number of vehicles per service supported

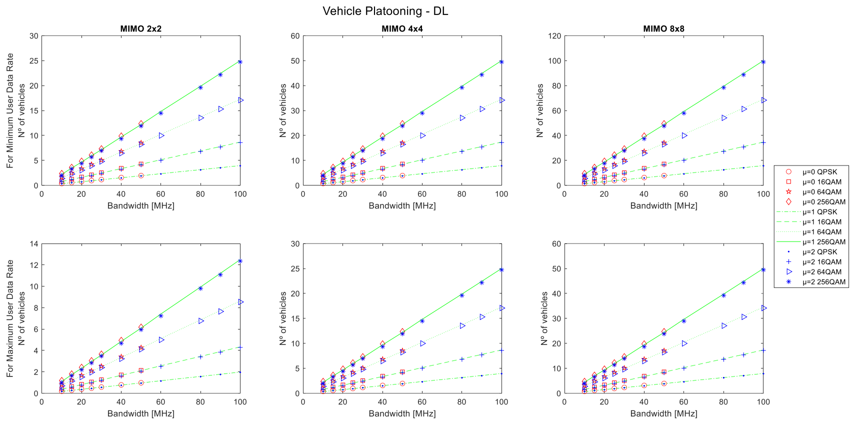

Figure H.1 - Number of vehicles supported for vehicle platooning in DL.

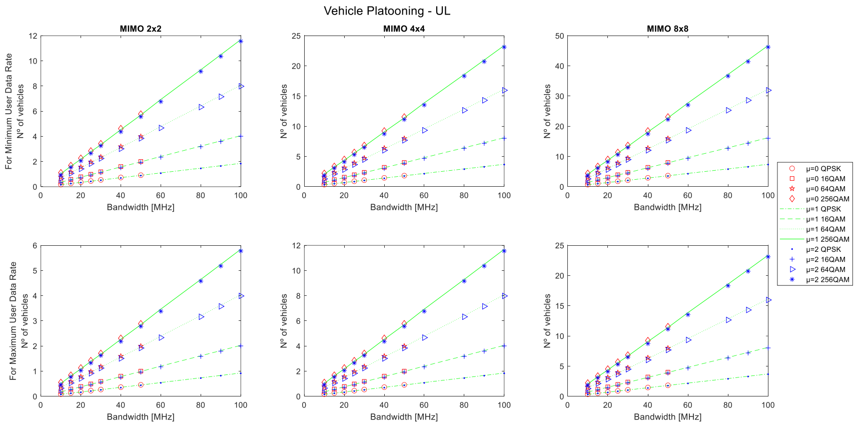

Figure H.2 - Number of vehicles supported for vehicle platooning in UL.

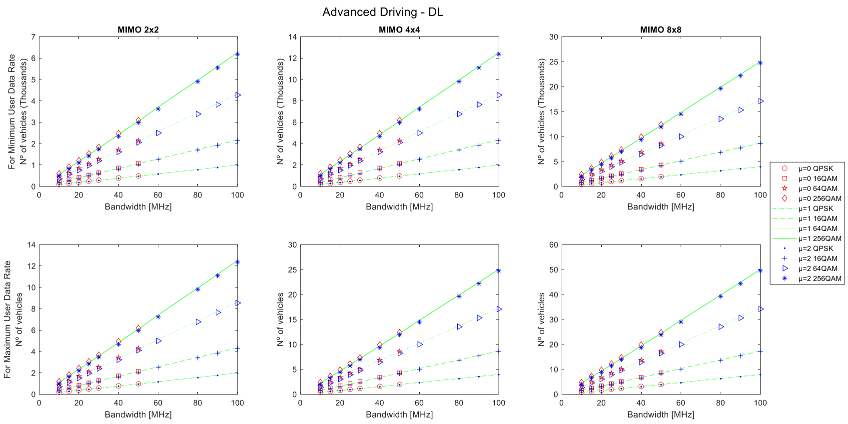

Figure H.3 - Number of vehicles supported for advanced driving in DL.

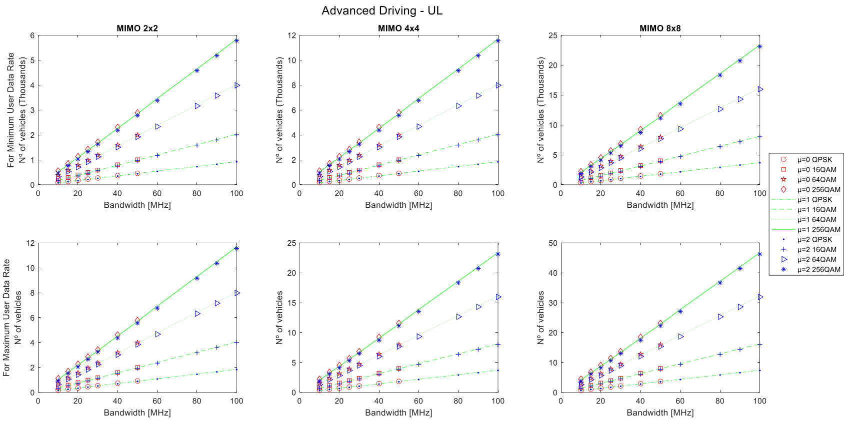

Figure H.4 - Number of vehicles supported for advanced driving in UL.

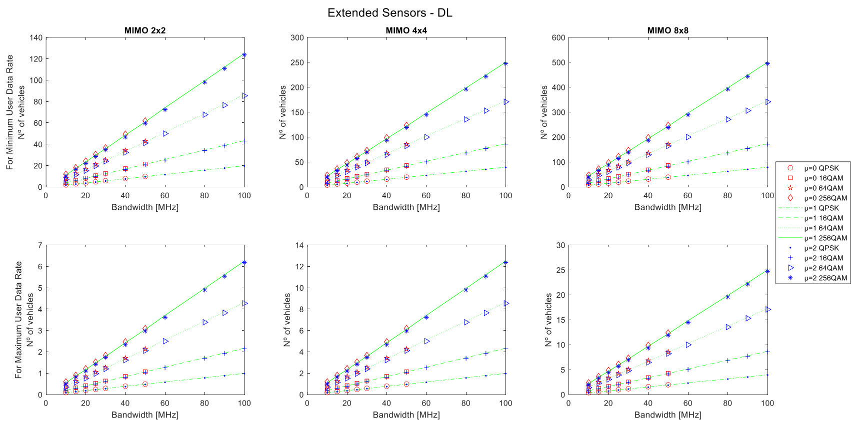

Figure H.5 - Number of vehicles supported for extended sensors in DL.

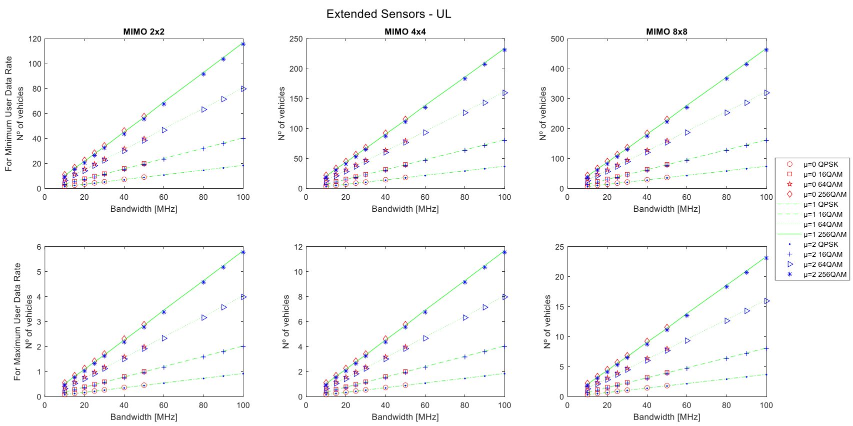

Figure H.6 - Number of vehicles supported for extended sensors in UL.

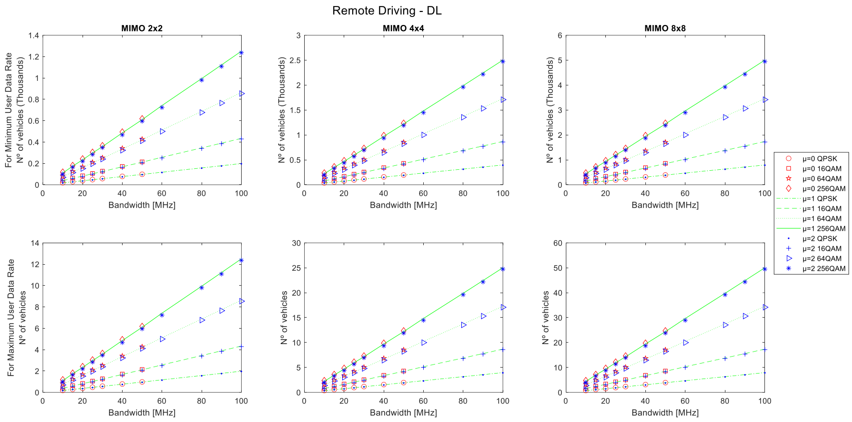

Figure H.7 - Number of vehicles supported for remote driving in DL.

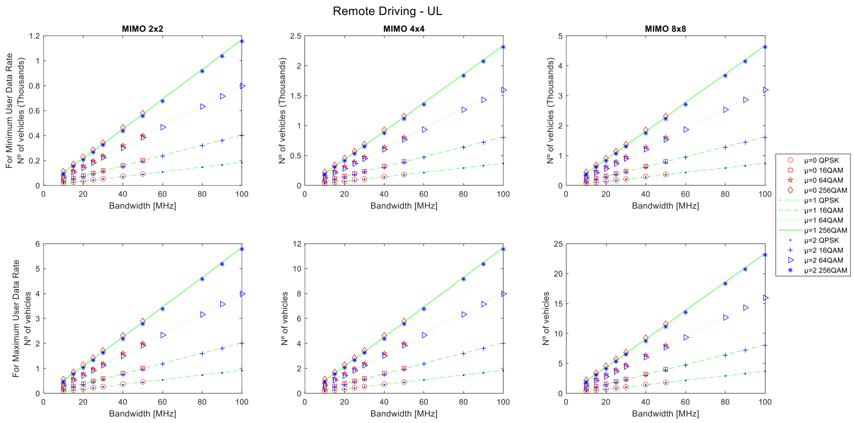

Figure H.8 - Number of vehicles supported for remote driving in UL.

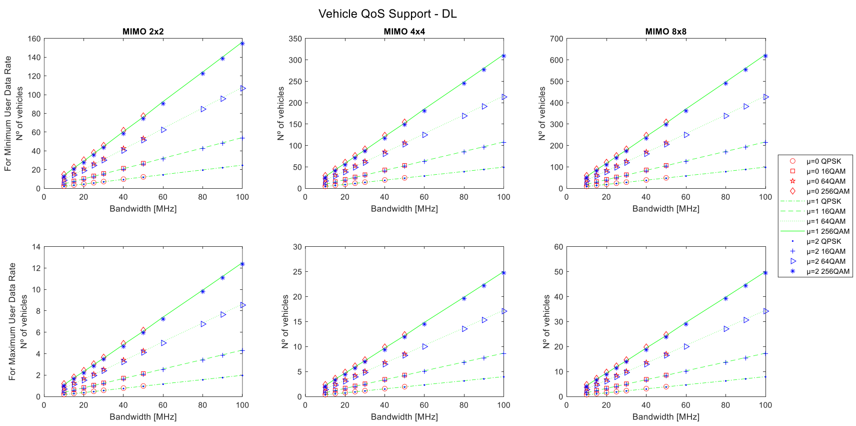

Figure H.9 - Number of vehicles supported for vehicle QoS support in DL.

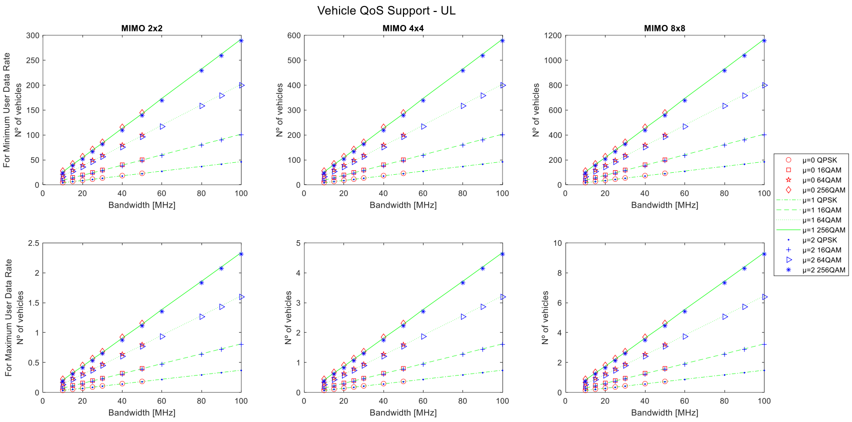

Figure H.10 - Number of vehicles supported for vehicle qos supported in UL.

Annex I. Inter-site distance by capacity

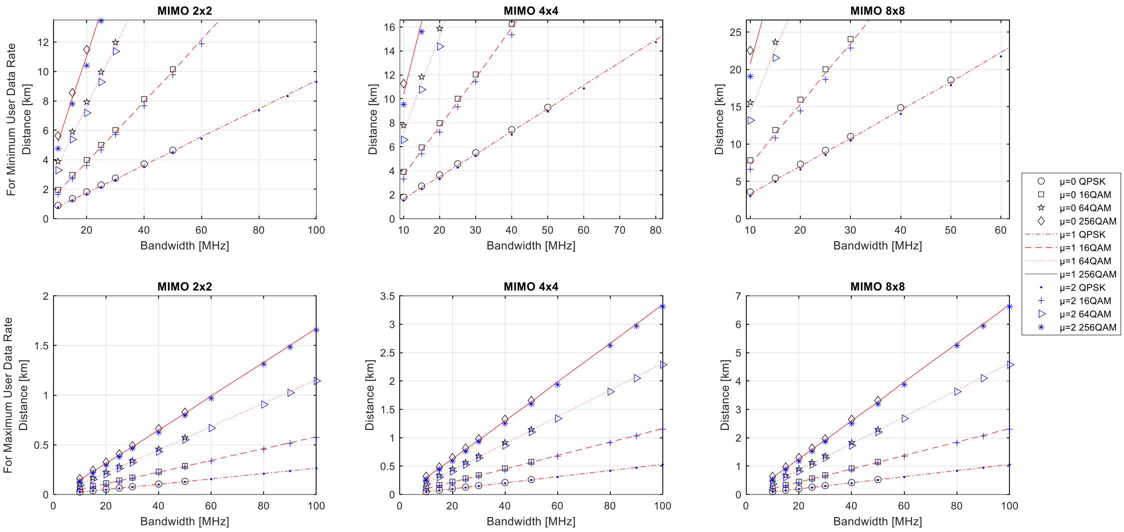

Figure I.1 - ISD computation by capacity on rural DL scenario.

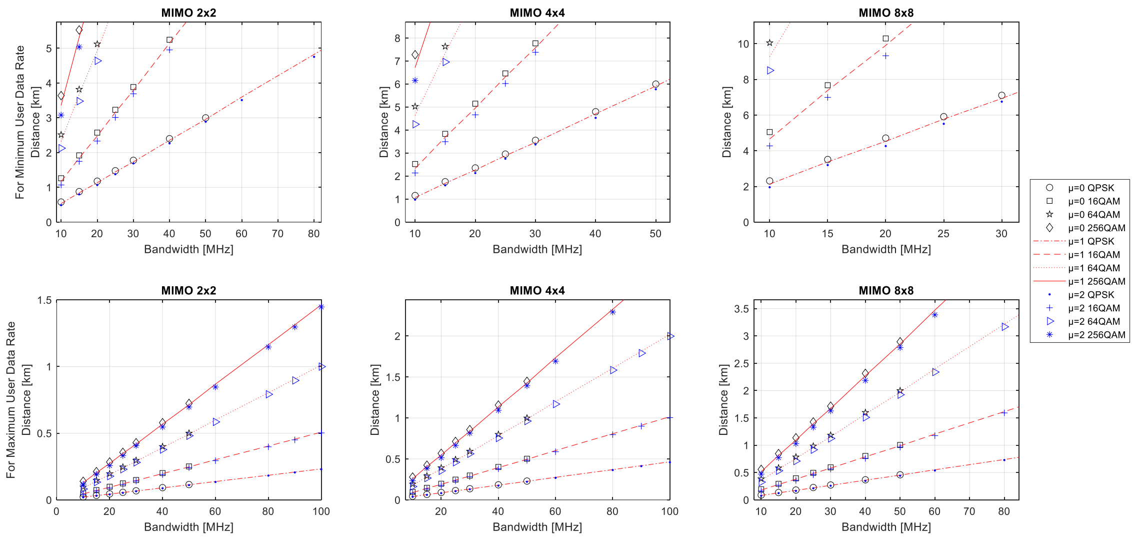

Figure I.2 - ISD computation by capacity on rural UL scenario.

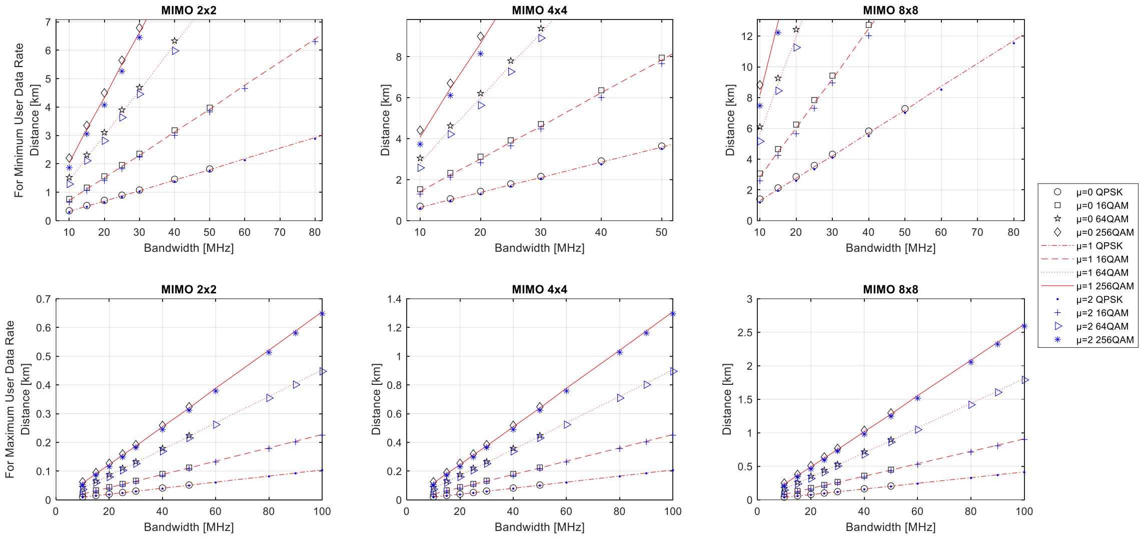

Figure I.3 - ISD computation by capacity on urban DL scenario.

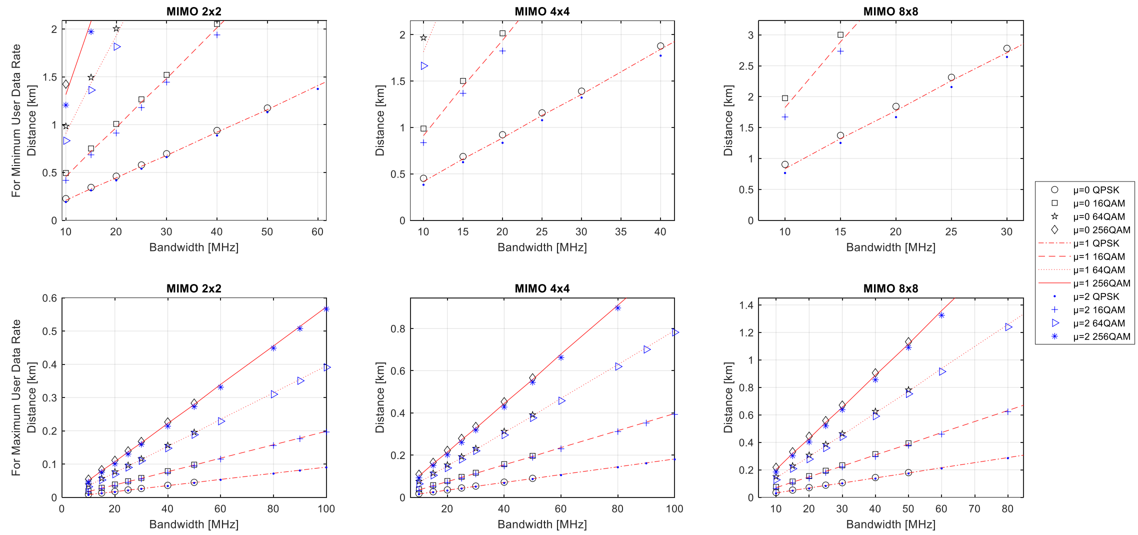

Figure I.4 - ISD computation by capacity on UMa UL scenario.